



UNIVERSITY OF
BATH

University of Bath

Department of Chemical Engineering

**Project Title: Chocolate Cooling
Tunnel
ES-2**

Individual's Name: Sohail Shaikh

Supervisor's Name: Tom Arnot

Product & Process Design (Individual)

Unit Code: CE30243

Academic Year

2024-2025

Contents

Nomenclature	4
1 Executive Summary	5
1.1 Aims and Objectives	5
1.2 Market Overview	5
1.3 Product Scoping and selection	6
1.4 Chocolate manufacturing Unit design overview	8
1.5 Economic Viability	9
1.6 Responsible innovation	10
1.7 Unit Brief	10
1.8 Chemistry of chocolate	11
2 Unit Design	12
2.1 Initial Shortcut Design	12
2.1.1 Calculation Check	13
2.1.2 Shortcut Energy Balance	17
2.2 Rigorous design	20
2.2.1 Dynamic variable adjustment	20
2.2.2 Surface Temperature Analysis	23
2.2.3 Internal Temperature Analysis	25
2.2.4 Modelling of air flow	30
2.2.5 Calculation Check	35
2.2.6 Computer flow diagram	39
3 Unit Optimisation	40
3.1 Varying Cooling Time	40
Varying mould thickness	41
3.2 Varying Cooling temperature	43
3.3 Varying inlet Velocity	45
3.4 Operational limits	48
4.1 Mechanical Engineering Design	49
4.1.1 Engineering drawings	49
4.1.2 Belt transfer	52
4.1.3 Conveyor belts	53

4.1.4 Frame & Housing.....	54
4.1.5 Airflow distribution system.....	54
4.1.6 Material Selection	55
4.1.6.1 Frame.....	55
4.1.6.2 Conveyor	56
4.1.6.3 Airflow system	56
4.1.7 Material Summary	57
5 Control Systems	58
5.1 Control Considerations	58
5.2 Operational influence on other units in the process.....	59
5.3 Safety considerations.....	60
5.4 Startup Shutdown	62
5.5 Cleaning / Maintenance	62
5.6 P&ID & HAZID.....	63
5.7 LOPA.....	70
5.8 Critical Review	71
6 Summary.....	72
6.1 Spec Sheet.....	72
6.2 Conclusion	73

Nomenclature

Symbol	Meaning	Units
C_p	Specific heat capacity	$\text{kJ}\cdot\text{kg}^{-1}\cdot\text{K}^{-1}$
ρ	Density	$\text{kg}\cdot\text{m}^{-3}$
λ	Thermal conductivity	$\text{W}\cdot\text{m}^{-1}\cdot\text{K}^{-1}$
T	Temperature	$^{\circ}\text{C} / \text{K}$
m	Mass	kg
\dot{m}	Mass flowrate	$\text{kg}\cdot\text{s}^{-1}$
Q	Heat transfer rate	W
U	Overall heat transfer coefficient	$\text{W}\cdot\text{m}^{-2}\cdot\text{K}^{-1}$
h	Convective heat transfer coefficient	$\text{W}\cdot\text{m}^{-2}\cdot\text{K}^{-1}$
A	Heat transfer area	m^2
dx	Change in distance	m
μ	Dynamic viscosity	$\text{Pa}\cdot\text{s}$
ν	Kinematic viscosity	$\text{m}^2\cdot\text{s}^{-1}$
k	Thermal conductivity	$\text{W}\cdot\text{m}^{-1}\cdot\text{K}^{-1}$
Pr	Prandtl number	—
Re	Reynolds number	—
Nu	Nusselt number	—
V	Air velocity	$\text{m}\cdot\text{s}^{-1}$
D_h	Hydraulic diameter	m
t	Time	s
ΔT	Temperature difference	$\text{K} / ^{\circ}\text{C}$
ε	Efficiency	—
α	Thermal diffusivity	$\text{m}^2\cdot\text{s}^{-1}$
P	Power	W
L	Pipe or tunnel length	m
\dot{V}	Volumetric flowrate	$\text{m}^3\cdot\text{s}^{-1}$

1 Executive Summary

1.1 Aims and Objectives

The purpose of the design project is to develop the production process of a chocolate bar. This project focuses on three core objectives: product, process and business. Firstly, the manufactured product needs to be designed to be an affordable and sustainable chocolate bar that appeals to the target market of 18-25 year old consumers. Secondly, the production process needs to include both the chocolate manufacturing process as well as an integrated wastewater treatment system that treats clean-in-place (CIP) water. CIP water is used to clean equipment throughout the process, addressing its management will mitigate the potential environmental impact posed by wastewater. Finally, this project will provide a profitable business strategy that effectively operates within the UK market and adapts to volatile market conditions, such as rising cocoa bean prices to ensure long term commercial viability.

Addressing these objectives will help achieve 4 of the UN Sustainable Development Goals, which are as follows:

- Goal 6: Clean Water and Sanitation
- Goal 11: Sustainable Cities and Communities
- Goal 12: Responsible Consumption and Production
- Goal 13: Climate Action

By focusing on sustainability within both the product development and the production process, this project aims to contribute to Goals 12 and 13 (Responsible Consumption and Production and Climate Action). The integration of a wastewater treatment facility directly supports Goal 6 (Clean Water and Sanitation).

1.2 Market Overview

The UK chocolate confectionary market was valued at £4.5 billion in 2024, it is also projected to grow at a compound annual growth rate of 6.2% from 2025 to 2032 (Richard Caines, 2024). Indicating a thriving market with sustained customer demand for confectionary products. The high valuation demonstrates chocolates status as a staple indulgence, whilst the stable growth rate indicates continued opportunities for innovation within the industry. However, traditional chocolate companies remain dominant within the market, where around 85% of the market is captured by five of the largest companies by market valuation (IBISWorld, 2024). This reveals a challenge for emerging brands in this competitive, consolidated industry. Despite this, a rising demand for ethically and sustainably sourced products driven by shifting consumer preference provides an opportunity for emerging businesses to capitalise on these trends when developing new chocolate products. Another challenge the industry faces is supply chain issues, such as volatile cocoa prices and rising production costs caused by events like agricultural issues in West Africa shrinking cocoa supply. Market regulations and restrictions regarding the content of food also put pressure on the impact of production. The sugar tax employed in 2018 by the UK government provides an increased scrutiny on products with sugar content, pushing manufacturers to re-evaluate product formulation (Public Health England, 2023).

1.3 Product Scoping and selection

Evolving consumer preferences are driving changes within the market, prompting innovation and the development of products that align with new demands. Market research was conducted to gain insights into consumer preferences and behaviour, this research would be used to drive the decisions in the development of the product. A survey was conducted with 168 participants. Participants were roughly evenly split by gender, with the majority falling within the young age range of 20–24 years old, accounting for 115 of the 168 respondents.

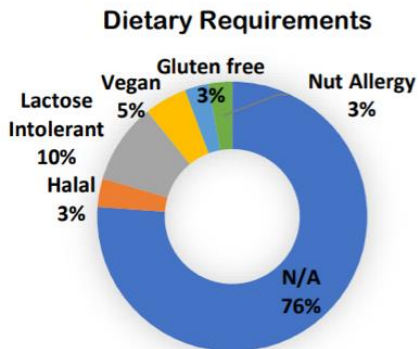
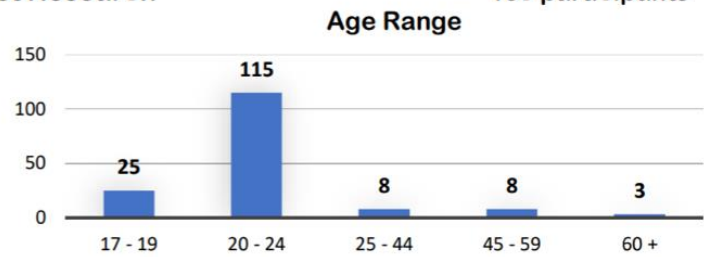
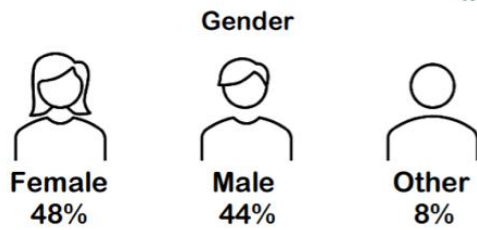
Findings from the survey revealed key chocolate buying habits among consumers. The most common purchasing frequency is once a week, with 31% of consumers surveyed falling into this group. Monthly and fortnightly purchases were the next most common. These patterns were taken into account when planning production and inventory management, helping to ensure consistent product availability for customers. It was also important to find out price that consumers would be willing to pay. Participants were asked how much they would be willing to spend for 100g worth of chocolate. The highest proportion of customers, 37% were willing to pay between 1.50£ and 2£, indicating preference to affordable options. As the price decreases from this range the willingness to pay remains relatively high. However, any higher than this price range results in a sharp decline in popularity.

Consumer preferences are integral in when deciding upon the product. In order to reach a wide range of consumers dietary requirements have to be considered. Despite this, the wide majority (76%) of consumers do not have any dietary requirements. Therefore, whilst it is important to consider these requirements, this is not something that will define the final product. An aspect that is important to consider is the chocolate type, with milk chocolate being the most popular choice, 62% of customers expressing a preference for it. This was followed dark chocolate (30%) and then white chocolate (8%). Texture also plays a crucial role, the data indicates a clear preference to a smooth texture, with 44% of consumers favouring it, the next popular is a crunchy texture, with 28% of people preferring it.

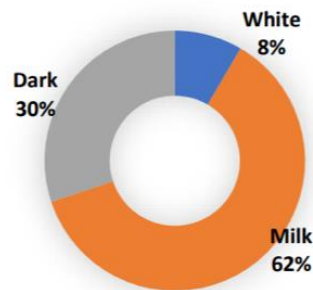
What makes a product stand out in the market is a distinctive flavour, the survey provided the participants with a wide range of flavours to choose from. The two most popular flavours were sea salt and caramel, with 49% and 43% of customers respectively indicating a desire for them. Honey, coffee, and nuts are amongst the other highly desired flavours. Lastly, the appropriate product size must be determined, participants were given a choice of three different chocolate bar sizes. The survey results revealed that the family bar (180g) was the most popular option, with 56% choosing it. This was followed by the standard 100g bar, with bite-sized options being the least preferred. The data clearly suggests a stronger consumer preference for larger chocolate bar formats.

Market Research

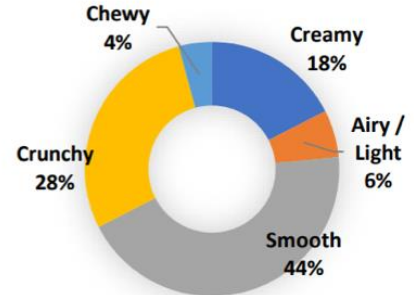
168 participants



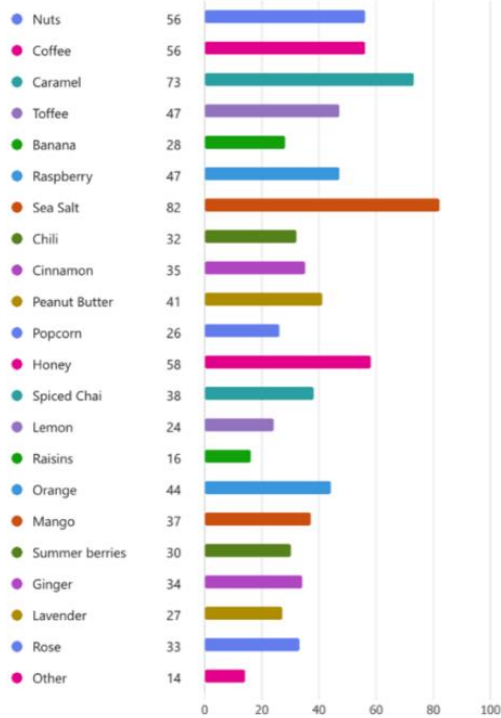
Chocolate Preference



Texture Preference



Desired New Flavours



Where do people buy their chocolate from



Super Market:
87%



Chocolate shops:
11%



Online
3%

Product Size Preference



Standard (100g):
30%



Family bar (180g):
56%

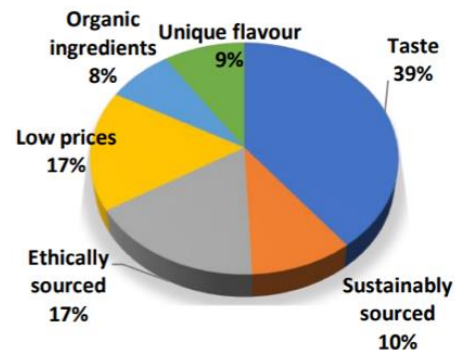


Multiple bite sized:
14%

Price willing to pay for a 100g standard bar



What is valued in a chocolate product



Frequency of purchasing chocolate



Daily: 1%

Once every other day: 10%

Once a week: 31%

Once a fortnight: 24%

Monthly: 27%

Figure 1.3.1 shows the visual depiction of the market research

Survey results suggest that a family-sized 180g bar would be the most effective option for maximising sales. In terms of flavour, a milk chocolate base combined with caramel and sea salt emerged as the most popular choice. The sweet-and-salty pairing offers a well-balanced taste, with caramel included as solid chunks rather than a liquid filling. The liquid chocolate takes up 90% of the whole chocolate bar, the remaining 10% is composed of the salted caramel inclusions. This texture contrast complements the smoothness of the milk chocolate, aiming to enhance overall appeal and attract a broad range of consumers. To fit the 180g requirement, the dimensions of the bar were 1.2 cm x 18.50 cm x 8.9 cm, as shown in *Figure 1.3.2*.

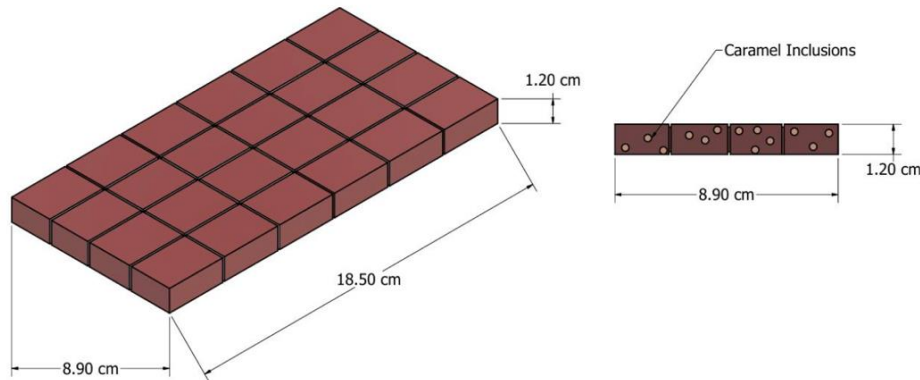


Figure 1.3.2. Dimensions of the salted caramel chocolate bar

1.4 Chocolate manufacturing Unit design overview

The chocolate production line is designed to produce 1000 chocolate bars per hour. The process begins with liquid chocolate being prepared and stored in a liquid chocolate vessel. The vessel takes the liquid chocolate feed and maintains it at 47 °C using an external water jacket, whilst being agitated via a paddle to avoid any hot or cold spots. The vessel was sized with the capability to carry 2 hours' worth of chocolate, to provide a buffer for upstream issues. This would require a capacity of 446kg of chocolate and a vessel volume of 0.42m³.

The tempering unit is essential in developing the final product's texture and flavour by ensuring the formation of the desired stable type V cocoa butter crystals. The correct crystallisation structure allows for the glossy appearance, smooth texture and characteristic snap that high quality chocolate provides. This is achieved through three cooling sections and two heating sections; the cooling section reduces the chocolate from 47 °C to 27 °C and a heating section reheats the chocolate to 30 °C at the exit of the tempering unit. The unit has impellers to provide shear stress which enhances nucleation of fat crystals. The temperer has a consistent flowrate of 223 kg/h with a residence time of 1 hour, a height of 0.55m and a diameter of 0.3m.

Around 20% of the chocolate then enters the Degrainer, a plate heat exchanger which helped maintain the efficiency of tempering process, through reheating the chocolate back up to 47°C and recycling it seamlessly back into the system without disrupting tempering flow.

Liquid chocolate that does not get recycled enters the depositor, where it is mixed with sea salt and caramel pieces via a helical ribbon agitator for 10 minutes with a constant rotational speed of 10 rpm. An agitator is used is due to the highly viscous non-Newtonian nature of liquid chocolate. The Tank is 0.525m in diameter and 0.525 m in height and requires a water-based

cooling jacket to keep the mixture at 30°C. The chocolate mixture is poured into moulds that have been preheated to match the temperature of the tempered chocolate. This is achieved using a mould heating unit that blows warm air over the moulds. It takes around 12 seconds for each mould to heat from 20°C to 29°C. The heater itself measures 0.48 m in width, 0.057 m in height, and 5.3 m in length.

The chocolate within its mould then enters a cooling tunnel via a conveyor belt, where chocolate is cooled and solidified into its optimal form and temperature for packaging. To match the required production rate, the conveyor belt moves at 0.5 m/s. The chocolate is cooled through air circulation gradually in order to ensure proper crystallisation. Gradual cooling is achieved through dividing the tunnel into three separate zones each with different cooling temperatures, residence times and air flowrates. The chocolate enters as a liquid at 30°C and exits at 19°C as a solid, ready for packaging. The tunnel has a total length of 14.53m, a height of 0.036m and a width of 0.368m.

The process also includes a water treatment setup, designed to clean the water used during equipment washing in the chocolate manufacturing plant, to make it pure enough to be safely discharged into the sewage or be reused as process water. The water treatment begins with a balance tank, which is responsible for evening out the flow and the concentration of the wastewater before the treatment begins, acting as a buffer and homogenising the flow. From there, the water moves to a cooling unit, that brings the temperature from 60°C down to 35°C, a suitable temperature for biological treatment to occur. Due to the acidic nature of wastewater, a neutralisation tank is required to control the pH before the water enters the anaerobic membrane bioreactor (aMBR), to protect the microbial culture. This is achieved by an addition of 1.23 L/hr of a caustic dose (sodium hydroxide) during normal operation, this raised the pH from 5 to 8.

The anaerobic membrane bioreactor reduces the concentration of organic contaminants through a combination of biological treatment and membrane filtration to remove organic pollutants by 95%, allowing for a safe discharge. The unit consists of a suspended hollow fibre ultrafiltration module contained in a 2 m³ glass lined stainless steel tank, 3.58 m in diameter and a height of 7.16 m. Methane is produced as a by-product in this process, so is captured and utilised for energy in a methane boiler. The methane boiler converts the biogas into thermal energy via combustion, producing 48.9 kWh of energy to be used on site.

1.5 Economic Viability

The chocolate was priced at £2.80; this was based on the price willing to pay from the participants in the market research. It also helps to ensure competitiveness within the market and maintain profitability. The product is sold through a distributor at £1.90, with a continuous production rate of 1,000 bars and hour, this gave an annual revenue of roughly £7.88 million.

The Capital expenditure (CAPEX) was calculated based on the cost of the major equipment, whilst other costs such as: buildings, structures, land, installation, instrumentation and control, piping, and electrical equipment were added as percentages of the base major equipment cost. Collectively, the total capital expenditure of the project was £8.81 million. The Operating

expenditure (OPEX) include both fixed costs like maintenance, labour and insurance, as well as variable costs such as packaging, raw materials and waste disposal. Based on these expenses, the annual operational expenditure was calculated to be £6,396,000.

Under the assumption that cocoa prices remain stable, the net present value was calculated, giving a payback time of 6 years, a return of investment of 83.3% and an annual rate of return of 4.2%. Indicating an economically viable project.

1.6 Responsible innovation

Both environmental sustainability and ethics have to be strongly considered when designing and operating food manufacturing processes. The project was designed to align with the UN Sustainable Development Goals, these include; Goal 6: Clean Water and Sanitation, Goal 11: Sustainable Cities and Communities, Goal 12: Responsible Consumption and Production, and Goal 13: Climate Action.

To address the environmental concern of excessive water usage, the Clean-in-Place (CIP) water was treated to remove organic pollutants and neutralise the pH within the water. This means that the water can either be safely discharged into the sewage or be reused as process water, hence reducing water wastage. Waste reduction initiatives are also implemented, the process incorporates a closed loop system that recycles 99% of all chocolate feedstock. This significantly reduces food waste and increases resource efficiency. Less feedstock waste also minimises greenhouse gas emissions, through reduced international shipping.

Ingredients are sourced sustainably and ethically from Fairtrade and Rainforest Alliance certified suppliers. This ensures local farmers are supported through fair wages as well as encourages responsible ecology and regenerative farming. This is key to both helping the welfare of farmers as well as limiting deforestation and carbon emissions, which are all major issues in the cocoa industry,

To increase energy efficiency, the plant captures and combusts methane biogas during wastewater treatment and uses it to generate 48.9kWh of energy. The cooling and heating requirements are also optimised in a strategy that to minimises unnecessary heat loss, saving another 27kWh. Both of these initiatives help reduce dependence on fossil fuels and improves overall energy efficiency, thus reducing the environmental impact.

Packaging was also chosen with sustainability in mind. Each chocolate bar is wrapped in biodegradable cellulose film rather than plastic. Due to the high production volume, considering the wrapping material is essential in reducing the impact of the process on the environment. Therefore, having a wrapper that can be recycled or degrade naturally will help the project align with its goals surrounding sustainability.

1.7 Unit Brief

Throughout the manufacturing process of chocolate, temperature control is an imperative factor when influencing the properties of the final product of the chocolate bar. This is especially true during the cooling stage, which is no exception to the precise temperature controls required to ensure the desired texture, structure and quality. A cooling tunnel is incorporated into the

process, it plays a critical role in making sure the chocolate solidifies into its optimal form for packaging under controlled conditions.

The cooling tunnel gradually reduces the temperature of the chocolate to avoid thermal shock. Since cocoa butter is a fat, it can crystallise in several different polymorphic structures, so if cooled too quickly or slowly incorrect crystallisation may occur. Rapid cooling increases the risk of forming unstable crystals which would interfere with the formation of the chocolate's desired texture, snap and gloss, instead resulting in a dull, brittle and inconsistent finish (Beckett, 2000). It also can result in fat bloom, where unstable cocoa butter crystals form on the surface of the chocolate, causing a white, greasy appearance (Kinta and Hatta, 2012). Prolonged cooling causes similar issues, as unstable crystals are allowed to develop over time. This also leads to fat bloom, as well as a range of other issues, such as soft, sticky texture with a weak snap (Tewkesbury, Stapley and Fryer, 2000). These textural and visual properties significantly influence the consumers experience of the chocolate, demonstrating the importance of precise and gradual cooling in chocolate manufacturing.

After deposition, the chocolate within moulds enters the cooling tunnel as a liquid at 30°C, via a conveyor belt. The purpose of the tunnel is to ensure the chocolate exits as a solid at 19°C, whilst having its required texture, consistency, quality and appearance. 19°C is chosen as the chocolate's exit temperature for packaging, as it is optimal for maintaining the carefully crafted properties and preventing defects. (Sensitech, 2023)

In order to provide the chocolate with the gradual cooling conditions required, the tunnel is split into multiple cooling zones, all with different temperature settings to ensure a controlled and consistent cooling process. The chocolate is cooled through air circulation, with compressors and fans. It is moved through the tunnel with conveyor belts that are powered by motors all moving at the same speed of 0.052 m/s. However, in each zone the air is circulated with different flowrates and at different temperatures, this variation allows for precise control. The air is cooled with a glycol cooling system, where a mixture of water and propylene glycol is used to create a cooling medium for the air. The flowing glycol mixture collects latent heat from the air before it comes in contact with the chocolate in the tunnel (ASHRAE Handbook, 2020).

1.8 Chemistry of chocolate

Controlling the temperature of the chocolate its formation is essential in achieving the desired characteristics. Chocolate in its liquid state is a suspension of cocoa butter and a range of different solids such as protein, sugars and cocoa solids. Both the solids and the cocoa butter play an important role in the final taste and structure. The size distribution of the solid particles impacts the grittiness, smaller particles contribute to a smoother texture, while larger ones can leave a rougher mouthfeel (Beckett, 2000).

Cocoa butter is a fat, mainly made up of molecules called triacylglycerols, these molecules are composed of three fatty acids: palmitic acid, stearic acid, and oleic acid with a glycerol backbone. The fatty acids can be arranged in different ways when they solidify, this can form

different solid structures of the fat molecules. The ability to form different solid structures during crystallisation is what makes cocoa butter highly polymorphic (Sato, 2018).

The cocoa butter can crystallise in six different polymorphic forms, these being: γ (Form I), α (Form II), β_{III} (Form III), β_{IV} (Form IV), β_V (Form V) and β_{VI} (Form VI) (Sato, 2018). The structures increase in thermal stability with their increasing number, shown by their increasing melting point in *Table 2.2.1*. Form I is the least thermodynamically stable, having the lowest melting temperature, Form VI is the most stable and has the highest melting point, but results in a sandy texture, so the V form is the desired structure chosen for chocolate. Form V crystal provides the ideal qualities of a glossy finish, firm snap, and smooth melting in the mouth. If lower forms of crystals are formed then fat bloom may occur (Beckett, 2000).

Vaeck	Wille and Lutton	Melting points (°C)
γ	I	17.3
α	II	23.3
β'	III	25.5
β'	IV	27.5
β	V	33.8
β	VI	36.3

Table 1.8.1 Cocoa butter polymorphic structures and their melting points (Sato, 2018)

Prior to cooling, chocolate undergoes pre-crystallisation in the tempering unit. A proportion of the form V crystals are created and act as the nuclei for further crystallisation in the cooling unit. The temperer then reheats the chocolate to around 30°C, where it melts the unstable crystals (forms I-IV) but keeps form V crystals (Staff, 2022).

The cooling unit maintains a gradual temperature gradient so the liquid cocoa butter begins to solidify, allowing for the pre-formed stable form V crystals to fully form. As the chocolate cools, the crystals grow and lock into a solid structure.

2 Unit Design

2.1 Initial Shortcut Design

An initial design was done on the cooling tunnel through short cut design within the group project. The group project involved the design of the entire chocolate manufacturing and water treatment process, therefore designing each component in detail would be overly extensive and impractical. Instead, shortcut design and assumptions were used to develop a conceptual framework for the overall process, where the design of each component was comprehensive enough to integrate into the overall process. This approach enabled the team to efficiently design numerous critical components without excessive complexity. However, this method required a range of assumptions that would not necessarily be feasible in practical application.

A more rigorous design with limited assumptions is required to ensure performance accuracy of the cooling tunnel.

Shortcut design relies on approximations and assumptions rather than rigorous calculations. In a practical setting precision is imperative, so relying on estimations could result in mechanical, electrical and process failures. Without detailed design, fluctuations in process conditions such as variations in temperatures, throughput or humidity may not be accounted for. If there are no considerations in the system to deal with the variations then the process's performance will be inconsistent and ineffective.

The short cut design includes three different zones, each zone contains different air flow temperatures and air flowrates. Splitting the tunnel into different zones, allows for gradual cooling.

- Zone 1: Liquid chocolate exits the depositor at 30°C. The first zone allows for chocolate to stabilise, without forming large unwanted crystals. Most of the latent heat of crystallisation is also removed at this stage. The air temperature is at 21°C and results in the chocolate exiting at 25°C.
- Zone 2: This is the zone where the chocolate is solidifies and where most of the specific heat is removed. The chocolate enters at 25°C and is cooled to 20°C via air of 14.5°C . It is also where the formation of the desired cocoa butter crystals (Form V) occurs.
- Zone 3: The chocolate leaves the previous zone at 20°C and is stabilised in the final cooling zone. Cooling air of 18.5°C is used to refine the chocolate to have optimal packing properties, as it is brought down to 19°C. The slower controlled cooling helps stabilise the crystals.

2.1.1 Calculation Check

The time required for cooling is calculated through *Equation 2.3.1* below, derived in *Appendix section 1* and the results are in *Table 2.1.1.1*.

$$t = \ln \left(\frac{T_{choc} - T_{air}}{T_0 - T_{air}} \right) \times \frac{\dot{m} C p_{choc}}{-hA}$$

Equation 2.1.1.1

Where t is the time required for cooling (measured in s), T_{choc} is the bulk temperature of the chocolate, T_{air} is the temperature of the cooling air and T_0 is the initial chocolate temperature (30°C), all the temperatures are in °C. \dot{m} is the mass flowrate and stays constant at 3 kg/s in order to reach the required production rate, h is the convective heat transfer coefficient of air (W/m² °C) and A is the area of chocolate exposed to air (m²).

	Zone 1	Zone 2	Zone 3
$T_{chocolate}$ [°C]	25	20	19
T_{air} [°C]	21	14.5	18.5

T_0 [°C]	30	25	20
Time [s]	354.61	282.76	480.42

Table 2.1.1.1

The conveyor speed (m/s) was calculated via

$$v_{Conveyor} = (L_{bar} + d_{gap}) \times \dot{b}$$

Equation 2.1.1.2

Where L_{bar} (m) is the length of each bar and d_{gap} (m) is the space between each bar. This was multiplied by the production rate, \dot{b} (bars/min).

With this the dimensions of the tunnel could be calculated.

$$L_{tunnel} = \frac{t \times v_{Conveyor}}{N_{bar}}$$

Equation 2.1.1.3

The equation above calculates the length required (m) for the tunnel, where $N_{bar,l}$ is the number of bars per row. In the mould used there were 4 bars per row.

The number of bars in each row and line within the mould is shown below, *Figure 2.1.1.1* also shows how the mould would fit onto the conveyor belt.

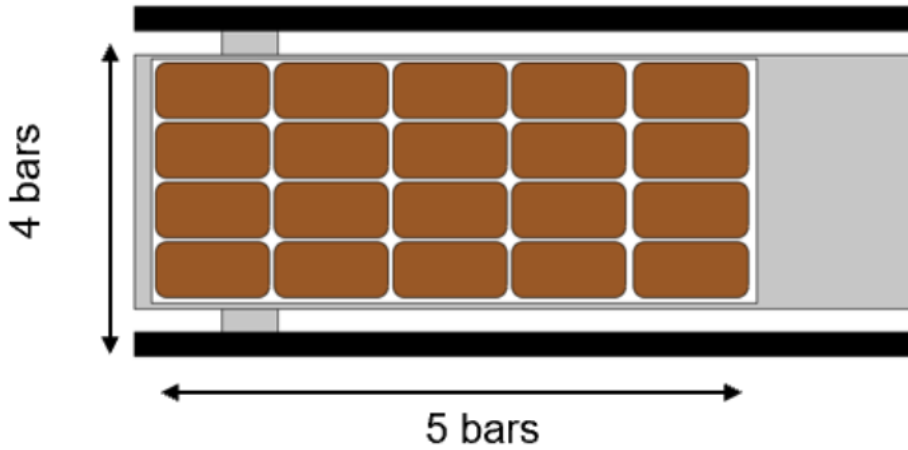


Figure 2.1.1.1

The required width of the tunnel (m) was subsequently calculated.

$$W_{Tunnel} = (W_{bar} \times N_{bar}) + d_{gap}$$

Equation 2.1.1.4

Where W_{bar} is the width of each bar and N_{bar} is 4 bars.

The height of the tunnel is calculated to be 3 times the height of the chocolate bar, this is based on industry standards to allow sufficient height for convective currents (ASHRAE Handbook, 2020).

$$H_{Tunnel} = H_{Bar} \times 3$$

Equation 2.1.1.5

Where H_{Bar} is the height of the bar (m).

The total dimensions of the cooling tunnel are 14.53 m x 0.368 m x 0.036 m. Given a wall thickness of 0.01 m, the inner dimensions of the cooling tunnel are 14.51 m x 0.345 m x 0.016 m. Therefore, the inner surface is of the tunnel can then be calculated to be 10.58 m².

A glycol cooling system is used to create a cooling medium for the air before it comes in contact with the chocolate. Once the air is cooled by the glycol, it will be distributed around the cooling tunnel via 3 different compressor blowers.

The mass and volumetric flowrates of the cooling air are given by *Equation 2.1.1.6* and *Equation 2.1.1.7* respectively.

$$\dot{m}_{air} = \frac{Q}{C_{p_{air}} \times \Delta T}$$

Equation 2.1.1.6

The mass flow rate, \dot{m}_{air} of each compressor (kg/s) is calculated based of the heat removed from the chocolate, Q at each stage (W), the specific heat capacity of air, $C_{p_{air}}$ (J/kg°C) and the difference in temperature, ΔT between the cooling air and the atmospheric air (°C).

$$\dot{V} = \frac{\dot{m}}{\rho}$$

Equation 2.1.1.7

The mass flowrate was then divided through by the density of air, ρ (kg/m³) to get the volumetric flow rate, \dot{V} (m³).

Turbulent flow is required to ensure consistent and effective cooling (New Food Magazine, 2017), to determine if the flow is turbulent *Equation 2.1.1.8* is used.

$$Re = \frac{\rho_{air} v_{air} L_c}{\mu_{air}}$$

Equation 2.1.1.8

Where v_{air} is the velocity of the air assumed to be 5 m/s. Turbulent flow can occur at velocities of 5m/s, any higher than that provides little advantage, (New Food Magazine, 2017). The ρ_{air} is the density of the air, which is assumed to be constant at 1.212 kg/m³. The μ is the dynamic viscosity of air, which is also assumed to be constant at 1.803×10^{-5} Pa.s. The L_c is the characteristic length, equivalent to the diameter, D of the pipe which is calculated below.

To find the diameter of the pipe (m), *Equation 2.1.1.9* is used

$$D = \sqrt{\frac{4 \times \dot{V}}{\pi \times v_{air}}}$$

Equation 2.1.1.9

The required length to cool 4 bars per row is 14.53m, instead of having one long segment, the conveyor can be split into a ‘U-Turn’ system, which consists of 3 belt systems. The different belts are aligned and meet each other in a synchronised manner to ensure smooth material transfer and a precise transfer point. Each segment will have their required length and air-cooling temperature that relates to each section of gradual cooling process. This will optimise the shape and reduce the overall footprint area, the shortcut optimised design is shown in *Figure 2.1.1.2* and the calculated parameters in *Table 2.1.1.2*.

	Zone 1	Zone 2	Zone 3
Mass Flowrate [kg s⁻¹]	0.746	0.284	0.092
Volumetric Flowrate [m³ h⁻¹]	2192.4	790.72	255.6
Pipe diameter [m]	0.360	0.237	0.134
Re	132,400	39,780	22,520
Fluid type	Turbulent	Turbulent	Turbulent

Table 2.1.1.2

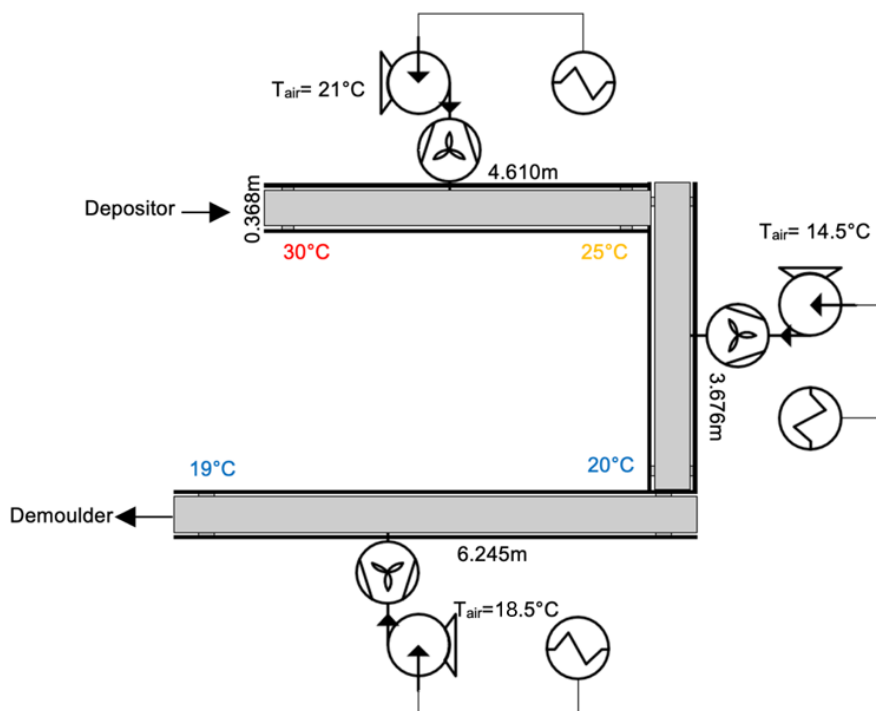


Figure 2.1.1.2

2.1.2 Shortcut Energy Balance

The overall energy balance is given by the difference between the energy inputs and outputs.

$$\text{Energy Variation} = \text{Energy inputs} - \text{Energy Outputs}$$

Where:

$$\text{Energy inputs} = \text{Energy required by the Conveyor Motor} + \text{Energy Required by the Fans} + \text{Heat removed from the chocolate}$$

$$\text{Energy outputs} = \text{Heat removed from the chocolate} + \text{Heat lost due to the environment}$$

Firstly, the **Energy Inputs** are calculated, starting with the mechanical energy required.

The power required for the conveyor belts is given by *Equation 2.1.2.1*.

$$P_{motor} = \frac{F v_{conveyor}}{\eta_{motor}}$$

Equation 2.1.2.1

The efficiency, η is assumed to be 0.8, this is based on industry standards (Demirel, 2018). $v_{conveyor}$ is the conveyor belt speed (m/s) and F is the force required to move the belt, this is the frictional force and is calculated below in *Equation 2.1.2.2*.

$$F = \mu W g$$

Equation 2.1.2.2

The friction coefficient (μ) is assumed to be 0.3, this based on common materials used in industry (Iso.org, 2024). W is the weight of the conveyor belt and its contents (Calculated in *Appendix 1*).

There are three fans used in the cooling tunnel. To calculate the power requirement for one fan, $P(W)$, *Equation 2.1.2.3* is used

$$P = \frac{\Delta P * \dot{V}}{\eta_{fan}}$$

Equation 2.1.2.3

\dot{V} is the volumetric flow rate of air in m^3/s (previously calculated) and η_{fan} is the efficiency of the fan, assumed to be 0.7 (Sntoom.net, 2024). The pressure drop ΔP is measured Pa and is given by the Hagen Poiseuille equation, *Equation 2.1.2.4*.

$$\Delta P = \frac{8\mu_{air}L_{pipe}\dot{V}}{\pi R^2}$$

Equation 2.1.2.4

Where L_{pipe} is the length of the pipe (m) and R is the radius of the pipe (m).

Once the mechanical energy input was calculated, the energy inputs surrounding the heat of chocolate was calculated.

Warm chocolate enters the cooling tunnel with thermal energy that needs to be removed for the chocolate to solidify. The heat removed, Q is measured in W and given by 2.1.2.5.

$$Q_{removed} = \dot{m}Cp_{choc}\Delta T$$

Equation 2.1.2.5

Where \dot{m} is the mass flowrate of chocolate going through the system and the specific capacity of chocolate used, Cp_{choc} (W/m² °C), ΔT is the difference in temperature between the inlet and outlet of the chocolate in each section (°C).

Next, the **Energy Outputs** are calculated.

Energy losses, Q_{loss} (W) via tunnel walls to external surroundings is found using Equation 2.1.2.6.

$$Q_{loss} = hA_{Tunnel}\Delta T$$

Equation 2.1.2.6

Where A_{Tunnel} is the surface area of the tunnel exposed to the environment. The heat transfer coefficient, h , is assumed to be 50 W m² K⁻¹ for all the walls in the tunnel. ΔT is the difference in temperature between the cooling air and the ambient air.

The thermal energy extracted by the cooling air is given by Equation 2.1.2.7.

$$Q = \dot{m}_{air}Cp_{choc}\Delta T$$

Equation 2.1.2.7

Where ΔT is the difference in temperature (°C) between the cooling air and the inlet let chocolate at each section.

The results of the energy inputs and outputs are shown in Table 2.1.2.1 and Table 2.1.2.2 respectively.

Energy Inputs			
	Zone 1	Zone 2	Zone 3
Pressure change, ΔP [Pa]	3.6 x 10 ⁻³	3.6 x 10 ⁻³	3.63 x 10 ⁻³
Air volumetric flowrate, \dot{V} [m³ s⁻¹]	0.609	0.220	0.071
Fan Power [W]	3.1 x 10 ⁻³	1.13 x 10 ⁻³	3.7 x 10 ⁻⁴
Total Conveyor Belt Force [N]	344.83		
Total Conveyor Motor Power [W]	22.41		
Heat Removed from Chocolate [W]	30000	30000	6000
Total Energy Input [W]	66,022.42		

Table 2.1.2.1

Energy Outputs			
	Zone 1	Zone 2	Zone 3
Thermal Energy Extracted By Air [W]	3001.9	2999.9	601.59
Surface Area [m²]	3.36	2.68	4.56
Heat Energy lost to environment [W]	672	1407	1482
Total Energy Output [W]	10,164.38		

Table 2.1.2.2

This concludes the shortcut design. Due to the extensive nature of the overall group report a lot of assumptions were made to simplify the design. Whilst the calculations provide an initial understanding there was not enough time to employ rigorous calculations, providing a lot of scope for criticism.

- Cp is initially assumed to be constant, however in practice this will vary with temperature so needs to be considered when calculating heat energies and cooling times.
- Dynamic viscosity is also assumed to be constant and will also vary with temperature. This will lead to inaccuracies when calculating pressure drop and Reynolds number which would compromise the accuracy of the fan power.
- Air density is assumed to be constant when calculating flow rates and pressure drops. However, it varies with temperature, humidity and pressure so therefore variations need to be considered in a more rigorous calculation.
- The shortcut design assumes consistent cooling within the chocolate bar uses the value of the surface of the bar. However, due to non-uniform cooling the surface will cool faster than the core, due to the direct contact with air. Chocolate has a low thermal conductivity so heat will transfer slowly to the core, this will result in an underestimated required cooling time. Therefore, more comprehensive heat transfer models need to be used.
- The airflow behaviour in the cooling tunnel was oversimplified. The design assumes uniform air velocity and perfect mixing of air in each tunnel section. In reality airflow would be uneven due to eddies and boundary layers, this would result in inconsistent cooling of chocolate. Computational fluid dynamic needs to be employed to decide upon the properties of the fluid flow.
- The heat transfer coefficients are approximated at a constant value for both the chocolate and the tunnel walls. In reality it will vary with air velocity, turbulence and surface geometry. Overestimations will predict faster cooling (undercooled chocolate) and underestimation will extend the cooling time unnecessarily resulting in a brittle chocolate.

- Power calculations also use of assumptions and chosen values, such as chosen motor efficiencies and friction coefficients which may not reflect real world conditions. These inaccuracies can affect the accuracy of system performance.

2.2 Rigorous design

The process includes equipment that was selected to ensure efficiency, reliability and effectiveness. This would be a multi-zone tunnel, with different air temperatures and airflows to ensure the chocolate cools at a controlled rate. Chocolate is transported in a mould with a conveyor belt system, which is surrounded by tunnel walls to keep the air in. Fans and ducts are utilised to distribute the airflow with a refrigeration unit to cool the air before it reaches the fan, this provides uniform airflow at a uniform temperature to help ideal product formation.

Alternatives to a conveyor-based cooling tunnel include batch cooling chambers and spiral cooling systems. Batch chambers work through sequentially placing liquid chocolate in a refrigerated room (Vantagehouse.com, 2024). This however lacks the efficiency and large-scale production potential that a conveyor belt offers. Spiral systems offer the benefit of saving floor space, however it does not offer the precise cooling conditions that is needed for optimal chocolate properties due to the complexity of the dimensions.

To improve upon the shortcut design, discretisation was used to develop a more gradual temperature profile, to allow for stepwise thermal analysis. The continuous system was divided into a different section, at which the temperature of the chocolate was calculated. This allowed for a more precise estimation of how heat is transferred over time. The variables used were also individually calculated at each stage based on the conditions at each instantaneous moment, whereas in the shortcut design they were assumed to be constant throughout.

2.2.1 Dynamic variable adjustment

In practice data for both air and chocolate properties will vary based on temperature, since the process has varying temperatures, polynomials are used to calculate these properties at each instantaneous moment, thus improving the accuracy of the overall temperature profile. These polynomials were based on empirical data, (Zografos, Martin and Sunderland, 1987).

Each zone tunnel was discretised into 4 sections, therefore there was a total of 12 sections. The residence time was divided equally within each segment and the mass flowrate remained constant. The temperature dependent chocolate properties were calculated via empirical polynomials.

The Specific Heat Capacity of chocolate (Cp_C) is temperature dependent. Calculating the dynamic thermal behaviour of chocolate during cooling allows the model to capture subtle changes in energy storage across the different zones. As with most food materials, the specific heat capacity of chocolate increases with temperature, shown in *Equation 2.2.1.1*.

$$Cp_C = 1.7778T_C + 1563.33$$

Equation 2.2.1.1

Where T_C is the temperature of chocolate surface

A temperature dependent polynomial was applied to model the density of chocolate (ρ_C), density tends to increase during cooling in a non-linear manner.

$$\rho_C = 7.98 \times 10^{-7} T_C^3 - 4.44 \times 10^{-5} T_C^2 - 2.15 \times 10^{-3} T_C + 1.19$$

Equation 2.2.1.2

Thermal conductivity (k_C) was also modelled with a temperature dependent polynomial to show the chocolate's ability to conduct heat changes with temperature. As temperature decreases, the structure of the cocoa butter becomes more ordered, thus increases the efficiency of conduction.

$$k_C = -0.3326805 + 6.4 \times 10^{-2} T_C - 2.1587 \times 10^{-3} T_C^2 + 2.32 \times 10^{-5} T_C^3$$

Equation 2.2.1.3

These would be used to calculate the heat transfer via conduction inside the chocolate

$$Q_{Conduction} = -k \times A \times \frac{(T_c - T_{air})}{dx}$$

Equation 2.2.1.4

Where A is the area of the top layer of the chocolate exposed in each zone of the tunnel (m^2) and dx is the distance over which conduction is considered (m).

The heat transfer of air and thus the dynamic properties air also need to be considered. The specific heat capacity of air (Cp_A) increases with temperature. In a similar manner to chocolate, additional energy is required to raise the temperature of air as the kinetic energy increases.

$$Cp_A = 1.386 \times 10^{-13} T_C^4 - 6.474 \times 10^{-10} T_C^3 + 1.023 \times 10^{-6} T_C^2 - 4.328 \times 10^{-4} T_C + 1.0613$$

Equation 2.2.1.5

Where T_A is the temperature of the inlet air

The dynamic viscosity (μ_A) is the air's resistance to flow, it also increases with temperature, this is due to increased molecular activity affecting the flow. Calculating the dynamic viscosity will help determine whether the airflow in the cooling tunnel is laminar or turbulent.

$$\mu_A = 2.5914 \times 10^{-15} T_C^3 - 1.4346 \times 10^{-11} T_C^2 + 5.0523 \times 10^{-8} T_C + 4.113 \times 10^{-6} T_C$$

Equation 2.2.1.6

The thermal conductivity of air (k_A) also varies with temperature, generally increasing as molecular collisions become more frequent at higher temperatures, thus increasing the rate of heat transfer. This directly impacts how effectively heat moves from the air to the chocolate.

$$k_A = 1.5797 \times 10^{-17} T_A^5 + 9.46 \times 10^{-14} T_A^4 + 2.2012 \times 10^{-10} T_A^3 - 2.3758 \times 10^{-7} T_A^2 + 1.7082 \times 10^{-4} T_A - 7.488 \times 10^{-3}$$

Equation 2.2.1.7

These properties were used to calculate the Prandtl number of air (Pr), which defines the ratio of momentum diffusivity to thermal diffusivity in a fluid. Pr is used to determine how effectively heat is being drawn from the surface of the chocolate.

$$Pr = \frac{\mu_A \times Cp_A}{k_A}$$

Equation 2.2.1.8

Reynolds number (Re), another key dimensionless number, is also highly relevant to heat transfer of air. It determines the flow regime of air (either laminar or turbulent). A high Re indicates turbulent flow, which is desired for effective heat transfer.

$$Re = \frac{\rho_A \times v_A \times d_T}{\mu_A}$$

Equation 2.2.1.9

Where d_T is the characteristic length (hydraulic diameter) of the cooling tunnel, this is calculated to be 0.06558m. v_A is the velocity of the inlet cooling air, set to be constant at 5 m/s.

ρ_A is the density of air, this is dynamic and varies with temperature, so can be calculated through the following equation.

$$\rho_A = \frac{345.57}{T_A - 2.6884}$$

Equation 2.2.1.10

The final dimensionless number used is the Nusselt Number (Nu), which describes the relative contribution of convection to the total heat transfer. A high Nusselt number indicates efficient cooling.

$$Nu = 0.023 \times Re^{0.8} \times Pr^{0.4}$$

Equation 2.2.1.11

The convective heat transfer coefficient (h) quantifies the rate of heat transfer between the solid surface of the chocolate and the cooling air. It directly indicates how fast the chocolate loses heat.

$$h = \frac{Nu \times k_A}{d_T}$$

Equation 2.2.1.12

The overall heat transfer coefficient (U) represents the combined effect of both convection and conduction to heat transfer.

$$\frac{1}{U} = \frac{1}{h} + \frac{dx}{k_c}$$

Equation 2.2.1.13

2.2.2 Surface Temperature Analysis

Firstly, the surface temperature of the chocolate was calculated, this would be heavily influenced by convection, however the point of temperature that was calculated was at 1mm into the chocolate ($dx = 0.001$), so conduction still had to be included. The rest of the internal chocolate temperature would be calculated via conduction finite difference analysis later on.

A differential equation is found that describes the rate of temperature change, however it is not sufficient to predict the temperature of the chocolate at specific times. It does not give the explicit temperature values at any given point, just the rate and direction of the temperature change.

$$\frac{dT}{dt} = \frac{U \times A \times (T_A - T_C)}{\dot{m} \times Cp_A}$$

Equation 2.2.2.1

To go from the rate of change to the actual temperature values, the differential equation needs to be integrated with respect to time. This will allow for predictive analysis for the surface temperature as a function of time, giving an outlet temperature for the chocolate in each segment. The derivation can be found in *Appendix 2*.

$$T_{C,out} = T_A + (T_C - T_A) \times e^{-\frac{U \times A \times \Delta t}{\dot{m} \times Cp}}$$

Equation 2.2.2.2

This can be plotted against the cumulative residence time to get a gradual temperature profile, showing the temperature of the chocolate at each segment in the cooling tunnel.

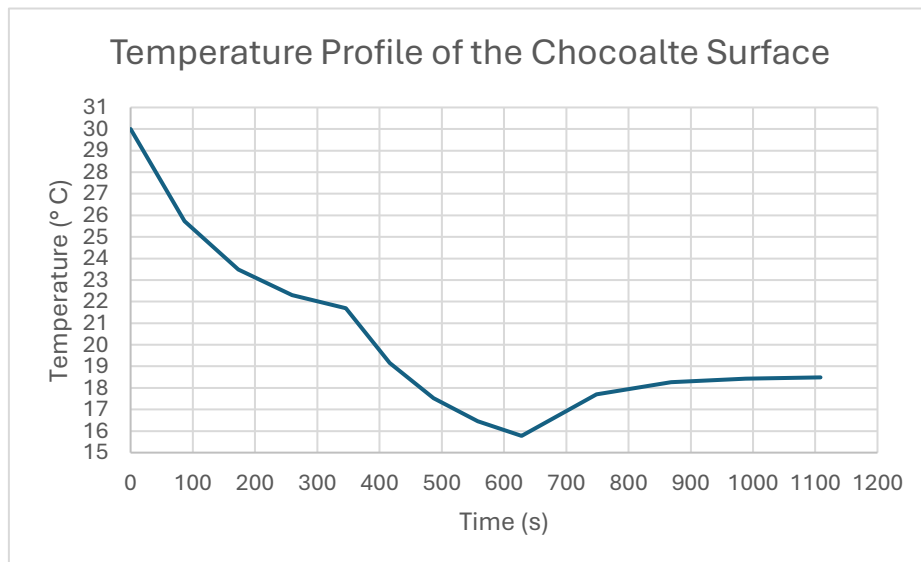


Figure 2.2.2.1

The chocolate starts at 30°C as it enters the tunnel in liquid form. There is then a sudden drop in temperature as the surface is initially exposed to the 21°C air, due to the relatively large difference heat is rapidly lost from the surface to the cooler environment. This cooling continues until the surface of the chocolate reaches a minimum just below 16°C. At this point there is a slight raise in temperature and then stabilises at 19°C, the desired temperature for storage and transport.

The mould which houses the chocolate is preheated to match the temperature of the deposited chocolate, this is done to prevent damage to the chocolate's crystallisation structure. If the moulds are too cold, the chocolate might stick onto the surface, on the contrary, if the moulds are too hot then the chocolate might lose its temper and the formation of the stable *type V* crystals will be compromised. Polycarbonate was the selected mould material, due to its optimal physical qualities including; high temperature resistance, durability and non-reactive nature (FOW Mould, 2022). The Mould dimensions are L: 93.7 cm, W:32.8 cm, H: 2.6 cm and the mass of the mould is 5.76 kg. The area of the base of the mould is 0.343m³, this is the interface that will be considered for heat exchange.

To calculate the heat transfer for the mould, the properties of polycarbonate used vary with temperature, just like with chocolate. They can be calculated using polynomials made from experimental data (Fsri.org, 2025).

The specific heat capacity (Cp_M), where T_M is the mould temperature:

$$Cp_M = -0.0025T_M^2 + 4.255T_M + 1097.75$$

Equation 2.2.2.3

The density (ρ_M), where ρ_0 is the reference density (1200 kg/m³), T_0 is the reference temperature (25°C) and β is the volume expansion coefficient ($195 \times 10^{-6} \text{ } ^\circ\text{C}^{-1}$).

$$\rho_M = \frac{\rho_0}{1 + \beta(T_M - T_0)}$$

Equation 2.2.2.4

The thermal conductivity (k_M) is calculated with data from

$$k_M = -7.58 \times 10^{-7}T_M^2 + 8.33 \times 10^{-5}T_M + 0.2303$$

Equation 2.2.2.5

These variables were used in *Equation 2.2.2.2* for predictive analysis for the surface temperature of the mould as a function of time, giving an outlet temperature for the chocolate in each segment. Shown in the figure below.

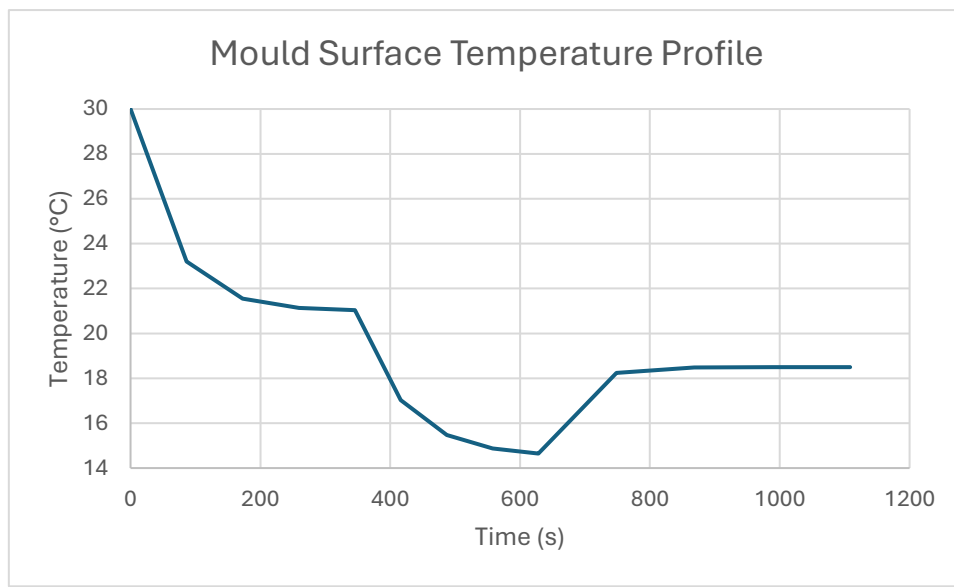


Figure 2.2.2.2

2.2.3 Internal Temperature Analysis

Conduction is the mechanism for heat transfer within the chocolate bar. When checking to ensure proper cooling it is not sufficient to only consider the surface temperature of the chocolate. The chocolate will have a temperature distribution within the bulk of the bar.

The general heat conduction equation (based on energy conservation) describes the change of heat flow with distance and time, for a flat slab it is given by the following equation. (Rodgers, 2013).

$$\frac{\partial}{\partial x} \left(k_c \frac{\partial T}{\partial x} \right) + g = \rho_c c p_c \frac{\partial T(x, t)}{\partial t}$$

Equation 2.2.3.1

Where T (measured in °C) is the temperature, as a function of distance x (measured in m) and time t (measured in s). g is the internal heat generation (measured in w/m³), since this = 0, it can be cancelled out. The equation is then rearranged to get the 1D unsteady heat conduction equation, which will model how chocolate cools over time.

$$\frac{\partial T}{\partial t} = \alpha \frac{\partial^2 T}{\partial x^2}$$

$$\text{Where } \alpha = \frac{k_c}{\rho_c c p_c}$$

Equation 2.2.3.2

The equation is a partial differential and thus is too complex to solve analytically, so the finite difference method is used. It approximates the continuous derivative by discretising the points and gathering the temperature at each stage.

Only the heat transfer in the y-direction was modelled, this is because the thickness of the bar is the shortest dimension, so will complete the heat transfer first. Once the heat transfer in the y direction is complete, then it is safe to assume the chocolate has cooled to the required temperature across the whole bar, as shown below.

The conveyor surface beneath the mould is made from a highly porous mesh with holes which air can freely pass through, therefore the cooling air reaches the mould base freely and heat transfer is modelled accordingly.

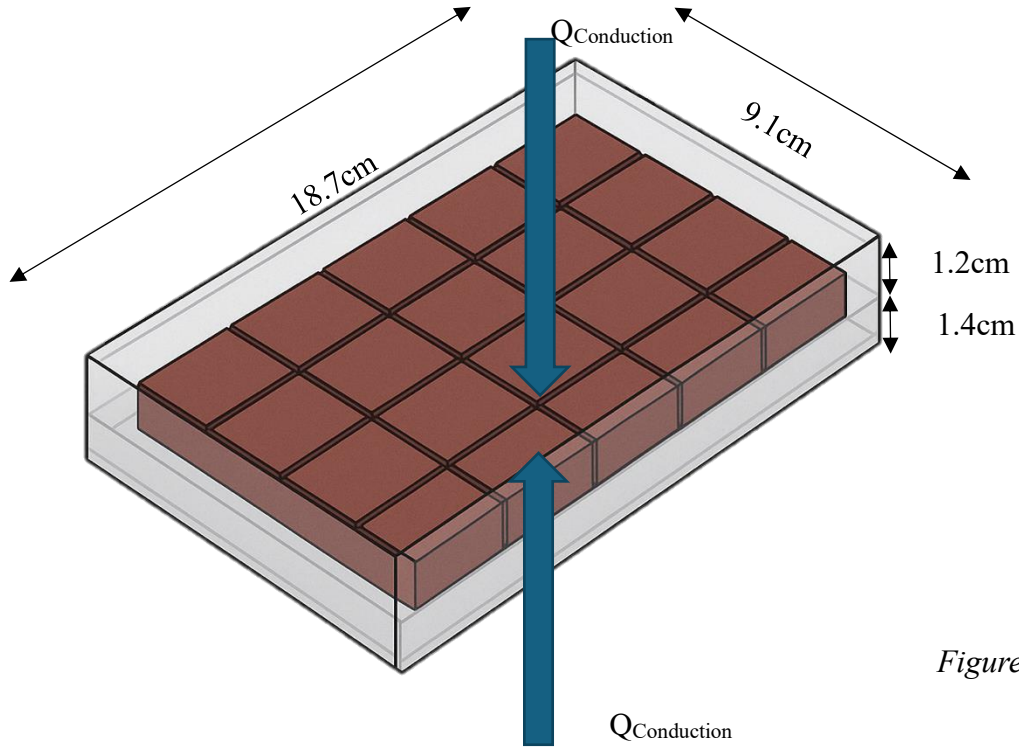


Figure 2.2.3.1

The figure above shows one bar of chocolate in its respective mould, the dimensions in the figure are the dimensions of the bar added to the thicknesses of the mould on each side. When all the dimensions of the chocolate in the mould are considered, it is clear to see the shortest distance for conduction to occur in is the thickness, the y direction. Therefore, the conduction in the y direction would be completed first. So, when the conduction is being modelled, it is only necessary to consider the y direction.

The temperature changes with both time and distance. The partial derivative in the 1D heat conduction equation were approximated by using a difference in both time and distance. Both time and distance need to be discretised, the thickness of the bar is 1.2cm, so the chocolate bar is divided up into 12 points of 1 mm each. The time spent cooling is discretised into 1 second intervals, for an accurate model.

The time derivative is given by the forward difference approximation:

$$\frac{\partial T}{\partial t} \approx \frac{T_i^{n+1} - T_i^n}{\Delta t}$$

Equation 2.2.3.3

Where T_i^n is the temperature at distance i at time n. T_i^{n+1} is the temperature in the same position, i at the next time interval. The time interval, Δt is 1s.

The distance derivative is given by the central difference approximation:

$$\frac{\partial^2 T}{\partial x^2} \approx \frac{T_{i+1}^n - 2T_i^n + T_{i-1}^n}{\Delta x^2}$$

Equation 2.2.3.4

Where T_{i+1}^n is the temperature at the next distance interval and T_{i-1}^n is the temperature at the previous distance interval. The distance interval, Δx is 1mm.

These two can be equated to each other in the original heat conduction equation (derivation found in *Appendix Section 3*) to give:

$$T_i^{n+1} = T_i^n + \frac{\alpha \Delta t}{\Delta x^2} (T_{i+1}^n - 2T_i^n + T_{i-1}^n)$$

Equation 2.2.3.5

For the finite difference method boundary conditions are required for providing information to define the how the model behaves at its edges. The initial condition, which we know already is that the chocolate enters the tunnel at around 30°C. In a well-mixed liquid chocolate, there will be an internal temperature variation of $\pm 0.4^\circ\text{C}$, (Dreger, 2014). The other boundary condition is the surface temperature of the chocolate, which was previously calculated.

Initial Condition: At $t=0$, the whole chocolate bar is around 30°C.

Distance (mm)	1	2	3	4	5	6	7	8	9	10	11	12
Temperature (°C)	29.6	29.6	29.65	29.7	29.75	29.8	29.85	29.9	29.95	30	30.1	30.2

Table 2.2.3.1

Boundary Condition: At $x=1$, the temperature of the layer just beneath the surface has been calculated previously.

Time (s)	0	100	200	300	400	500	600	700	800	900	1000	1100
Temperature (°C)	30	25.3	23.0	22.2	19.7	17.3	15.9	16.8	18.1	18.3	18.5	18.5

Table 2.2.3.2

The interface at which the chocolate and mould came in contact also was considered, therefore the conduction of the mould also had to be considered. This meant that there was one overall system where each point would use the temperature from its same location in the previous time, as well in the forwards and backwards position, in order to predict the current temperature in that certain location. This calculation was done on Microsoft Excel, each cell would gather information from the cells around it in order to predict the next temperature iteration, an example of a section from the first, middle, and last few rows can be found below. Each cell uses *Equation 2.2.3.5*.

		Using Equation 2.2.5.3.																											
		Mould														Chocolate													
		1	2	3	4	5	6	7	8	9	10	11	12	13	14	Interface	12	11	10	9	8	7	6	5	4	3	2	1	
Time[s]	0	30	29.6	29.65	29.7	29.75	29.8	29.85	29.9	29.95	30	30.1	30.2	30.12	30.16	30.2	30.2	30.1	30	29.95	29.9	29.85	29.8	29.75	29.7	29.65	29.6	29.6	
	1	29.87204	29.67356	29.65	29.7	29.75	29.8	29.85	29.9	29.95	30.00817	30.1	30.17058	30.13962	30.16	30.19346	30.18554	30.1	30.100723	29.95	29.9	29.85	29.8	29.75	29.7	29.65	29.60723	29.9337	
	2	29.74546	29.70215	29.66202	29.7	29.75	29.8	29.85	29.9	29.95134	30.01367	30.09653	30.15398	30.14801	30.16214	30.1867	30.17432	30.09896	30.01237	29.95104	29.9	29.85	29.8	29.75	29.7	29.65104	29.6606	29.86786	
	3	29.62027	29.70267	29.67479	29.70197	29.75	29.8	29.85	29.90022	29.95313	30.01703	30.09237	30.14361	30.15129	30.16384	30.18066	30.16522	30.09733	30.01602	29.95253	29.90015	29.85	29.8	29.75	29.70015	29.6595	29.68918	29.80248	
	4	29.49645	29.68464	29.68379	29.70538	29.75032	29.8	29.85004	29.90066	29.95493	30.0189	30.08843	30.13649	30.15209	30.16454	30.17539	30.15764	30.09539	30.0186	29.95414	29.90047	29.85002	29.8	29.75002	29.70148	29.66967	29.70127	29.73755	
	5	29.37399	29.65374	29.68746	29.70919	29.75109	29.80006	29.85013	29.90126	29.95651	30.01981	30.08492	30.13119	30.15158	30.16428	30.17071	30.15121	30.09329	30.02038	29.9557	29.90094	29.85008	29.80001	29.75023	29.7039	29.67883	29.70194	29.67308	
	6	29.25288	29.61352	29.6855	29.71249	29.75225	29.80004	29.85003	29.90193	29.95783	30.02011	30.08184	30.12696	30.15082	30.16325	30.16647	30.14565	30.09112	30.02157	29.95713	29.9015	29.8502	29.80005	29.75073	29.70697	29.6858	29.69443	29.69005	
	7	29.13313	29.56634	29.67815	29.71458	29.75359	29.80058	29.85056	29.90263	29.95887	30.02002	30.07913	30.1234	30.14861	30.16167	30.16254	30.14078	30.08895	30.02231	29.9584	29.90213	29.85036	29.80017	29.75153	29.71024	29.69011	29.68084	29.54547	
	8	29.01471	29.5138	29.66583	29.715	29.7549	29.80107	29.8509	29.90331	29.95967	30.01968	30.0767	30.12029	30.14663	30.15968	30.15884	30.13643	30.08681	30.0227	29.95951	29.90278	29.85059	29.80039	29.75259	29.7133	29.69168	29.66261	29.48234	
	9	28.89762	29.45707	29.64901	29.71348	29.75592	29.80167	29.85132	29.90396	29.96027	30.01919	30.07451	30.11747	30.14445	30.15741	30.15532	30.1325	30.08472	30.02283	29.96044	29.90344	29.85088	29.80074	29.75382	29.71585	29.6906	29.64076	29.41966	
	10	28.78185	29.397	29.62818	29.70988	29.75646	29.80231	29.85181	29.90456	29.9607	30.0186	30.07249	30.11486	30.14216	30.15495	30.15193	30.12889	30.08268	30.02276	29.96122	29.90408	29.85123	29.80121	29.75512	29.71769	29.68705	29.616	29.35741	
	11	28.6674	29.33423	29.60374	29.70414	29.75634	29.8029	29.85234	29.90511	29.96099	30.01795	30.0706	30.11239	30.13979	30.15236	30.14866	30.12554	30.0807	30.02253	29.96186	29.9047	29.85164	29.80177	29.75637	29.71867	29.68121	29.5889	29.2956	
	12	28.55426	29.26929	29.5761	29.69626	29.75542	29.80337	29.85289	29.90562	29.96116	30.01724	30.06883	30.11004	30.13736	30.1497	30.14548	30.1224	30.07877	30.02216	29.96236	29.90529	29.8521	29.80242	29.75748	29.7187	29.67328	29.55984	29.23423	

548	14.97188	16.25734	17.47751	18.62289	19.6844	20.65414	21.52595	22.29552	22.9604	23.51972	23.97381	24.3238	24.57121	24.71753	24.76398	24.71129	24.54669	24.26963	23.87904	23.37354	22.75182	22.01301	21.15708	20.18509	19.0994	17.9036	16.60218
549	14.96262	16.24667	17.46528	18.60918	19.6694	20.63813	21.50924	22.27841	22.94315	23.50252	23.95679	24.30703	24.55468	24.7012	24.74777	24.69511	24.53043	24.25322	23.86243	23.35674	22.73489	21.99608	21.1403	20.16865	19.08348	17.88833	16.5876
550	14.9533	16.23597	17.45307	18.59595	19.65444	20.62217	21.49257	22.26134	22.92592	23.48534	23.93979	24.29026	24.53815	24.68486	24.73155	24.67892	24.51417	24.2368	23.84582	23.33995	22.71798	21.97917	21.12355	20.15224	19.06758	17.87307	16.573
551	14.94392	16.22525	17.44086	18.58185	19.63953	20.60627	21.47596	22.24431	22.90873	23.46818	23.92279	24.27349	24.52161	24.66851	24.71532	24.66271	24.49789	24.22038	23.82921	23.32317	22.70109	21.96219	21.10683	20.13586	19.05171	17.85781	16.55839
552	14.93447	16.21451	17.42867	18.56824	19.62467	20.5904	21.45939	22.22732	22.89157	23.45104	23.90581	24.25673	24.50507	24.65215	24.69907	24.64649	24.4816	24.20395	23.81261	23.30639	22.68422	21.94543	21.09013	20.1195	19.03584	17.84256	16.54375
553	14.92495	16.20374	17.41647	18.55465	19.60984	20.57459	21.44287	22.21037	22.87445	23.43393	23.88883	24.23996	24.48852	24.63578	24.6828	24.63026	24.4653	24.18751	23.796	23.28963	22.66736	21.92859	21.07346	20.10316	19.02	17.8273	16.52909
554	14.91537	16.19294	17.40429	18.54108	19.59506	20.55882	21.4264	22.19347	22.85735	23.41683	23.87187	24.22319	24.47196	24.61939	24.66653	24.61401	24.44899	24.17108	23.7794	23.27288	22.65052	21.91177	21.05681	20.08685	19.00416	17.81205	16.5144
555	14.90571	16.18212	17.3921	18.52755	19.58031	20.5431	21.40997	22.1766	22.84028	23.39976	23.85492	24.20643	24.4554	24.603	24.65024	24.59775	24.43267	24.15463	23.7628	23.25613	22.6337	21.89497	21.04019	20.07055	18.98835	17.7968	16.49969
556	14.89598	16.17126	17.37992	18.51403	19.5656	20.52742	21.39359	22.15977	22.82325	23.38271	23.83797	24.18967	24.43883	24.58659	24.63394	24.58147	24.41634	24.13818	23.7462	23.2394	22.61689	21.87819	21.02359	20.05428	18.97254	17.78154	16.48496
557	14.88618	16.16037	17.36773	18.50054	19.55093	20.51179	21.37724	22.14298	22.80625	23.36568	23.82104	24.17291	24.42225	24.57018	24.61762	24.56519	24.4	24.12173	23.7296	23.22267	22.60009	21.86144	21.00701	20.03803	18.95675	17.76628	16.47019
558	14.87631	16.14945	17.35555	18.48707	19.5363	20.49619	21.36094	22.12623	22.78927	23.34867	23.80413	24.15615	24.40567	24.55375	24.6013	24.54889	24.38366	24.10527	23.71301	23.20596	22.58331	21.8447	20.99045	20.02179	18.94096	17.75101	16.4554
559	14.86636	16.13849	17.34335	18.47362	19.52169	20.48064	21.34469	22.10952	22.77233	23.33168	23.78722	24.13939	24.38909	24.53732	24.58496	24.53258	24.3673	24.08881	23.69641	23.18925	22.56655	21.82799	20.97391	20.00558	18.92519	17.73574	16.44058
560	14.85635	16.12749	17.33116	18.46018	19.50712	20.46513	21.32847	22.09284	22.75542	23.31471	23.77032	24.12264	24.37251	24.52088	24.56861	24.51626	24.35094	24.07234	23.67982	23.17255	22.5498	21.81129	20.9574	19.98938	18.90942	17.72046	16.42574

1096	18.5501	18.6936	18.8234	18.9436	19.0563	19.1618	19.2597	19.3489	19.428	19.4956	19.5503	19.5909	19.6164	19.6264	19.6204	19.5985	19.5591	19.5029	19.4313	19.3456	19.2477	19.1393	19.0225	18.8989	18.7697	18.6356	18.4963
1097	18.5466	18.6913	18.8218	18.9424	19.0551	19.1605	19.2583	19.3472	19.4261	19.4935	19.548	19.5884	19.6139	19.6238	19.6178	19.596	19.5566	19.5007	19.4292	19.3438	19.2462	19.1381	19.0215	18.8981	18.769	18.6349	18.4952
1098	18.5431	18.689	18.8202	18.9411	19.0539	19.1593	19.2568	19.3456	19.4242	19.4914	19.5457	19.586	19.6113	19.6212	19.6152	19.5934	19.5542	19.4984	19.4272	19.3421	19.2447	19.1369	19.0205	18.8972	18.7683	18.6341	18.4941
1099	18.5395	18.6866	18.8185	18.9398	19.0527	19.158	19.2554	19.3439	19.4224	19.4893	19.5434	19.5835	19.6088	19.6186	19.6126	19.5909	19.5518	19.4962	19.4252	19.3403	19.2432	19.1356	19.0195	18.8964	18.7675	18.6332	18.493
1100	18.5358	18.6841	18.8168	18.9384	19.0514	19.1567	19.2539	19.3423	19.4205	19.4872	19.5411	19.5811	19.6063	19.616	19.61	19.5884	19.5494	19.494	19.4232	19.3385	19.2417	19.1344	19.0185	18.8956	18.7667	18.6324	18.4919
1101	18.5319	18.6816	18.815	18.937	19.0502	19.1554	19.2525	19.3406	19.4186	19.4851	19.5388	19.5787	19.6038	19.6134	19.6075	19.5859	19.5471	19.4918	19.4212	19.3368	19.2402	19.1331	19.0175	18.8947	18.7659	18.6315	18.4907
1102	18.528	18.6789	18.8131	18.9356	19.0489	19.1541	19.251	19.339	19.4167	19.483	19.5366	19.5763	19.6012	19.6109	19.6049	19.5834	19.5447	19.4896	19.4192	19.335	19.2386	19.1319	19.0165	18.8939	18.7651	18.6306	18.4894
1103	18.5239	18.6762	18.8112	18.9341	19.0475	19.1527	19.2495	19.3373	19.4149	19.4809	19.5343	19.5739	19.5987	19.6083	19.6024	19.5809	19.5423	19.4874	19.4172	19.3332	19.2371	19.1306	19.0154	18.893	18.7643	18.6296	18.4881
1104	18.5197	18.6734	18.8092	18.9325	19.0462	19.1514	19.2481	19.3356	19.413	19.4789	19.532	19.5715	19.5962	19.6058	19.5998	19.5784	19.5399	19.4852	19.4152	19.3315	19.2356	19.1294	19.0144	18.8921	18.7634	18.6286	18.4868
1105	18.5154	18.6704	18.8072	18.931	19.0448	19.15	19.2466	19.334	19.4111	19.4768	19.5298	19.5691	19.5937	19.6033	19.5973	19.576	19.5376	19.483	19.4132	19.3297	19.2341	19.1281	19.0133	18.8912	18.7625	18.6276	18.4854
1106	18.511	18.6674	18.8051	18.9293	19.0434	19.1486	19.2451	19.3323	19.4092	19.4747	19.5275	19.5667	19.5913	19.6007	19.5948	19.5735	19.5352	19.4808	19.4112	19.328	19.2326	19.1269	19.0123	18.8902	18.7616	18.6266	18.484
1107	18.5065	18.6644	18.8029	18.9277	19.0419	19.1472	19.2435	19.3306	19.4074	19.4726	19.5253	19.5643	19.5888	19.5982	19.5923	19.5711	19.5329	19.4786	19.4092	19.3262	19.2311	19.1256	19.0112	18.8893	18.7607	18.6255	18.4826
1108	18.5018	18.6612	18.8006	18.9259	19.0405	19.1457	19.242	19.3289	19.4055	19.4706	19.5231	19.5619	19.5863	19.5957	19.5898	19.5686	19.5306	19.4764	19.4073	19.3245	19.2296	19.1243	19.0101	18.8883	18.7597	18.6244	18.4811

Figure 2.2.3.2

The 3D plot of temperature varying with both time and distance within the chocolate was plotted in MATLAB (code can be found in *Appendix section 2*) and can be found below.

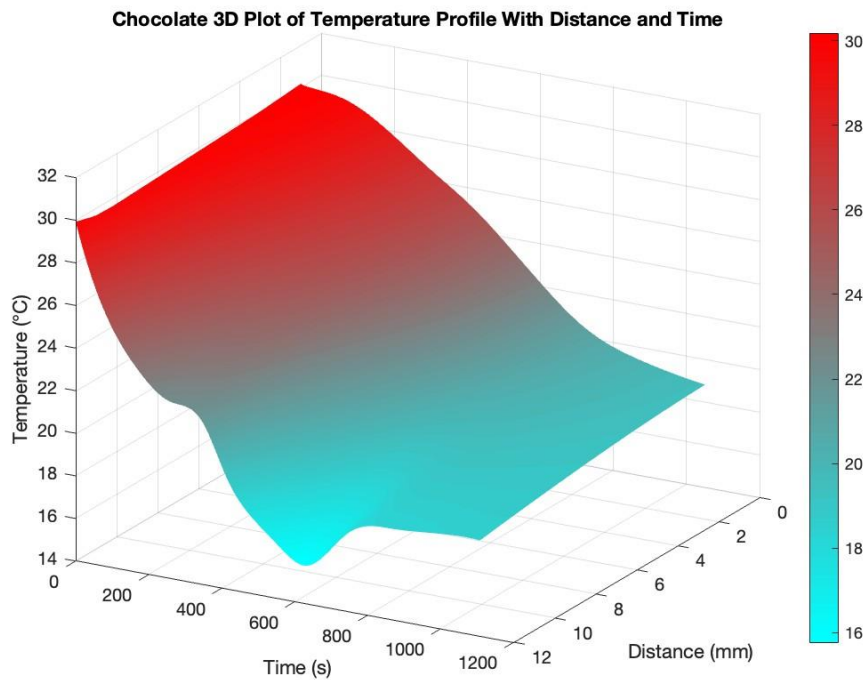


Figure 2.2.3.3

The Heat map of temperature with time and distance was also plotted. The graph below shows the heat transfer vertically in the Y direction.

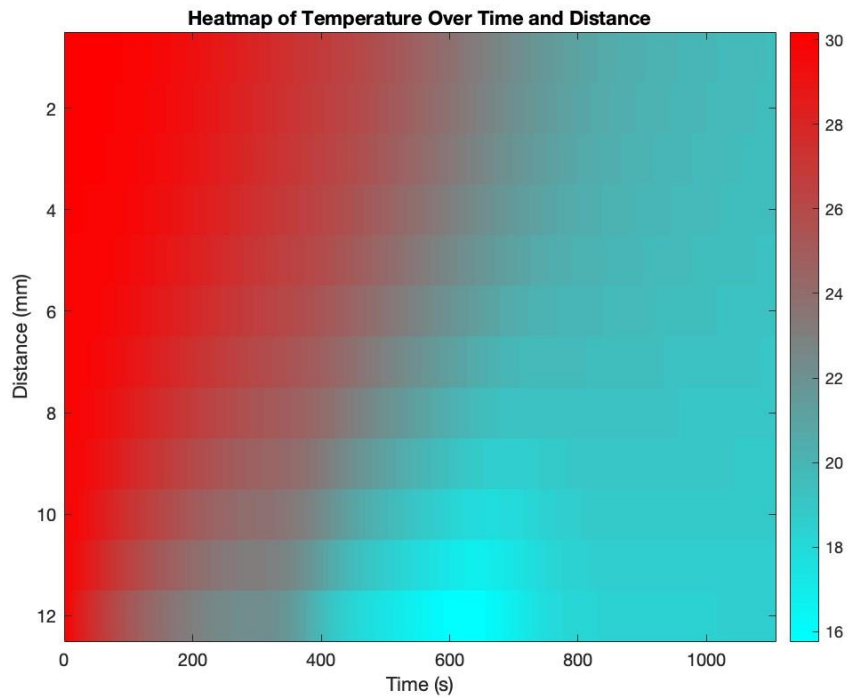


Figure 2.2.3.4

The plots reveal a gradual decrease in temperature, with the layers closer to the surface cooling faster than the interior. This is to be expected due to the time it takes for the conductive transfer to reach the interior. The lack of uniform temperature distribution reveals the varying rate of heat dissipation. The smooth continuous temperature transitions are ideal for formation of the desired crystalline structure, the chocolate also cools to the desired temperature range of around 18°C, which is optimal for storage and transportation. The temperature at the end is uniform, which shows that the whole bar has been properly cooled.

Since the conduction of the mould affected the conduction of the chocolate, they were both modelled as one overall system. The temperatures of each component affected each other, as can be shown in the 3D graph and heat map below.

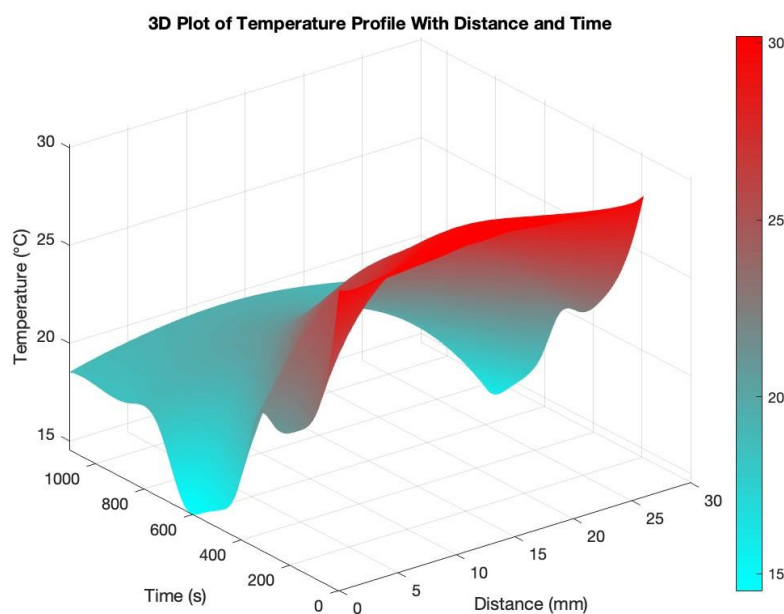


Figure 2.2.3.5

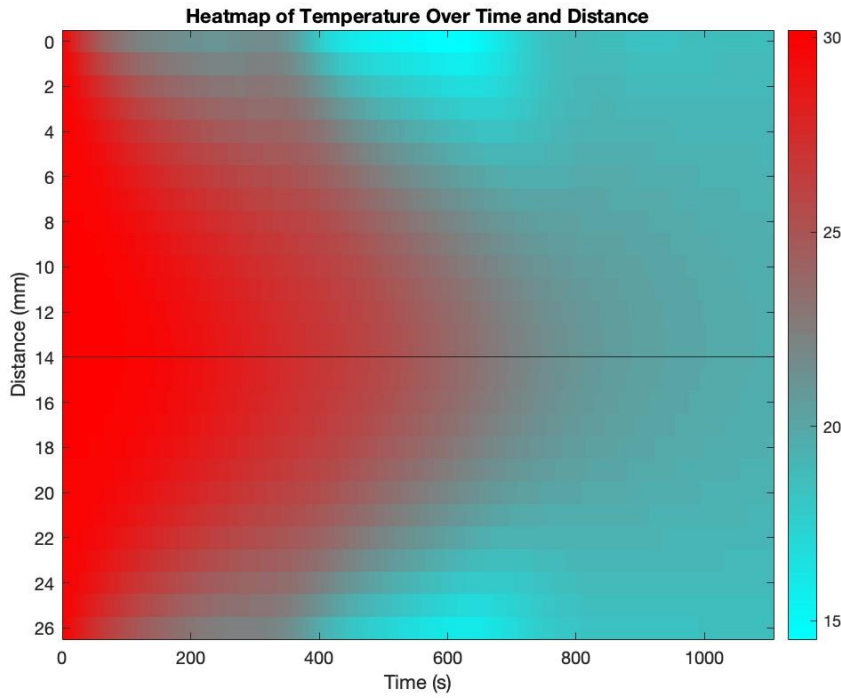


Figure 2.2.3.6

The plots display the combined thermal behaviour of the chocolate and the mould as one system during cooling. The cool air reaches the top of the chocolate, as well as the bottom of the mould, these surface temperatures were previously calculated and thus used as boundary conditions in this model. The cooling effect then goes down from the chocolate and up from the mould, as the desired temperature is eventually reached in the middle. There is a clear temperature gradient, with the outer regions cooling first. It is also clear that the mould acts as a insulator, as is a smooth temperature transition near the boundaries.

2.2.4 Modelling of air flow

The calculations for the heat transfer are done based on the assumption that the cooling air will reach the chocolate surface at the required velocity. Having a relatively uniform airflow is beneficial for consistent cooling performance. This had to be validated through modelling the motion of the air throughout the tunnel.

The movement of fluid is driven by various properties, these include viscosity, velocity, pressure, density and temperature. Fluid flow is governed by the conservation of mass and momentum, described the incompressible Navier–Stokes equation for the (x direction) below (NASA, 2015).

$$\rho \left(\frac{\partial u}{\partial t} + u \frac{\partial u}{\partial x} + v \frac{\partial u}{\partial y} + w \frac{\partial u}{\partial z} \right) = - \frac{\partial p}{\partial x} + \mu \left(\frac{\partial^2 u}{\partial x^2} + \frac{\partial^2 u}{\partial y^2} + \frac{\partial^2 u}{\partial z^2} \right) + \rho g_x$$

Equation 2.2.4.1

Where ρ density of air (kg/m^3), u is the velocity component in the x-direction (m/s), v is the velocity component in the y-direction (m/s), w is the velocity component in the z-direction (m/s), p is pressure (Pa), μ is the dynamic viscosity of air, g_x is the gravitational acceleration (m/s^2). $\frac{\partial u}{\partial t}$ is the acceleration in the x direction and $\frac{\partial p}{\partial x}$ is the pressure gradient.

The equation is divided into different components: $u \frac{\partial u}{\partial x}, v \frac{\partial u}{\partial y}, w \frac{\partial u}{\partial z}$ are the convective acceleration terms and $\frac{\partial^2 u}{\partial x^2}, \frac{\partial^2 u}{\partial y^2}, \frac{\partial^2 u}{\partial z^2}$ are the viscous diffusive terms.

The Navier Stokes equation is a nonlinear partial differential equation that can only have analytical solutions in very simplified cases, solving this numerically would be too complicated to do. Therefore, Computational Fluid Dynamics is used to solve approximations and simulate the airflow. Computational Fluid Dynamics uses a variety of techniques like finite difference, finite volume, finite element, and spectral methods (NASA, 2015). In this case finite element analysis is used.

COMSOL Multiphysics is a simulation software that is used for modelling fluid dynamics, it uses finite element analysis to solve the Navier Stokes equation and thus simulate how physical systems behave under real world conditions.

This approach allowed for the discretisation of finite elements, where the Navier Stokes equation was solved iteratively at each stage. This enabled the identification of varying airflows, specifically highlighting regions of high and low airflows, eddies, recirculation zones and stagnant points. This helped visualise whether the cooling air was reaching the chocolate surface in a uniform manner.

The model included a 2-D schematic of the cooling tunnel, based on the previously calculated dimensions. To account for the mould height (which was not previously considered in the shortcut design) the new tunnel height modelled is 7.8cm. This was based on industry standard, where the height of the tunnel is calculated to be 3 times the height of the object being cooled to allow sufficient height for convective currents. The chocolate blocks were represented as internal obstructions to the air. A single fan was placed at the top centre in each tunnel.

Air enters the tunnel through the top of the tunnel, this should allow for the highest degree of uniform distribution of air across the tunnel and should target the surface of the chocolate. This type of flow is called Jet Flow, where the cooling air perpendicularly approaches the surface to be cooled (Grob, 1991), as shown in the figure below.

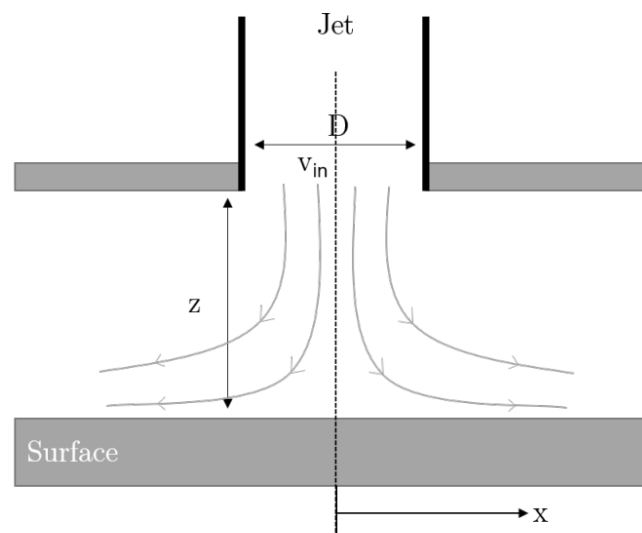


Figure 2.2.4.1

The properties of the cooling air that were inputted into the model were based on their temperature and were as followed:

	Zone 1	Zone 2	Zone 3
Temperature, T (°C)	21	14.5	18.5
Dynamic Viscosity, μ (Pa s)	1.817×10^{-5}	1.786×10^{-5}	1.805×10^{-5}
Density, ρ (kg/m ³)	1.2	1.227	1.21
Fan diameter (m)	0.360	0.237	0.134

Table 2.2.4.1

Appropriate boundary conditions were also applied to help accurately represent to airflow, these included:

- No slip condition on all solid surfaces, including tunnel walls, mould, and the chocolate surface. This means that the air has zero velocity at the surface of these objects.
- Velocity inlet of the fan was 5 m/s. This is where air enters the tunnel and the speed was chosen during the short cut design based on the requirements to achieve turbulent flow. The direction of the flow was also chosen to be from the ceiling of the tunnel, in a downwards vertical direction.
- The pressure outlet at the exit and entrance to the tunnels was set to zero. This boundary condition was applied to allow for the free flow of air in and out of the tunnel. This allowed for the model to predict the flow velocity based accurately.

The software also included a setting to vary the grid size, this refers to the spatial discretisation of the model into smaller regions, each region is where the Navier Stokes equation is solved over. The grid size determines how many regions there are in a set area. Having a smaller grid size increases the accuracy of the model, since there are more regions and thus more variations in velocities can be captured. However, having too small of a grid size could increase computation time so would therefore be unnecessary and impractical. The grid size in the system was set to 0.002, this allowed for a high degree of accuracy whilst keeping the computation time to a reasonable length.

The air reaches the base of the mould through the porous mesh conveyor that allows air to freely pass through. This means the cooling air will reach the bottom surface unaffected by the conveyor system.

Result from the simulation can be found below in Figure 2.2.4.2, the dimensions of the tunnel are wide and narrow, making it difficult to see, therefore a zoomed in version was displayed in Figure 2.2.4.3 to show the air flow near the entrance to the tunnel. On the right hand side there is a scale which shows of the velocity of the air, where red is the highest (30 m/s) and blue is the lowest (0 m/s). Streamlines have also been added to assist visualisation of the airflow. The chocolate inside the mould was modelled by the white rectangles, where the air cannot flow through.

The simulation was ran for all three sections of the tunnel but the results are presented for the first section only. The design alterations and checks for the first section apply to all sections of the tunnel.

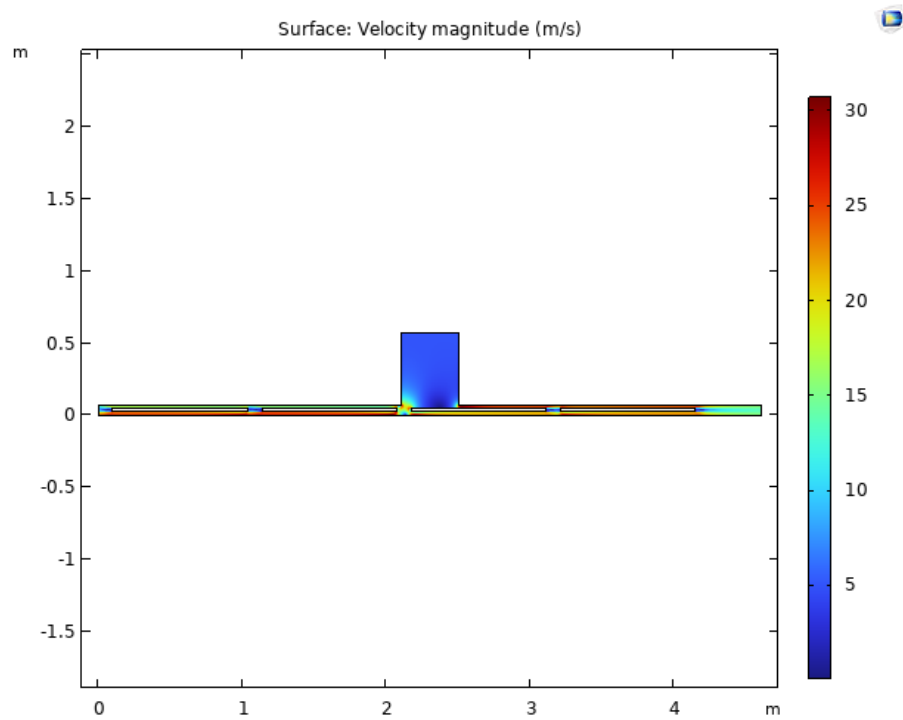


Figure 2.2.4.2

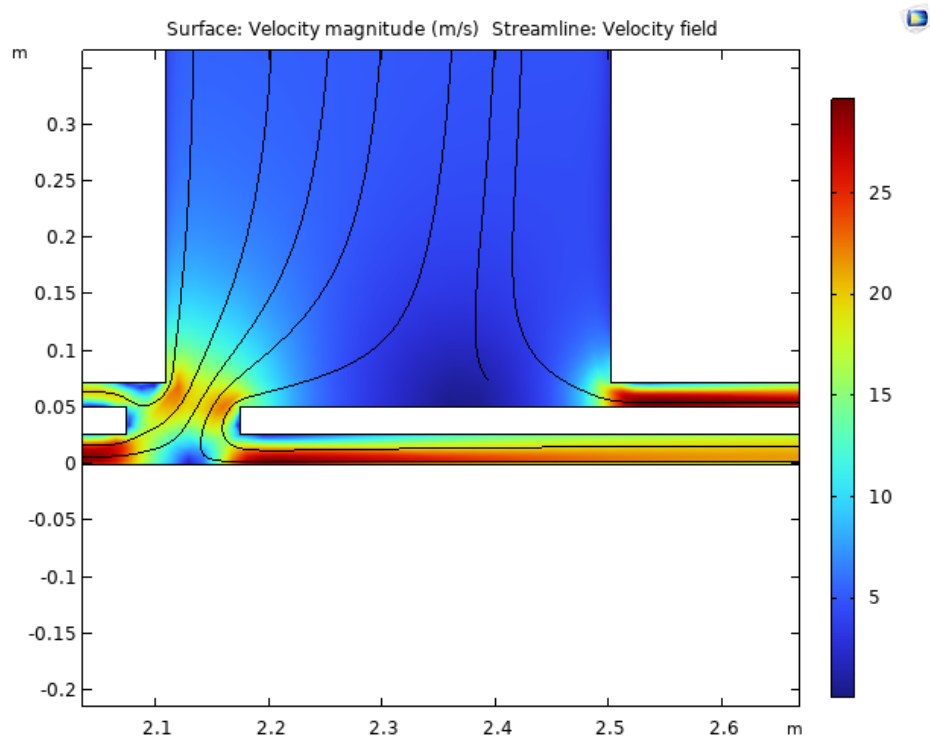


Figure 2.2.4.3

An initial obvious observation from the simulation is that with an inlet velocity of 5m/s, the air velocity between the chocolate surface and the tunnel roof increases sharply. The high velocity in the narrow horizontal duct is due to the reduced cross-sectional area, shown by the equation below. If the volumetric flowrate is constant, then as the area gets smaller then the velocity increases.

$$v = \frac{\dot{V}}{A}$$

Equation 2.2.4.2

Where v is the air velocity (m/s), A is the cross-sectional area that the air travels through (m^2) and \dot{V} is the volumetric flowrate (m^3/s).

These high velocities of around 25m/s near the surface of the chocolate are problematic, they can lead to overly rapid and uneven cooling through disrupting the gradual cooling gradient required for the process. High velocities can also physically damage the product through the stress inflicted on the surface.

Therefore, the design needed to be altered in order to eliminate this issue. This can either be done by reducing the inlet velocity or the cross-sectional area. This balance will be further refined in the optimisation section, but an initial adjustment was necessary in order to get a reasonable internal airflow. The height of the tunnel was doubled to 0.144m and the inlet velocity was set to 2 m/s. The results are shown below.

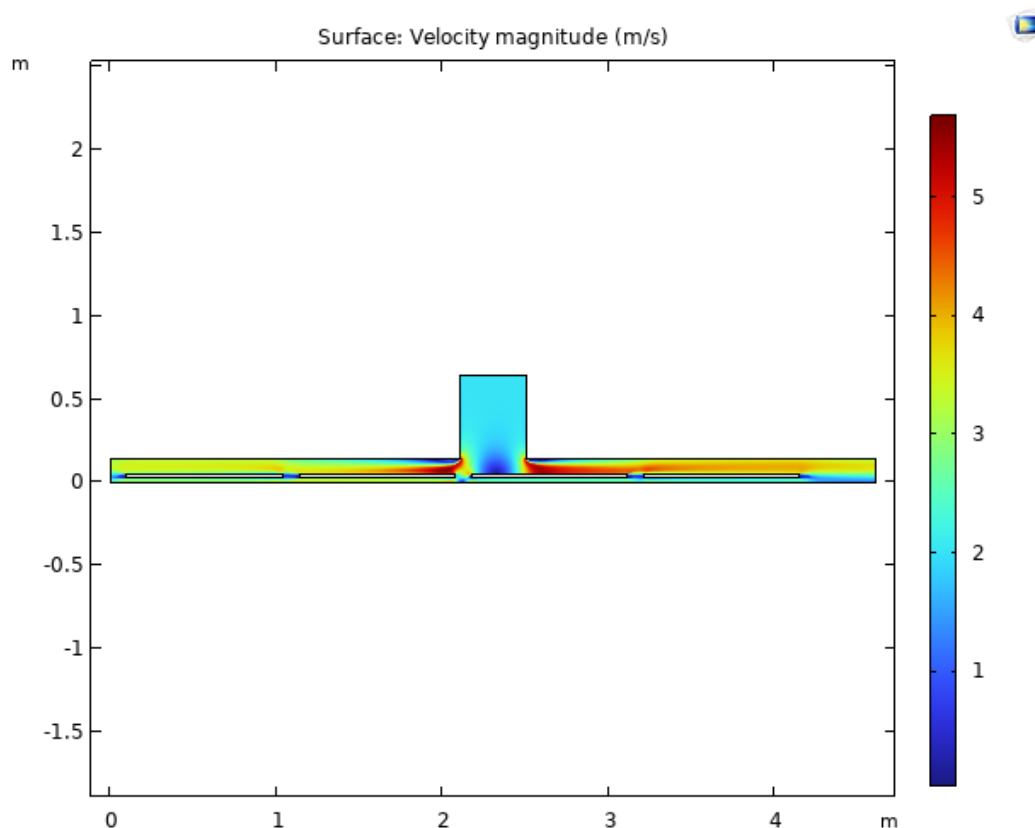


Figure 2.2.4.4

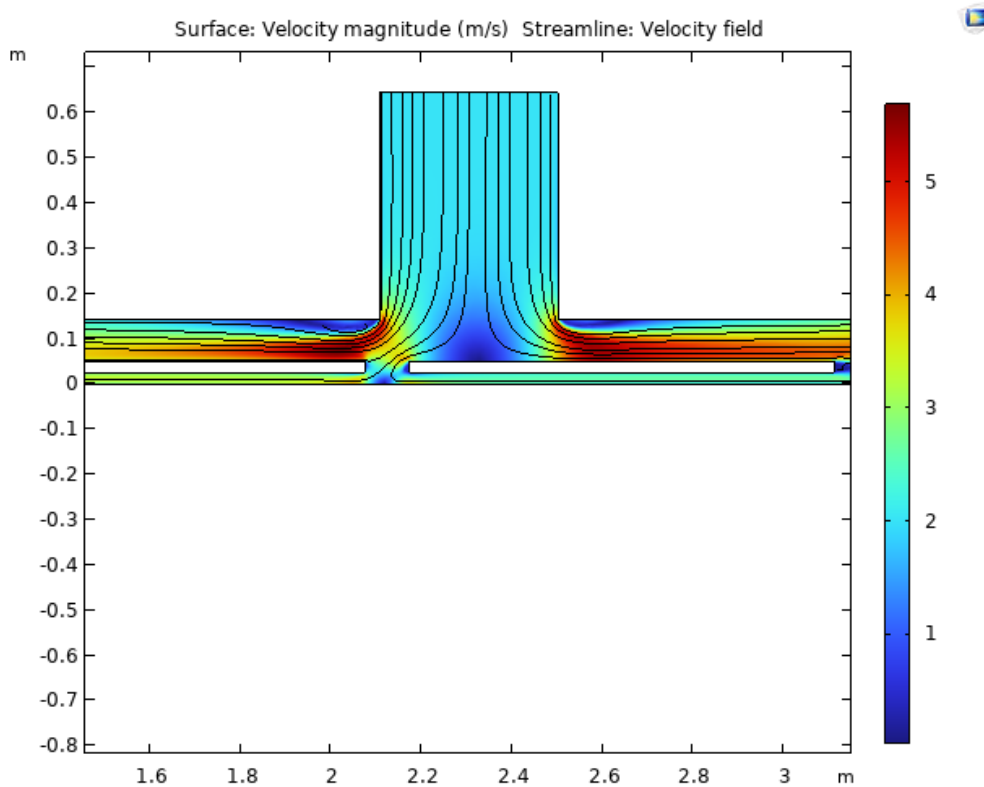


Figure 2.2.4.5

Figures 2.2.4.4 and 2.2.4.5 show the effect on airflow on the system when the tunnel height and inlet velocity was adjusted to reduce the internal air velocity. The new velocity range is from 1 m/s to 6 m/s. This is range is what is considered optimal in industry (Grob, 1991).

Cold air enters the tunnel through a duct and a fan from the cooling unit and that is where the initial cooling via convection occurs. The fan diverts cold air to the space above the surface of the chocolate. The air also circulates via the space below the conveyor so that chocolate in that area is cooled from the bottom, via conduction through the mould. Air exits at the end of the tunnel section, where it returns to the atmosphere.

After the changes air is distributed in a more uniform manner along the tunnel, after it enters the tunnel vertically, demonstrating a significant improvement in flow distribution. The velocity does not exceed 6 m/s, therefore the chocolate is not at risk of being damaged and cooled incorrectly.

2.2.5 Calculation Check

To ensure robustness of the system, the results need to be validated through comparisons with similar designs from literature. This will both check the precision of the calculations and confirm the integrity of the design.

The literature used for comparison was Lucas Grob's thesis, titled: "Aero and thermodynamical optimization of cooling tunnels for chocolate systems" (Grob, 1991). This study explores how airflow and heat transfer, specifically aspects such as influence of airflow patterns, mould geometry, and material conductivity on the efficiency of chocolate cooling. The research conducted within this report uses measurement techniques such as ultrasound tracking, optical surface analysis and heat flux sensing to comprehensively analyse and optimise the cooling process. The findings from the research in the report were used as a benchmark to validate the calculations done in this project.

2.2.5.1 Heat transfer validation

Grob investigates the cooling dynamics of a chocolate sample to get a relationship between temperature and time. *Figure 2.2.5.1.1* shows the temperature distribution of chocolate at different depths and with different cooling temperatures. The different depths are at the top of the bar ($d = 2\text{mm}$), the centre of the bar ($d = 5\text{mm}$) and at the bottom near the mould interface ($d = 7\text{mm}$). The different cooling airs used are 18°C , 12°C and 12°C .

The cooling airs used in this project are 21°C then 14.5°C and finally 18.5°C and the chocolate bar is 12mm deep. Although these vary from the numbers used in the reference literature. Grob's research still provides a valuable insight into the way the temperature is supposed to behave.

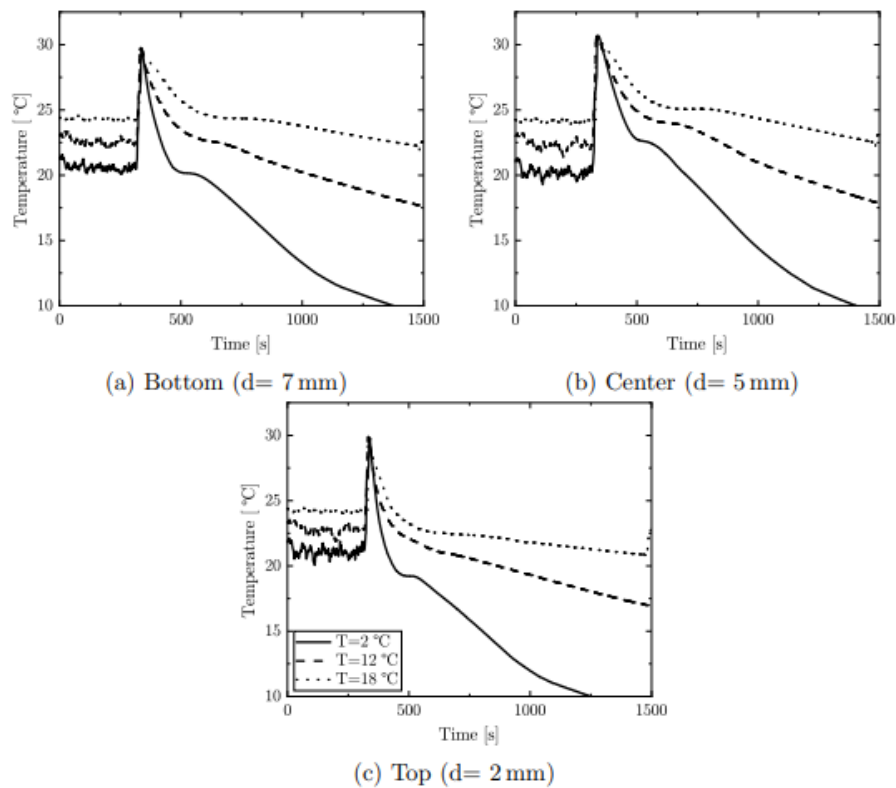


Figure 2.2.5.1.1

The curves all show an initial plateau of temperature, this may be due to for the time taken to overcome the thermal resistance of the chocolate mass, where energy will be released without a corresponding temperature drop. There is then a sharp increase in temperature, this can be attributed to the latent heat of crystallisation. As the cocoa butter is exposed to the cool air, it will crystallise and thus release latent heat, this is because crystallisation is an exothermic process. The release of latent heat briefly overcomes the rate of heat removal by air. There is then a rapid temperature drop at the beginning of each cooling stage, especially at the surface. This is driven by the temperature difference between the warm chocolate and cooler air, which creates a thermal gradient and transfers heat from the chocolate to the surrounding air. The centre and base of the bar experience a slightly more gradual temperature drop than the surface, due to the surface being in direct contact with the air. The centre and base have to wait for the conduction to occur at their position. The cooling continues until the temperature stabilises as thermal equilibrium is reached.

The model in this report similarly shows that surface layer of the chocolate cool fastest, with a clear temperature gradient toward the centre, aligning accurately with Grob's experimental data and what is expected from conduction. Grob's temperature sensors at multiple depths (2 mm, 5 mm, and 7 mm) reveal the similar pattern of internal cooling via conduction as the model in this report. The time taken for cooling is also similar with roughly 1500s for Grob's model and 1200s required for this model.

The surface profile in Grob's report also validates the surface temperature gradient modelled in this report (as shown in *Figure 2.2.5.1.1*). Although the behaviour is not identical, the profile shows a similar pattern. Both surfaces experience rapid drop in temperature before gradual slowing down of the cooling rate, ending in a stable plateau.

Despite the strong similarities in overall trends, there are still notable differences between the temperature profiles. Grob's experimental data captures the latent heat of crystallisation, as shown by the spike in temperature in *Figure 2.2.5.1.1*. The report in the conduction model does not account for latent heat of crystallisation and thus does not have an initial spike in temperature.

Grob measures his data empirically, via an industrial data logger that utilises ultrasound technology and temperature sensors to measure the temperature. The temperature development is measured at three different points along the depth of the chocolate. Whereas the model used in this report was the finite difference method and thus was purely theoretical. There are also key differences in the parameters across the models, Grob uses a fixed air temperature, not gradually decreasing the temperature across zones, this creates a steeper thermal gradient.

In Grob's report he mentions that when the cooling air was set to 2°C the formation of unstable polymorphs occurs, whilst cooling at the higher temperatures of 14°C and 18°C lead to more stable crystals. The impracticalities of cooling at 2°C are visualised in *Figure 2.2.5.1.1*, where the steep temperature gradient is evident. In the calculations done for this report the cooling air temperature was chosen to be 21°C, 14.5°C and 18.5°C, which are more reasonable than when Grob's model was set to 2°C, these temperatures are closer to the successful ones in Grob's model, reinforcing the validity of the calculations done.

It is evident that there are differences in the set-up of each model, therefore differences are expected to occur. So, variations such as the latent heat of crystallisation is the natural outcome of differences in model parameters. Grob's model relies on empirical data so will be more effective in capturing aspects such as the latent heat of crystallisation. Whereas this report uses a high level of discretisation to gradually approximate temperature changes. Both models have different strengths and techniques, therefore the differences do not undermine either model. The fact that the general behaviour and outcome of the temperature profiles are similar reinforces the validity and reliability of the model used in this report.

2.2.5.2 Fluid Behaviour Validation

It is important to confirm that the airflow pattern across the tunnel is consistent with that used in industry. Grob's report also simulates the velocity of the air around the mould. However, a key difference is that the air flows horizontally entering from the left-hand side of the tunnel. Regardless of the direction of flow, the velocity around the surface of the chocolate should still remain within the desired range. His model is found below.

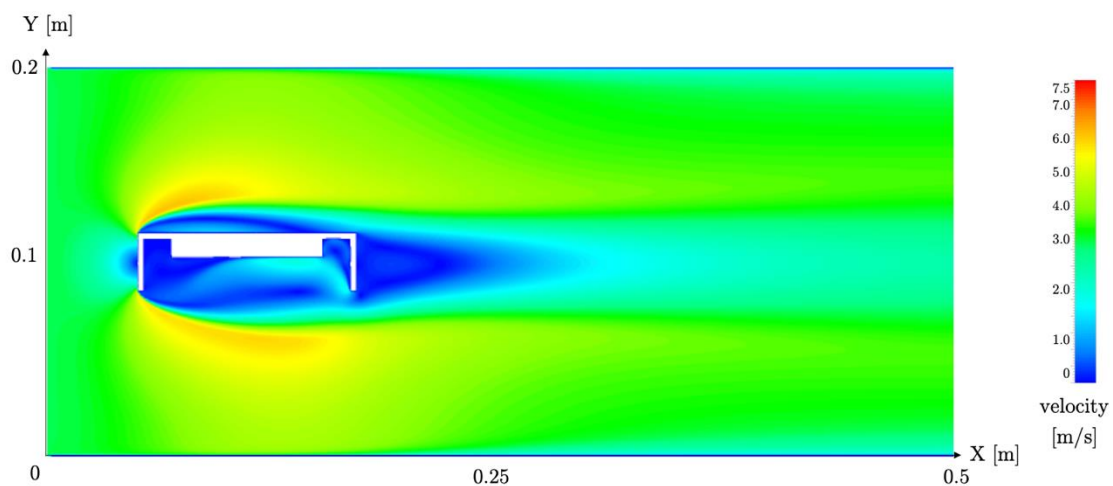


Figure 2.2.5.2.1

Grob's inlet air is set to 3.5m/s, where as the simulation in this report the inlet velocity is 2m/s, the velocity then varies around the dimensions of the mould. Both simulations closely align with each other, in terms of geometry and airflow. Both flows remain steady and streamlined with no visible eddies. This shows that the calculated model from this report demonstrates accurate and precise plausibility. In practice a design like this will ensure gentle and uniform cooling without surface disturbances.

2.2.6 Computer flow diagram

An algorithm was created that outlined the calculation steps for the design. The algorithm visualised the steps required for calculating the surface temperature, conduction model, and computational fluid dynamics model. This is shown in *Figure 2.2.6.1*.

- The outputs of the surface temperature was used in the conduction model.
- The output from the conduction model showed at which point the chocolate bar achieved uniform internal cooling. During optimisation this can be used to alter the residence time required for cooling as well as the cooling air temperature.
- The output from the computational fluid dynamic model can be used to optimise the number of fans and their placements, the velocity of air and the tunnel dimensions.

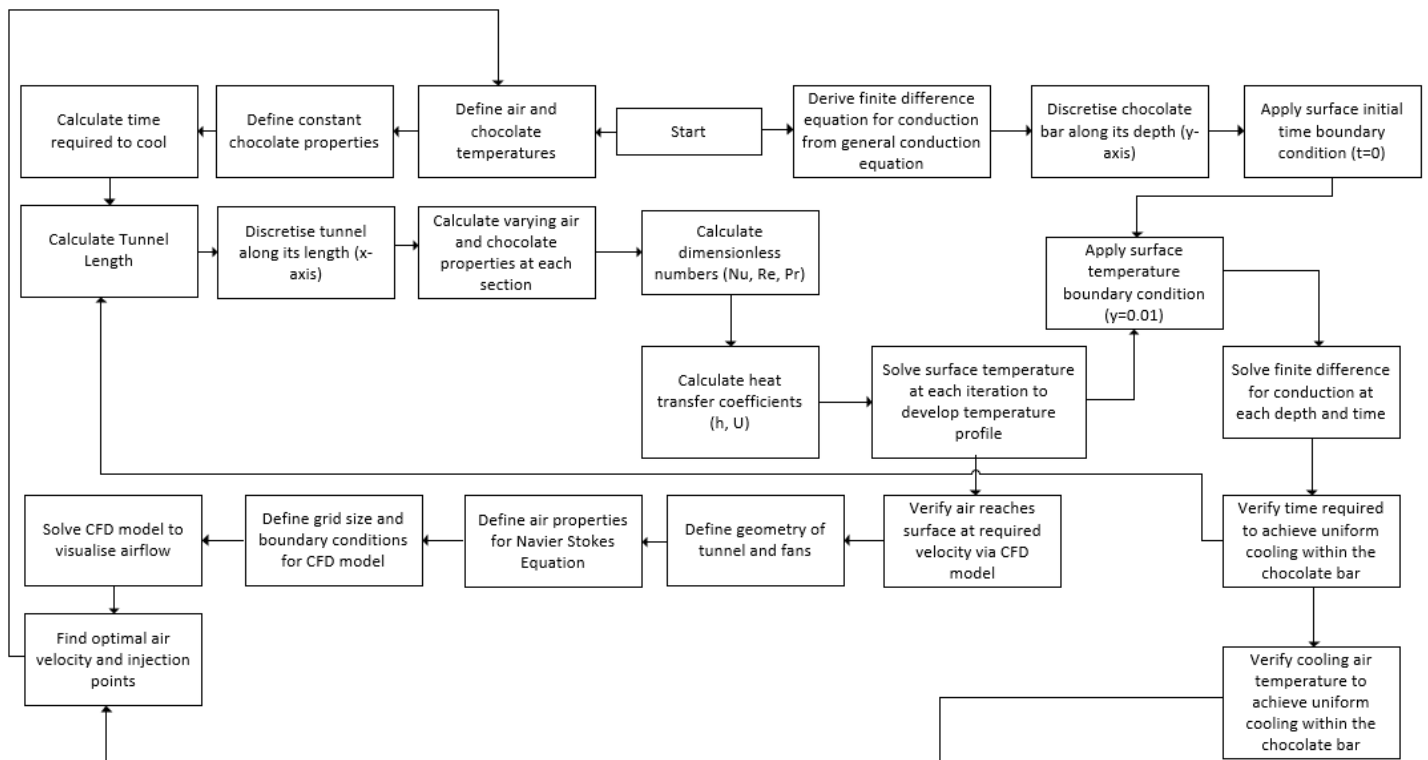


Figure 2.2.6.1

3 Unit Optimisation

The optimisation process aims to iteratively carry out the algorithm found in *Figure 2.2.6.1* in order to find the properties that create a system that is both efficient and effective.

When altering the properties and variables of the system, the parameters that need to be evaluated to assess the extent of how optimal the system is are as followed:

- Capital and operational expenditure have to be kept low to increase the economic viability of the process.
- The footprint are has to be considered, therefore having a reduced tunnel length will help this.
- Minimise total cooling time of the system, whilst not compromising chocolate quality.
- Reduce the energy usage of the tunnel's mechanical and pneumatic aspects.
- Ensure uniform cooling internally within the chocolate, at the required temperature for Form V crystal formation.

The impact of the variables to be iteratively analysed are as followed:

- Cooling air temperature in each zone: Having more moderate cooling air temperatures would both reduce energy usage and cost.
- Air velocity: Lower air velocities would both reduce energy usage and cost.
- Residence time: Less time spent cooling leads to a lower tunnel length and thus a smaller footprint, this will also reduce energy consumption and thus cost.
- Fan injection points. The number of fans has to consider both ensuring airflow distribution and the economic cost of having multiple fans.
- Mould thickness: lower mouth thicknesses will increase the rate of conduction but may compromise the structural integrity.
- Mould Material: Different materials may have different heat transfer properties, which will effect how effective and efficient they are at performing cooling via conduction.

3.1 Varying Cooling Time

Chocolate is required to be kept at between 18°C and 19°C during storage (Beckett, Fowler and Ziegler, 2017). Once it reaches this required cooling temperature, it should be left to stabilise to ensure desired form V cocoa butter crystals fully form. This stabilisation section should contain mild air circulation, but active cooling is not required, therefore it can occur outside of the cooling tunnel. Beckett states that for complete stabilisation to occur, chocolate should remain at the stabilisation temperature for 24 to 48 hours before packaging (Beckett, Fowler and Ziegler, 2017). Therefore, this is likely to occur outside of the cooling tunnel, this means that once the required temperature is reached, the chocolate can exit the tunnel and stabilise elsewhere.

As seen in the Heatmap of the internal chocolate temperature distribution, the chocolate reaches the required temperature of 18°C and 19° C at around 300 seconds before it reaches the exit of

the tunnel (*Figure 3.1.1*) This is validated by the excel model, where the first point where the entire chocolate bar is below 19°C is at t=813s, shown in *Figure 3.1.2*.

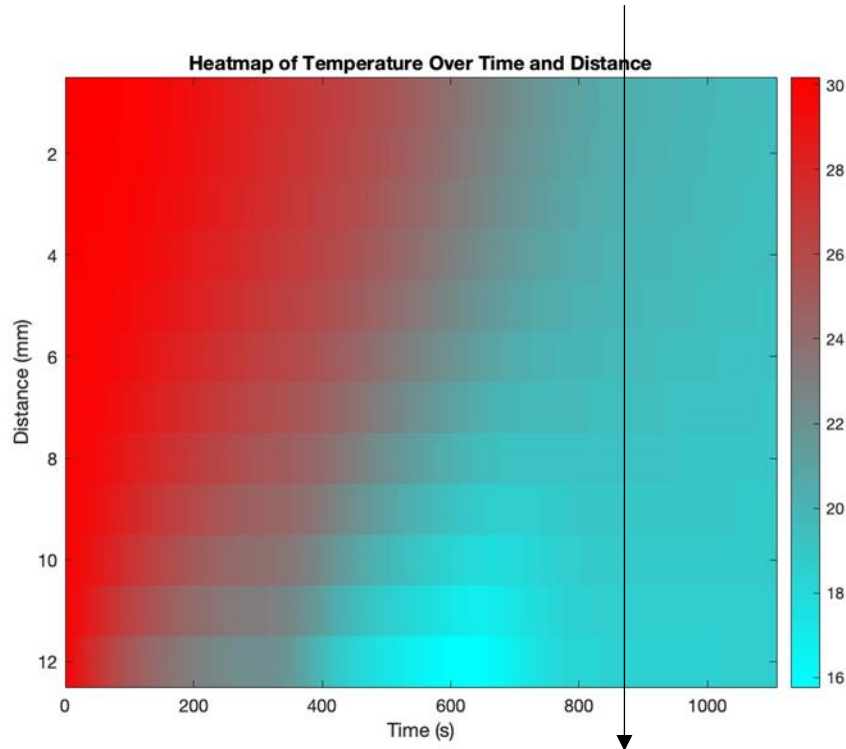


Figure 3.1.1

810	17.40963	17.65064	17.86842	18.06398	18.23832	18.39238	18.52711	18.6434	18.74207	18.82395	18.88978	18.94026	18.97607	18.99781	19.00608	19.00141	18.98272	18.95055	18.90544	18.84791	18.77844	18.69754	18.60568	18.50333	18.39096	18.26905	18.1381
811	17.40567	17.64684	17.86479	18.06051	18.235	18.38922	18.5241	18.64052	18.73933	18.82133	18.88727	18.93787	18.97377	18.99561	19.00396	19.00939	18.98077	18.94868	18.90365	18.84618	18.77679	18.69596	18.60416	18.50188	18.38958	18.26774	18.1368
812	17.40171	17.64305	17.86116	18.05704	18.23169	18.38606	18.52108	18.63764	18.73658	18.8187	18.88476	18.93546	18.97147	18.9934	19.00185	19.00736	18.97882	18.94681	18.90185	18.84446	18.77514	18.69437	18.60264	18.50043	18.3882	18.26643	18.1356
813	17.39775	17.63925	17.85752	18.05357	18.22838	18.3829	18.51806	18.63476	18.73383	18.81608	18.88225	18.93306	18.96917	18.9912	18.99973	18.99533	18.97687	18.94494	18.90005	18.84273	18.77348	18.69279	18.60113	18.49898	18.38682	18.26511	18.135
814	17.39378	17.63545	17.85389	18.0501	18.22506	18.37973	18.51504	18.63188	18.73108	18.81345	18.87974	18.93066	18.96687	18.98899	18.99762	18.9933	18.97493	18.94307	18.89825	18.84101	18.77183	18.6912	18.59961	18.49754	18.38544	18.2638	18.1331
815	17.38982	17.63166	17.85026	18.04662	18.22174	18.37657	18.51202	18.629	18.72833	18.81082	18.87723	18.92826	18.96457	18.98679	18.9955	18.99127	18.97298	18.94119	18.89646	18.83928	18.77017	18.68962	18.5981	18.49609	18.38406	18.26249	18.1318

Figure 3.1.2

This means that the new optimised residence time becomes 813 seconds, or 13.55 minutes. The new tunnel length subsequently becomes:

$$L_{tunnel} = \frac{t \times v_{conveyor}}{N_{bar}}$$

Equation 2.1.1.3

$$L_{tunnel} = \frac{813 \times 0.052}{4} = 10.569m$$

The initial length of the tunnel was 14.53m, therefore the optimisation process saves 3.96m of tunnel length, this will reduce the footprint area that is going to be calculated later in the mechanical design (Section 6).

Varying mould thickness

The mould used initially has a total thickness of 24mm with a cavity of 12mm for the liquid chocolate to sit in. This gives a distance of 14mm between the base of the mould and the interface with the chocolate, which is a large distance for conduction to cover. However, it was

found that the mould thickness can be drastically reduced. Grob uses a mould with 5mm of depth for a thinner option as can be shown in the figure below.



Figure 3.1.3

Having a thinner mould would greatly improve the rate of heat transfer. However, it is important to consider the fact that Grob used a different material in this thinner version of a mould. It was made from polylactide and the mould used in this project was polycarbonate, therefore the material properties may vary in a way that could have unpredictable effects on the process if the polycarbonate was made thinner. Despite this, after having investigated the material properties such as density, flexural strength, thermal conductivity and tensile strength (MakeItFrom.com, n.d.) it was evident that the variations in material properties were not significant enough to have an impact on the performance. For example the flexural strength of polycarbonate is 92-160 MPa, whilst the flexural strength of polylactide is 80Mpa. In fact, after investigation the properties for polycarbonate were superior to the ones of polylactide, due to the materials ability to perform more efficiently and last longer. Therefore the thickness of the polycarbonate mould can be reduced to 5mm safely, without risk of affecting the process.

Once this mould thickness was applied to the conduction model, the first point where the entire chocolate bar is below 19°C is at t=633s, as shown in the figure below.

631	14.6821	15.3486	16.0409	16.7136	17.3355	17.8848	18.3463	18.6964	18.9272	19.0338	19.0138	18.8673	18.5971	18.2091	17.7131	17.1251	16.4632	15.7816
632	14.6968	15.3528	16.0377	16.7053	17.3237	17.8704	18.3302	18.6792	18.9093	19.0155	18.9955	18.8495	18.5801	18.1935	17.6998	17.1153	16.4646	15.7848
633	14.7123	15.3576	16.0349	16.6973	17.312	17.8562	18.3142	18.662	18.8914	18.9773	18.8316	18.5632	18.178	17.6867	17.1057	16.4604	15.7884	
634	14.7284	15.3628	16.0324	16.6895	17.3005	17.8421	18.2983	18.6449	18.8735	18.9791	18.9591	18.8139	18.5463	18.1627	17.6737	17.0964	16.4565	15.7925
635	14.7452	15.3686	16.0304	16.6819	17.2891	17.8281	18.2824	18.6278	18.8557	18.9609	18.941	18.7962	18.5295	18.1474	17.661	17.0874	16.453	15.797

Figure 3.1.4

Reducing the depth of the mould will reduce the distance that heat must travel from the interior of the chocolate to the surface of the mould, which increases the rate of heat loss during the cooling process and thus reduces the required cooling time. Thermal conduction occurs faster over shorter distances, therefore a thinner mould releases the internal heat more efficiently, reducing the residence time and thus the length required for the tunnel.

Fourier's Law of Heat Conduction shows that if the distance heat must travel, d is reduced then the heat transfer rate, q will increase.

$$q = \frac{k \cdot A \cdot \Delta T}{d}$$

Equation 3.1.1

Where q is the rate of heat transfer (W), k is the thermal conductivity of the material (W/m K), A is the surface area through which heat is conducted (m²), ΔT is the temperature difference (°C), and d is the thickness or distance over which the heat is transferred (m).

The new tunnel length subsequently becomes:

$$L_{tunnel} = \frac{633 \times 0.052}{4} = 8.23\text{m}$$

Equation 2.1.1.3

Saving an extra 6.3m of tunnel length from the original tunnel design, further reducing the footprint area.

3.2 Varying Cooling temperature

Throughout optimisation the balance between air velocity and cooling temperature has to be considered. Lower air flows will required a higher temperature gradient and vice versa in order to achieve the same cooling effect (Beckett, Fowler and Ziegler, 2017). The optimal balance will be based on the option that has the lowest energy consumption, whilst still achieving efficient cooling. Lower energy consumption lead to reduced environmental effect as well as lower costs for the project. This is calculated from the cooling load equation below.

$$Q = \dot{m} \times c_p \times \Delta T$$

Equation 3.2.1

Where Q is the heat removal rate (kW), \dot{m} is the mass flow rate of air (kg/s), c_p is the specific heat capacity of air (kJ/kg °C) and ΔT is the difference in temperature between the ambient air and the chilled air supplied to each section of the tunnel (°C). The ambient air is set to 25°C.

The chiller efficiency needs to be accounted for to find the final power input required. Chiller efficiency is typically measured by the Coefficient of Performance (COP), in industry this ranges from 2.40 to 3.06 for air cooled chillers (Yu et al., 2014). In this system the COP is set to 2.73.

$$P = \frac{Q}{COP}$$

Equation 3.2.1

Where P is the Power input required (kW), Q is the cooling load (kW) and COP is the coefficient of performance and has no units.

Section	Mass Flowrate (kg/s)	Specific Heat Capacity (kJ/kg °C)	Temperature Difference (°C)	Cooling Load (kW)	Power input (kW)
1	0.746	1.006	4	3.00	1.10
2	0.284	1.005	10.5	3.00	1.10
3	0.092	1.006	6.5	0.60	0.22

Table 3.2.1

The required power input will be lowered if the temperature difference is lowered. The section with the largest temperature difference is section 2, therefore this was varied and evaluated first. Using *Equation 5.3.1* it can be seen that for every 1°C decrease in temperature difference (closer to ambient temperature) this saves 0.05kW. However, this needs to be balanced to ensure that the cooling of the chocolate still occurs effectively. The effect on surface temperature can be found on the graph below.

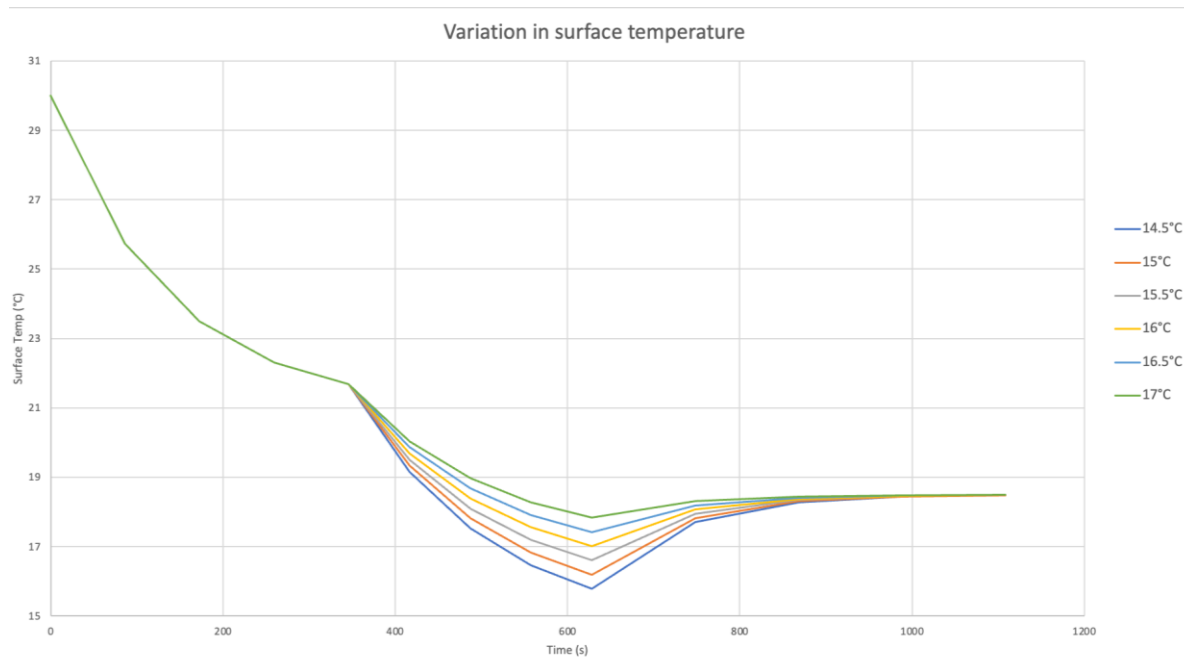


Figure 3.2.1

The varying surface temperature was then input into the conduction model to see if the internal target temperature of the chocolate was reached at what time. The time taken where the entire chocolate bar is below 19°C and its corresponding tunnel length was shown below.

Middle section cooling air (°C)	New time required to cool (s)	New Tunnel length (m)
15	640	8.32
15.5	649	8.437
16	658	8.554
16.5	668	8.684
17	683	8.879

Table 3.2.2

As Expected, there is more moderate the cooling air, the more time the chocolate bar needs to cool and thus the longer the tunnel needs to be. Therefore, a balance needs to be found between the cooling air and the length of the tunnel. Since one of the priorities of the overall project was to optimise footprint area, the length was kept as short as possible, as oppose to the temperature being moderate.

3.3 Varying inlet Velocity

The parameter which is important to consider when varying inlet velocity is whether or not the air reaches the chocolate surface at the required velocity. This has already been reduced from 5 m/s to 2 m/s in order to ensure gentle and uniform cooling without surface disturbances, however this can be further optimised to reduce the energy usage and cost of the system. Higher air velocities generally lead to increased energy consumption. The different inlet air velocities were modelled and compared on COMSOL Multiphysics and the results can be shown below.

Inlet velocity at 5m/s

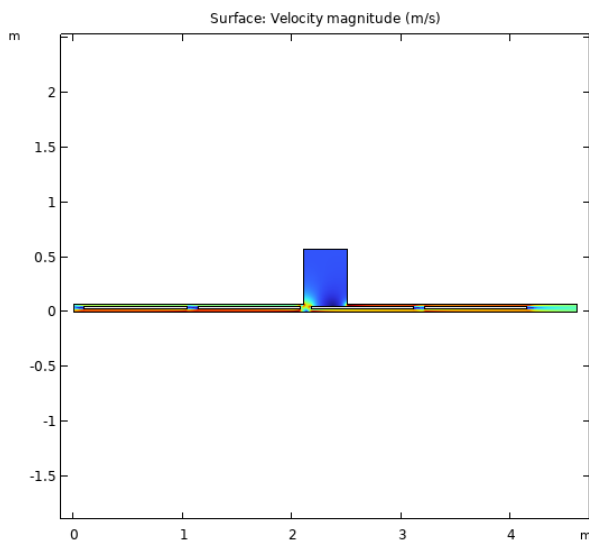


Figure 3.3.1

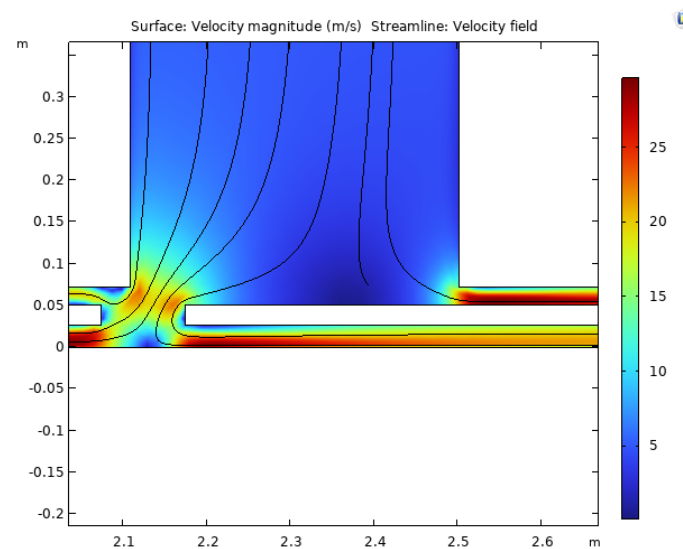


Figure 3.3.2

Inlet velocity = 2 m/s

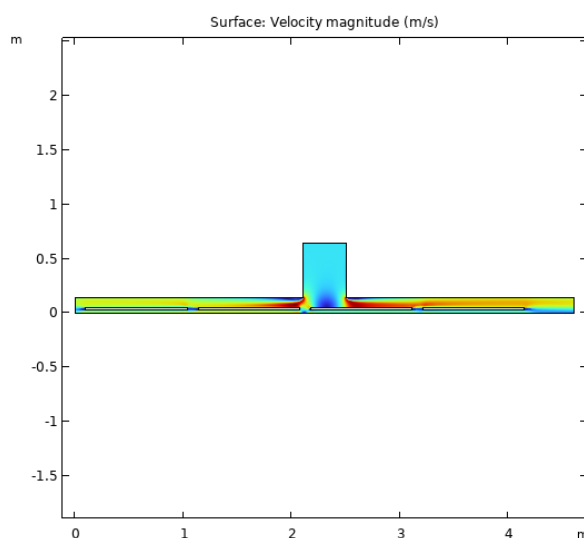


Figure 3.3.3

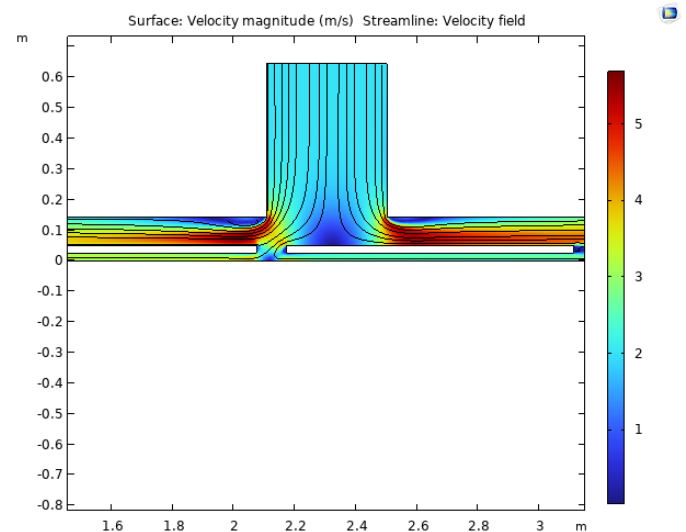


Figure 3.3.4

Inlet velocity = 1 m/s

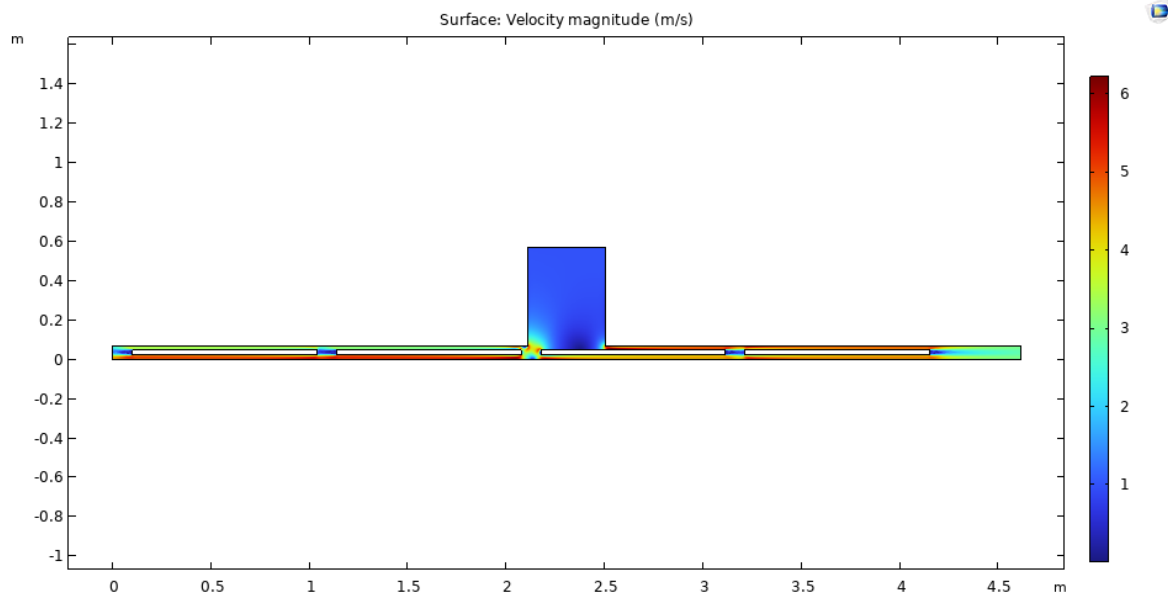


Figure 3.3.5

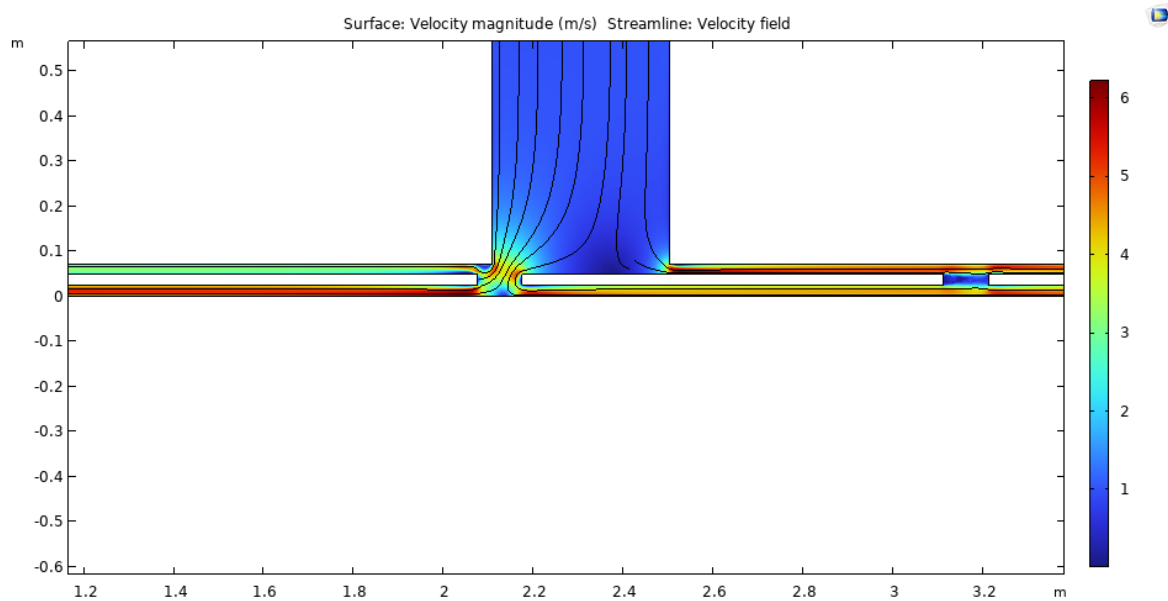


Figure 3.3.6

The internal air velocity when the inlet velocity is reduced to 1 m/s remains uniform and sufficiently distributed. Most importantly, the air stays between the desired range of 1m/s to 6 m/s that is used in industry. Therefore, making this velocity equally as effective, but more energy efficient than the higher velocities.

Inlet Velocity = 0.5

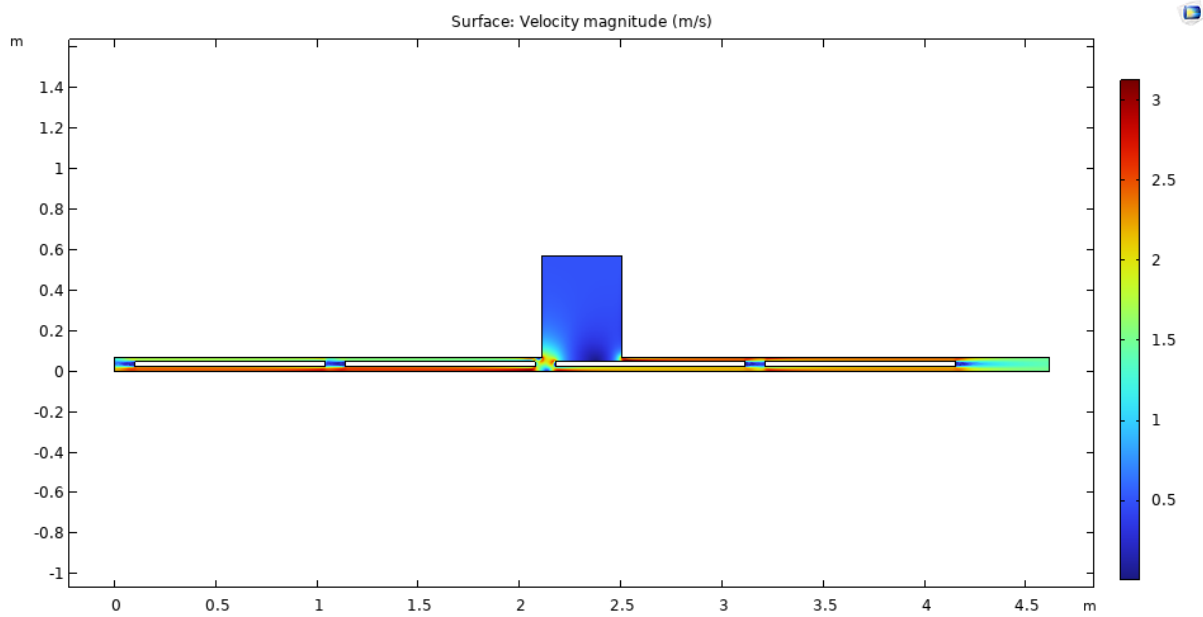


Figure 3.3.7

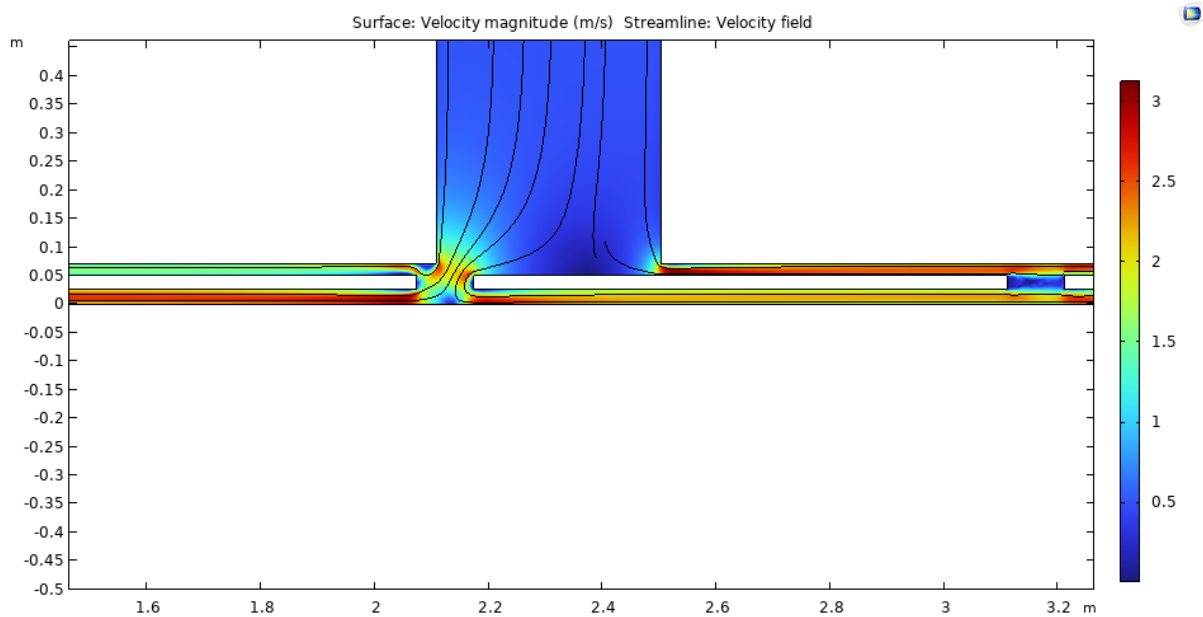


Figure 3.3.8

The internal velocity drastically decreases when the inlet velocity is set to 0.5 m/s. The maximum becomes 3 m/s and the minimum falls below 1 m/s. Therefore, it does not provide sufficient velocity to the system to allow for effective cooling.

The most efficient inlet velocity for the cooling air is 1 m/s.

The development from the optimisation is the drastic reduction in tunnel length from 14.53m to 8.23m, saving 6.3m. This will not only reduce the footprint area drastically, but also reduce the energy usage of the system. As a result of this reduction the final section of the cooling tunnel can be removed entirely, since the length of the final section is 6.245m. This creates an L shaped tunnel that can utilise even more floor space.

3.4 Operational limits

The Operational limits of a conveyor-based cooling tunnel depend on variables including maximum throughput, temperature variations of air, airflow capacity, composition of chocolate, temperature of chocolate.

If the conveyor speed increases, then there may not be enough time for the chocolate to fully form the desired crystals. If the conveyor speed is too slow, then the chocolate may 'overcool' leading to hard brittle chocolate. Brittle chocolate can also be caused by increased air flow or reduced cooling air temperature. This can be caused by malfunction in the refrigeration unit or the centrifugal fan. Brittle chocolate will lead to product cracking or shrinkage which will be undesirable for consumers. Also, if a stage in the upstream process such as tempering or deposition is not carried out properly, then the composition of the chocolate will vary. This inconsistency will disrupt the conditions required for the optimal cooling profile, likewise with the inlet temperature of the chocolate.

Regardless of these factors, it must be noted that the cooling process is an inherently stable process. These fluctuations in variables are highly unlikely. For example, the whole chocolate manufacturing process has set flowrate, so therefore there would be no logical reason for this to increase suddenly. The process is also a gradual one, with no sudden complex phase changes, therefore it is unlikely that operational limits need to be rigorously investigated. Instead, routine cleaning, maintenance and visual inspection would be sufficient in ensuring the system is performing in an adaptable manner.

If the entire manufacturing process wants to scale up in the future, the cooling tunnel would need to accommodate for an increase in production rate. The most practical option is to extend the length of the tunnel, to allow for a longer residence time. This means that additional chocolate will still cool sufficiently. The additional section will be identical to the one in the initial proposal with the design of all three lengths of the tunnel being utilised.

4.1 Mechanical Engineering Design

4.1.1 Engineering drawings

Front Section view

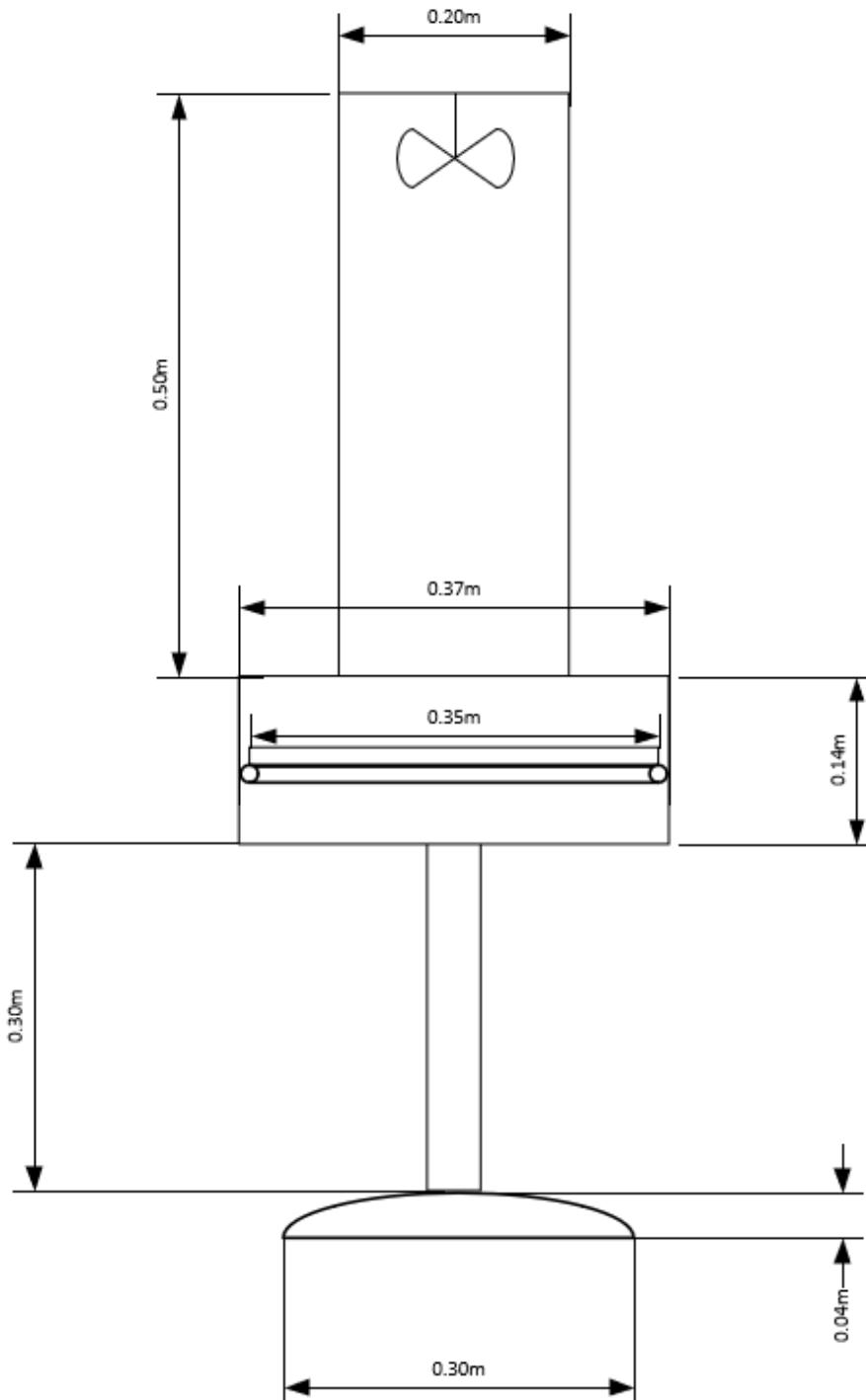


Figure 4.1.1.1

Side section view

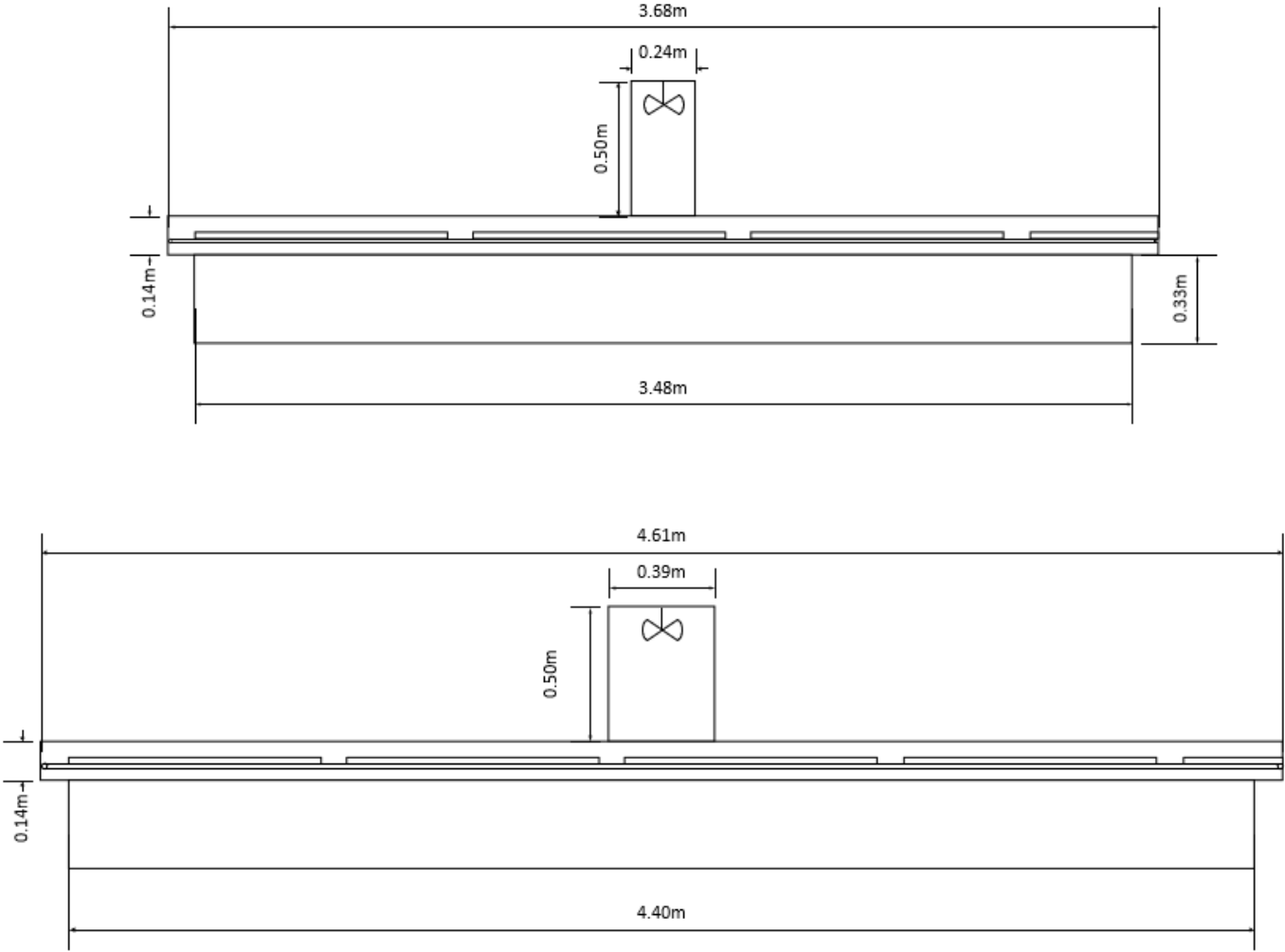


Figure 4.1.1.2

Front Section View

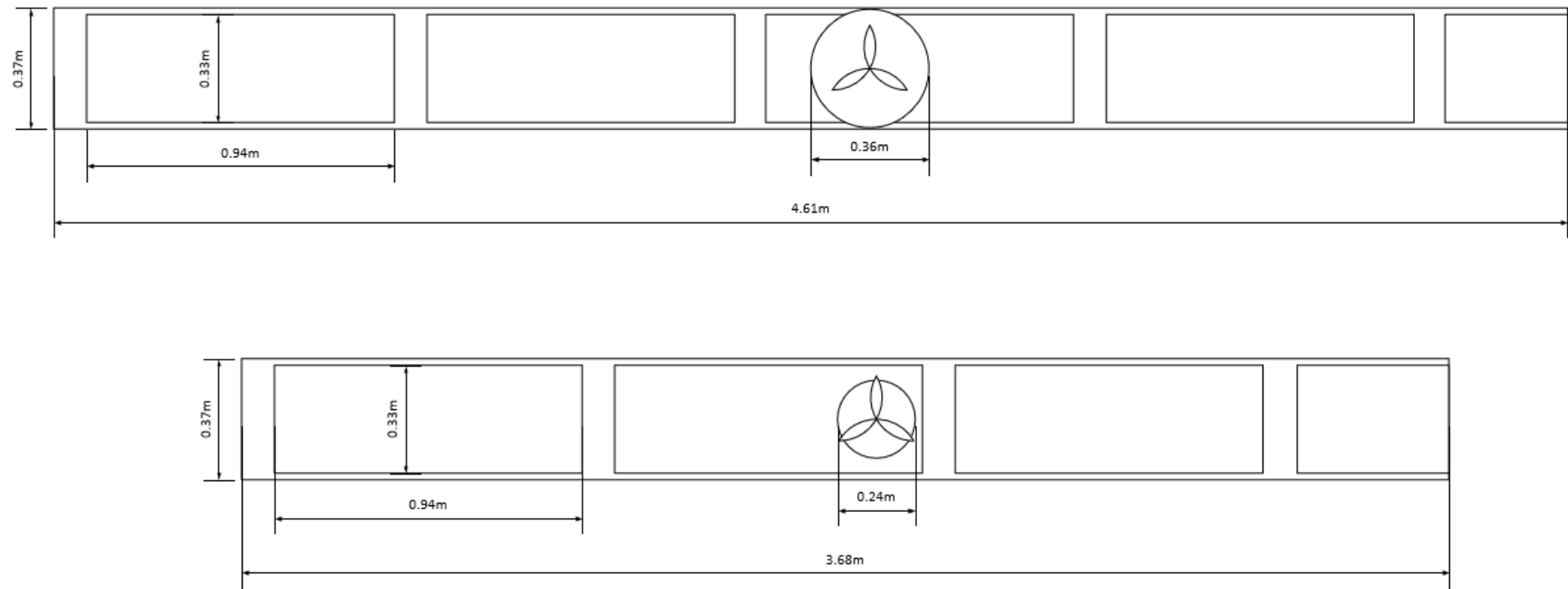


Figure 4.1.1.3

4.1.2 Belt transfer

As a result of the optimisation, the tunnel is divided into two sections as opposed to the previous three. This is because the reduced mould thickness, altered cooling air temperature and reduced residence time allowed for a shorter required tunnel length to achieve the same cooling effect. The two sections join at a right angle to create an “L” shape in order to reduce the footprint area. A corner transfer unit is used for the right angle transfer, this is in the form of a “Powered Pop-Up Belt Transfer”.

A Powered Pop-Up Belt Transfer is a set of timing belts that is placed just below the end of the first conveyor belt. When a mould reaches the end of the first belt, the belts are pushed up to come in contact with the base of the mould. The belts are motor driven and rotate perpendicular to the first conveyor, therefore moving the moulds sideways onto the second conveyor. As the base of the mould comes in contact with the second conveyor belt, it is moved along in the desired direction. After the transfer has commenced, the belts are lowered back down to allow for the next mould to reach the end of the first conveyor.

Pneumatic cylinders are used to create a lifting mechanism for the belts. Compressed air enters the cylinder from an air compressor and through a valve, causing the piston rod inside the cylinder to be pushed upwards and out of the cylinder. The pistons are directly connected to the underside of the belt platform, so the belts are raised. When the air is switched off, the piston retracts and brings the frame down with it.

The cylinders need to raise the belts at the right time, therefore information is required to have precise timing. Photoelectric sensors are used to detect the presence of a mould. A beam of light is emitted across the width of the conveyor belt which reaches a reflector on the opposing side. When this light is obstructed by a mould an electrical signal is sent to the PLC control system, this sends another signal to the solenoid valve in the cylinder, which allows air into the cylinder and causes the belts to rise. When the mould is transferred onto the next conveyor belt, there is no longer an object blocking the light beam, so the sensors send a new signal to the solenoid valve to allow the air out of the cylinder and thus lowering the frame.

There are two narrow belts that come in contact with either side of the base of the mould. These slide in parallel between the rollers of the first conveyor and rotate at a 90° angle. Each belt has a width of 10mm and a length of 360mm to match the dimensions of the rollers in the conveyor belt. There is a space of 200mm in between the two belts and they are raised by 20mm each time to provide enough lift to clear the initial conveyor of any moulds. These belts are looped around drive pulleys, which are connected to a shaft. The shaft is rotated by a motor, creating a motion which turns the belt. The motor is located under the frame and required 0.4 kW in order to match the belt speed of 0.5 m/s.

A frame is used to support the lifting and retracting system, it houses the motors, cylinders and belts. It is constructed from 304 stainless steel. It reaches from the floor to the base of the conveyor belt. The frame contains a movable platform that holds the timing belts and their shafts. This platform is raised up and down by the cylinders, which are held in place by mounting points. Mounting points are also used to hold the motors and sensors in place.

4.1.3 Conveyor belts

The two main conveyors are designed to transport the moulds smoothly through the cooling environment, this required synchronised movement between components. The conveyors are moved via geared motors, which power the system. The system transfer rotational energy from the motors to a series of rollers through a drive shaft. The motors are connected to a horizontal drive shaft by a chain, which runs along the length of the conveyor. This drive shafts connects to multiple sprockets, each connected to a corresponding sprocket mounted on the end of the rollers through a chain. So as the drive shaft is rotated by the motor, so are both sets of sprockets, causing all the rollers to rotate simultaneously. The components are held in place by a 304 stainless steel frame consisting of guards to house moving parts.

Each roller is 0.36m long, to suitably fit the conveyor width and provide enough space for the mould. The diameter of each roller is 40mm, as this is small enough for the required mould size but still strong and smooth. For a smooth continuous process the rollers should not be placed too far apart. Therefore, a spacing of $\frac{1}{4}$ of the width of the mould is chosen, an 82mm distance from centre to centre of each mould. On either end of the roller there is a bearing to allow for rotation. The sprocket sits on the outside of this, attached to the end of the roller, as it rotates it rotates the roller with it.

The conveyor speed is 0.052 m/s which directly links to the revolutions per minute (RPM) as shown by the equation below. This ensures that the rotation of the rollers is matched to the corresponding product flow rate. Where d_R is the radius of the rollers (m).

$$\text{RPM} = \frac{60 \times v_{\text{conveyor}}}{\pi \times d_R}$$

Equation 4.1.3.1

The RPM gives an indication for the motor power requirement, this also depends on the torque required to overcome the friction of the rollers and the weight of the moulds. Torque, T is the rotational force (Nm) needed to turn the rollers, given by the equation below. Where r_R is the radius of the rollers (m) and F is the force.

$$T = F \times r_R$$

Equation 4.1.3.2

Where;

$$F = m \times g \times \mu$$

Equation 4.1.3.3

m is the mass (kg), g is the gravitational acceleration (m/s^2) and μ is the coeefieint of friction.

4.1.4 Frame & Housing

The conveyor is held in place by a frame, this is a rigid stainless-steel structure that supports the conveyors, transfer units and cooling walls. Support brackets and mounting rails attach to the frame and support the conveyors. The brackets do not come in contact with the moving part, but instead are bolted to the conveyor bed. The rollers are mounted to the conveyor bed so they can move independently.

The frame is made from 304 stainless steel and it consists of two parts; a body and a base, these are connected through welding. The body is made from 2 parallel longitudinal beams attached to a curved base. The base distributes the load evenly across the floor, which provides stability. Each beam connects to the underside of the conveyor bed, the beams are 0.3m tall and 0.05m thick, they are placed on opposite sides along the conveyor. The base is 0.3m wide and 0.04m tall.

There is a cooling tunnel housing that encloses the conveyor system which keeps the temperature at the required level, by keeping the air inside. This is constructed from insulated 304 stainless steel panel with 10mm of thickness, there is a layer of extruded polystyrene on the inside for thermal insulation.

The panels are bolted onto the outside of the conveyor support frame using brackets. The conveyor will sit inside these walls and the panels will surround the sides and the top of the conveyor belt. There is food-grade sealing used between panel joints to prevent air leaks

The top of the housing has a duct in each section of the tunnel to allow for the fans airflow to enter the housing. There is also a baffle placed in between the two air sections to stop the mixing of air flows that have different temperatures. Temperature control thermometers can also be located inside the cooling tunnel.

4.1.5 Airflow distribution system

The airflow distribution is designed to ensure even consistent cooling across all the moulds. Centrifugal fans and air ducts are placed in the middle of the roof in each section of the tunnel. At the top of each section, there is a 0.2 m wide housing duct, this duct extends 0.5m where a centrifugal fan is located at the end. The fan drives cooling air downwards through the airduct, when the air reaches the end of the duct the air is evenly distributed across the width of the conveyor. The end of the duct has a slotted outlet which directs the air across the tunnel. The duct is welded onto the tunnel frame to prevent air leaks and maintain air pressure.

Turbulent airflow is generated using centrifugal fans. These fans have an impeller surrounded by casing. Air is drawn into the impeller, and it is accelerated rapidly through the centrifugal force of the impeller. The air then exits the impeller at a high velocity (1 m/s was used in the system) and it travels throughout the duct, out the duct and into the tunnel. The fan is mounted inside a stainless-steel enclosure which is directly connected to the duct. Motors are used to rotate the fan.

The final major mechanical component is the refrigeration system, which is responsible for supplying cooled air to the centrifugal fans. Previously, in the shortcut design a glycol heat

exchanger was used to cool the air, however a refrigeration unit was chosen due to its increased efficiency and ease of operation. The refrigeration system is an air-cooled chiller which is positioned outside the tunnel. Ambient air from the factory is drawn over cooling coil through a duct, where it is chilled before entering the centrifugal fan. Inside the coil chilled fluid is circulated through a coil and the warm factory air is drawn over the coil, therefore heat transfer occurs. The chilled fluid absorbs the heat from the air, so the air's temperature is lowered. R-404A (Hydrofluorocarbon) is a refrigerant fluid used in air conditioning, it is commonly used in the food industry due to its environmentally friendly nature and effective heat transfer capabilities. Due to its high energy efficiency, it is chosen as the chilled fluid in this system.

4.1.6 Material Selection

4.1.6.1 Frame

- Longitudinal Beams (Body) – Grade 304 stainless steel is the standard material used for food machinery frames, it's durable, strong and rust / corrosion resistance. This means that it can be cleaned frequently, without risk of degrading, so it is both hygienic and long lasting (AZoM, 2019). Each beam is 0.3 high and 0.05m thick and there are two beams per section. So the total beam volume is:

$$0.3\text{m} \times 0.05\text{m} \times 8.23\text{m} \times 2 = 0.2469 \text{ m}^3$$

The density of 304 stainless steel is 7,930 kg/m³ (Solitaire Overseas, 2024), therefore the weight is:

$$0.2469 \text{ m}^3 \times 7,930 \text{ kg/m}^3 = 1,958 \text{ kg}$$

The price of stainless steel is 0.7£/kg (Reclamet Limited, 2025). So, the price becomes:

$$1,958 \times 0.7 = 1370.6\text{£}$$

- Housing - Grade 304 stainless steel was used for the exterior of the tunnel. As previously mentioned, it provides a food-safe surface and is resistance to corrosion (AZoM, 2019). The inside of the tunnel is insulated with extruded polystyrene, to keep the desired air temperature inside the tunnel. The total tunnel dimensions is 8.29mx0.144mx0.366m therefore the total surface area becomes 8.456m². Using a thickness of 0.05m, then the volume becomes 0.4228m³, and thus the mass in 3124.39 kg and the price is 2187.14£.
- Housing insulation- On the inside layer of the tunnel housing there needs to be a layer of extruded polystyrene in order to retain the temperature of the cold air in the tunnel to minimise energy loss and ensure uniform product quality. The layer of insulation is based on industry standard (60-100mm) (ASHRAE Handbook, 2020). The thickness was chosen to be 60mm, this gives a volume of 0.812m³. With a density of 33kg/m³ (www.easycomposites.co.uk, n.d.), then the weight becomes 26.80kg, with a price of 4£/kg this becomes 107.18£
- Base- The base provides structural support for the entire tunnels weight, so therefore needs to be strong. It will also be made from 304 stainless steel, which helps with the simplicity of sourcing materials. The width of the base is 0.3m, the height is 0.04 and

the base runs the length of the whole tunnel. The base is a semi-circle, thus the volume is 0.132m^2 . This gives a weight of 975.48 kg and a price of £682.84.

- Baffles- In between the two tunnel sections there is a physical division to prevent mixture of air. This will also be made from stainless steel and will match the difference between cross sectional area of the tunnel and the cross-sectional area of the mould;

$$0.052992 - 0.00154 = 0.0515\text{m}^2$$

With a thickness of 1mm, the weight becomes 0.41kg and the price becomes £0.3.

4.1.6.2 Conveyor

- Conveyor belt – Polyurethane is commonly used in food production due to its compliance with FDA/US food standards. It is hygienic due to its natural resistance to bacteria, chemicals and water. Therefore, it can come in contact with food without any concerns (Bsbeltfactory.com, 2025). The typical weight for a belt of this material is $2\text{--}3\text{kg/m}^3$ and the cost is £50 per m^2 (www.alibaba.com, 2020). The total area of polyurethane is calculated below, this is the length and width multiplied by 2 to account for the top and bottom section of the belt. The thickness of the belt is 0.016m (Durabelt.com, 2019).

$$8.23\text{m} \times 0.368\text{m} \times 2 = 6.0592\text{m}^2$$

The belt also needs to wrap around half a roller (with diameter 0.04m) on either side.

$$\pi \times 0.04\text{m} \times 0.5 \times 2 = 0.1256\text{m}^2$$

The total area becomes.

$$0.1256\text{m}^2 + 6.0592\text{m}^2 = 6.18\text{m}^2$$

Thus, the cost becomes.

$$6.18 \times £50 = 309£$$

The weight of the belt is the volume multiplied by the density. The density of polyurethane is 1200 kg/m^3 (indiamart.com, 2017)

$$8.23\text{m} \times 0.368\text{m} \times 0.016\text{m} \times 1200\text{ kg/m}^3 = 58.17\text{ kg}$$

- Rollers- The rollers used under the belt will be made from 304 stainless steel. Since the rollers have a diameter of 0.04m and the conveyor length is 8.23m, there would roughly need 100 rollers for the belt. Each roller needs to have a hole in the middle to allow space for a bearing and shaft. A hole of 0.03m would be subsequent for this, therefore the weight of all the rollers becomes 146.2kg. The price of a roller and shaft with similar dimensions is £25 (Rollers UK, 2023), therefore all the rollers cost £250.

4.1.6.3 Airflow system

- Fan housing- 304 stainless steel is used again due to its ability to withstand pressure from airflows and hygienic nature. Each fan is placed in at the top of a 0.5m high duct that matches the required diameter of the pipe (0.360m for zone 1 and 0.237m for zone 2). With a thickness of 0.05m these two air sections thus required a total steel volume of 0.039m^3 . Giving a weight of 310.06kg and a price of £214.04.
- Impeller blades- 304 stainless steel will be used but will be much thinner, with a thickness of only 0.01m. The blades are organised in a circle that matches the required pipe diameter. There will be two sets of impeller blades (one for each section), zone 1's

impeller has a volume of 0.00102m^3 and zone 2's has a volume of 0.000441m^3 . This results in a weight of 11.59kg and a price of £8.11.

4.1.7 Material Summary

A summary of the materials and their relevant values can be found in the table below.

Component	Material	Dimension (m)	Weight (kg)	Price (£)
Frame	304 Stainless Steel	$0.3 \times 0.05 \times 8.23$	1,958	1370
Body	304 Stainless Steel	$8.29 \times 0.144 \times 0.366$	3124.39	2187.14
Body Insulation	Extruded Polystyrene	Volume = 0.812m^3	26.80	107.18
Base	304 Stainless Steel	$8.29 \times 0.3 \times 0.04$	975.48	682.84
Conveyor Belt	Polyurethane	$16.46 \times 0.368 \times 0.016$	58.17	309
Rollers	304 Stainless Steel	$\text{Ø}0.04 \times 0.36$	146.2	250
Fan housing	304 Stainless Steel	Zone 1: $\text{Ø}0.36 \times 0.5 \times 0.05$ Zone 2: $\text{Ø}0.237 \times 0.5 \times 0.05$	310.06	214.04
Impeller blades	304 Stainless Steel	Zone 1: 0.00102m^3 , 0.01m thick Zone 2: 0.000441m^3 , 0.01 m thick	11.59	8.11
Baffle	304 Stainless Steel	Cross sectional area = 0.0515m^2	0.41kg	0.3

Table 4.1.7.1

The total weight of the system is 6,611.10kg and the price of materials is £5,128.61.

5 Control Systems

5.1 Control Considerations

As previously discussed, the purpose of the system is to reduce the temperature of the chocolate gradually, in a manner that encourages desired crystal growth. Control systems are an essential to achieving this, it is a fundamental part of any manufacturing process and ensures that the process is carried out consistently and safely (Marketing, 2024). Control involves the regulations of key variables to achieve consistent product quality, increase production efficiency and reduce safety risks. Once the optimising and design of the system is completed, aspects such as tunnel length and number of fans cannot be varied. However, the process can be influenced by different control variables:

- Conveyor speed: This directly controls the residence time of the chocolate in the tunnel, which affects how thoroughly the chocolate cools and crystallises. Control systems can be used to dynamically vary the conveyor belt speed based on different inputs. This can be controlled not
- Airflow Temperature: Precise temperature control is needed to avoid defects such as fat bloom through maintaining target temperatures in each cooling zone, so the chocolate has stable crystal formation.
- Airflow velocity: The cooling rate is not just affected by the temperature but also the air velocity. Faster airflows increase the rate of heat transfer, increasing the rate of cooling. But too strong of an airflow is not energy efficient and can damage the surface of the chocolate.

Based on the optimisation, there are operational limits to these variables. The airflow simulation shows that the airspeed cannot be 0.5 m/s or below, as the flow will not reach the chocolate surface at the required velocity for cooling. Velocities of 5m/s and above provides little advantage to the cooling process and risk damaging the product, (New Food Magazine, 2017).

A Programmable Logic Controller (PLC) is a digital computer used to control and automate industrial processes. PLCs monitor inputs, process information and subsequently control outputs (UNITRONICS, 2023). This can be used to provide real time control for quick adjustments to ensure consistent operation in the cooling tunnel. The PLC will continuously monitor the different temperatures in the system to then correspondingly control outputs such as fan speeds, conveyor motor speeds and cooling unit temperatures.

PLCs utilise programmed logic to make decisions based on the values of input signals. This is called Ladder Logic, which consists of input conditions and output actions. When input conditions are met the programme will follow a logic sequence to make a decision on the form of output executed (Siemens AG, 2017). Operators can set target temperatures, conveyor speeds and air flow velocity through the human machine interface.

For temperature control, the PLC will receive inputs from temperature sensors throughout the cooling tunnel. These sensors continuously monitor the air temperature in each zone. The

signals are compared with reference set points and this information is processed through the programmed logic. If the temperature deviates from the setpoint, a control signal will be sent to the cooling unit. The temperature of the cooling unit is adjusted through opening or closing valves that control the flow of chilled R-404A fluid. This will subsequently adjust the cooling air to bring the temperature in the tunnel to the desired point.

The conveyor speed is regulated through the motor that drives the roller rotation. The variation in speed is achieved by adjusting the electrical power to the motor, this is controlled through a Variable Frequency Drive. The PLC monitors the inputs such as the temperature of the tunnel, process timings or operator instructions to send instructions to the Variable Frequency Drive that alters the speed. This changes the voltage provided to the motor, lower frequencies result in slower motor rotations and thus a slower conveyor, higher frequencies result in faster motor rotations and thus a faster conveyor. This will help ensure that the chocolate remains in each zone of the tunnel for the required duration that will result in uniform, gradual cooling.

Air velocity is controlled by a PLC through the control of the centrifugal fan. The fans are connected to motors that are also controlled by Variable Frequency Drives. The PLC receives input signals from airflow sensors, processes this information and sends corresponding output signals to the Variable Frequency Drives to either increase or decrease the fan speed. This will allow for accurate regulation of air velocity to ensure that the cooling rate is controlled.

5.2 Operational influence on other units in the process

Within the overall manufacturing process, changes to one component can influence the operation of the others. Understanding the interconnected nature of the system is essential in maintaining a consistent process. The performance of the cooling tunnel is depends on the preceding stages, and the performance of the subsequent stages depends on the performance of the cooling tunnel.

The tempering unit is responsible for starting the formation of the desired stable type V cocoa butter crystals. This is achieved in the tempering unit through three cooling sections and two heating sections, with impellers to provide shear stress which enhances nucleation of fat crystals. The temperer has a consistent flowrate of 223 kg/h with a residence time of 1 hour, a height of 0.55m and a diameter of 0.3m. If the temperature profile is not precisely controlled then the chocolate which enters the cooling tunnel will contain unstable, undesired polymorphs. These polymorphs will crystallise in the wrong structure during the cooling process, causing undesirable textures in the final product. This will disrupt the function of the cooling tunnel, as the process conditions are based on the expected type V crystals. If the tempering unit fails to produce the correct crystals, then the cooling tunnel must compensate by having to cool for longer or at a higher rate. This will lead to higher energy consumption and reduced operational efficiency, whilst also compromising the quality of the final product.

Another unit that can significantly influence the performance of the cooling tunnel is the depositor. The depositing stage occurs immediately before the cooling stage so can have an important impact on the cooling process. If the depositor dispenses inconsistent volumes of liquid chocolate into the mould then the thickness of the chocolate will vary. The thickness of

the chocolate is a highly important property during the calculations of all the heat transfer calculations. Therefore, if the thickness varies than the calculations that the design is based on becomes invalid. The variations in thickness affects how quickly each chocolate cools, therefore it will compromise the tunnels ability to provide uniform cooling. Also, if the chocolate is deposited at inconsistent temperatures, then the initial boundary conditions for the calculations also become invalid, which will lead to defects in the final product.

The performance of the cooling tunnel affects the properties of the solidified chocolate and thus the performance of the components later on in the process. The cooling tunnel must ensure the balance between the chocolate completely solidifying but not over hardening. Inadequate cooling can result in the chocolate being too soft to properly be removed from the moulds during the demoulding stage. On the contrary, overcooling can lead to reduced density and thus shrinkage of the chocolate. This can increase the likelihood of the chocolate breaking during the demoulding stage. Breakage can occur due to incomplete releases, sticking or brittle properties of the chocolate. Therefore, it must be ensured the chocolate reaches the optimal temperature at the end of the cooling tunnel.

Broken pieces of chocolate or chocolate that doesn't meet quality standards are rejected and recycled in a rework tank. This is where the chocolate is melted down and prepared to be reintroduced into the system. If the properties of the chocolate are inconsistent then it can affect the performance of the components downstream. Therefore, if the chocolate has not been cooled properly, there will be improper crystals formed that the system will not be suited for, affecting the delicate nature of the process.

5.3 Safety considerations

Process safety is a framework implemented to reduce the system's potential to cause damage. This required interdisciplinary considerations of engineering, operations, design, management and training.

Dangers in temperature related processes often occur due to extreme temperatures. However, in the cooling process the temperatures used are all moderate, so pose limited risk to the operators. Air velocities are also moderate and have been even further reduced after optimisation, making the cooling tunnel a safe process, relative to other units. Regardless, there are still safety aspects that need to be considered.

Firstly, mechanical hazards are present. These are mainly centred around the moving components such as the conveyor system and fans. These tend to move at high speeds so can cause damage to someone on impact or trap body parts if proper guarding is not in place. To prevent risk of these injuries, moving parts should be enclosed in protective covers and emergency stop buttons.

Electrical safety also needs to be considered due to the presence of electrical components such as sensors, motors and control panels, PLCs and variable frequency drives. All wiring and electrical parts need to be properly sealed, grounded and placed. Industry standard electricity rules need to be followed to reduce the chance of electric shocks.

The refrigeration unit can also pose safety risks if leaks occur. The coolant, R-404A is not highly toxic, however it can still pose potential health hazards. These include skin irritation and severe eye irritation if exposed to these parts. If inhaled it can cause symptoms of asphyxiation, loss of coordination and an increased pulse rate (Refrigerants.com, 2025). Therefore, a proper drainage system is needed underneath the cooling tunnel to allow for leaked fluid to be drawn away.

Hygiene is also a fundamental concern in food production. Materials used must be easy to clean to make sure that residue food does not cause microbial growth. Any surface that comes into contact with the chocolate should be made with food-grade material. Cross contamination should also be avoided, this is done by ensuring that the inlet air is not contaminated with air from the external air. This is achieved through a filtration system.

To reduce human errors accident prevention systems are needed. All operators and engineers must undergo specific equipment training before working with the process. These will come in the form of standard operating procedures (SOPs). SOPs are documents that contain instructions that ensure that the correct procedures are followed across all stages of the process. Each employees need to be trained with the SOP before using any equipment.

Another accident prevention system is the ‘Lock Out Tag Out’ procedure. This is used during maintenance when employees are carrying out work to ensure that machines are not powered on. This prevents machines from restarting when someone is working inside or near a machine, preventing risks of injury. Before cleaning or maintenance, the equipment will be shut down and all electrical, mechanical and pneumatic sources are isolated. These sources will be turned off and locked in place by each individual that works on the machine. Safety tags are attached to the locks to show others who is working on the machine.

Lock Out Tag Out is highly effective at preventing machinery from harming workers, it reduces the risks of moving parts colliding with workers and causing injuries. Once all the necessary work is carried out on the machines the locks and tags are removed from the equipment and the energy sources are restarted, the machine is now ready to resume production.

Protective Personal Equipment (PPE) is also important in protecting operators and engineers when they are near the machine. PPE is equipment worn by a worker that physically protects them from health and safety risks. In the chocolate manufacturing process, this would include overalls, safety glasses, steel cap boots, ear plugs and hair / beard nets. All these are necessary for workers to wear in order to protect them from unexpected damage. A visual depiction can be found below.



Figure 5.3.1

5.4 Startup Shutdown

Before operation of the cooling tunnel commences, a detailed inspection needs to be carried out. Operators should carry out all relevant safety checks. These include:

- Checking the mechanical guards and covers are in place.
- Confirm there are no loose objects that could interfere with moving parts.
- Checking for visible leaks in the chilling system.
- Test all isolation points and emergency stop buttons
- Verify electrical components are securely closed and sealed.
- Inspect floors for spills or residue.

Once the safety checks are done the electrical power can be turned on, followed by pneumatic and other fluid sources. Each component needs to be started in a gradual sequence to reduce the risks of sudden hazards. Throughout the start-up process operators need to continuously monitor the pressure, temperatures and mechanical velocities, to see if there are any sudden issues occurring.

Since only one product is being made, there is no requirement for different thermo and aerodynamic condition settings to be in place. The settings required for the product will be standard.

The cold air will be let into the system for 10 minutes before the chocolate flow commences, this is to allow for the air in the tunnel to reach the desired temperature uniformly.

When shutting down the tunnel, the steps must be followed in a rigorous manner, to ensure a smooth problem-free procedure. The first step of the procedure is that the flow of chocolate is turned off and any chocolate remaining in the tunnel should be allowed to fully pass through.

The next step is that the cooling system needs to be powered down. The refrigeration unit is switched off, but the fans are kept running for a period of time, this is to avoid sudden thermal shock. The airflow (fans) is then subsequently turned off, then the conveyor belt and its transfer unit. Once all the mechanical motion has stopped the machines are isolated and the main power is turned off. Once all the components have been turned off, then an inspection of the equipment and safety checks is carried out.

Before starting up and after shut down cleaning and maintenance of the equipment needs to be done, this is discussed in the section below.

5.5 Cleaning / Maintenance

Maintaining a clean tunnel is not only important for hygiene, but also for product quality and consistent operation. Since chocolate residue can lead to obstructions, the system can experience hazards, blockages and faults. Therefore, regular maintenance needs to be carried out to prevent this. Cleaning is done to prevent the built up of chocolate deposits, sugar residues, and microbial growth. Before any cleaning occurs, the machines need to be isolated and locked out, to ensure that no moving parts cause danger to operators.

- Surface wipe downs are carried out at the end of each shift, to remove any residue. This is done with food-safe cleaning chemicals such as a neutral pH food-grade detergent, along with nonabrasive cloths. Every surface needs to be cleaned, including the inside of the tunnel walls, conveyor belt and fan housing.
- The floors around the tunnels need to be washed and drained to remove condensation. Drying then needs to be done to prevent slips and injuries.
- Fan blades and ducts need to be cleaned less frequently, so can be done after every 7 shifts as opposed to after every shift. The conveyor belts also need to be inspected to check for stuck chocolate or dirt. Any dust particles need to be hoovered,

Regular maintenance is important because it increases the life of the equipment, which is beneficial both economically and environmentally. There are routine mechanical checks that can assist in avoiding unexpected failures. This can be done through Regular Maintenance (more frequent) and Planned Maintenance (less frequent).

- Lubrication of any moving part needs to be done as part of Regular Maintenance, this includes bearings in the conveyor belt rollers, motor bearings in the fans and conveyors, shafts in the fans and conveyors and any chains. Food grade lubricants need to be used, and over-lubrication needs to be avoided.
- The conveyor system needs to be mechanically inspected, this includes checking the belt alignment and tension during planned maintenance. Every 6 months, the conveyor belt needs to be replaced to remove any chances of having a degraded belt.
- The motors in the fans and conveyor systems also need to be checked regularly
- Electrical components also need to be checked during planned maintenance. The sensors need to be calibrated, and the PLC inputs and outputs need to be checked. The electrical panels also need to be checked for loose connections. Regularly test emergency stops, interlocks, and alarms to confirm they are fully operational.

The frequency of maintenance and cleaning depends on the volume of product that passes through the tunnel. Higher volumes increase the risk of residue build up as well as the strain on the mechanical parts. Therefore, if the process is at a high production efficiency, the equipment will require maintenance and cleaning more often. The environment also affects the frequency, varying temperatures can cause increased condensation or microbial growth, which would require more frequent cleaning.

5.6 P&ID & HAZID

A Piping and Instrumentation Diagram (P&ID) is a drawing that visualises the piping, equipment, control and instrumentation within a process. A diagram was drawn to support the engineering design of the cooling tunnel. This included all the pumps, fans, controls, sensors and valves that were required.

A Hazard Identification (HAZID) is a structured, systematic method used to identify possible hazards in a process. It involves evaluating components of the process and the possible

scenarios that could occur, with the causes. Then looking at the consequences and methods to mitigate and prevent the severity of the consequences. It is carried out in the preliminary stages of design to improve process safety. The HAZID also contains a hazard index based on the likelihood of the event and the severity of the event. This is shown in the table below.

Initiating event frequency (Events per year)		Severity				
		First aid injury (E)	Recordable injury (D)	Lost time injury (C)	Permanent injury or death (B)	Multiple deaths (A)
1	1 per 10 years	1E	1D	1C	1B	1A
2	1 per 100 years	2E	2D	2C	2B	2A
3	1 per 1,000 years	Tolerable	3D	3C	3B	3A
4	1 per 10,000 years	Tolerable	Tolerable	4C	4B	4A
5	1 per 100,000 years	Tolerable	Tolerable	Tolerable	5B	5A

Table 5.6.1

The conclusions drawn around the methods of mitigation and prevention of hazards are then used as a basis to improve the design of the P&ID. This was in the form of instrumentation and control throughout the process. A temperature and flow control loop were added to monitor and moderate the variables, to keep the process stable and safe. These additions were drawn in red to highlight the changes made.

Overall, it can be seen that the cooling process is a relatively safe one. The process does not use extreme temperatures or other process conditions, therefore the severity of hazards are low. The process also has precautions and protection layers in place to reduce the likelihood of hazards occurring.

The initial P&ID can be found below in *Figure 7.6.1*, with a key of symbols found in *Figure 7.6.2*. The HAZID was carried out in *Table 7.6.2* and the subsequent influence of the HAZID outcomes are depicted in the updated P&ID in *Figure 7.6.3*.

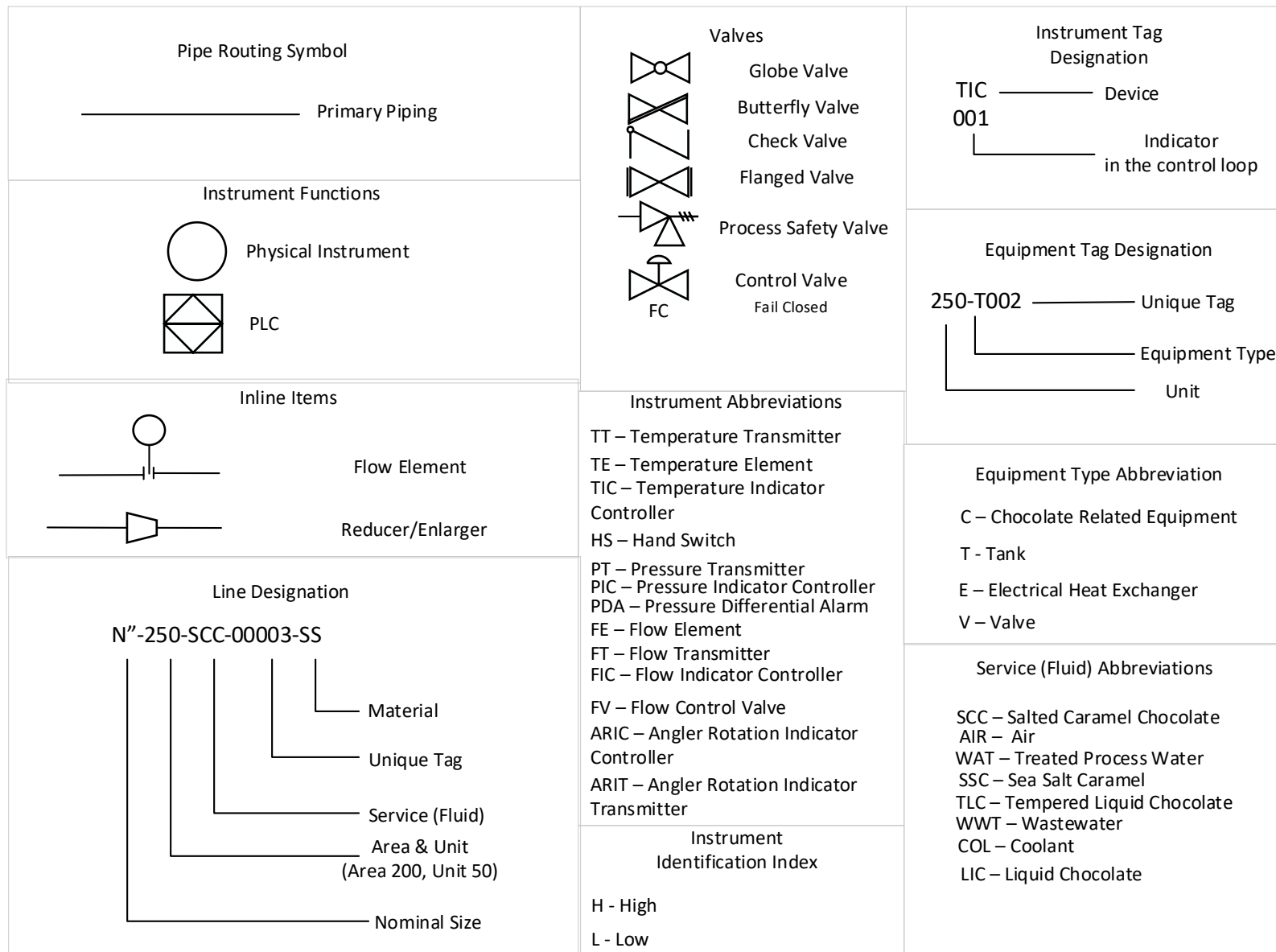


Figure 5.6.2

Guide Words	Consideration	Cause	Consequences	Hazard Index	Safeguard
Process Upsets	Flow	Valve Failure	Overpressure of air in the system, damaging the product and risking injury.	3D	Regular Maintenance of valves. Backup Valves.
		Pump Failure	Incorrect cooling conditions, damaging the product. Introduction of contaminants in the system.	4E	Regular maintenance of pumps. Manual hand switch for emergency stops
		Pipe Failure	Leakage of cooling air, causing incorrect cooling conditions and a contaminated product.	3C	Addition of flow indicator to monitor any sudden changes in flow.
	Temperature	Refrigeration Unit Failure	Inappropriate temperature in system causing incorrect cooling conditions and a damaged product.	4E	Regular maintenance and checks of refrigeration unit. Regular replacement of cooling fluid.
		Temperature control Failure	Inappropriate temperature in system causing incorrect cooling conditions and a damaged product.	3E	Regular manual checks and tests of the control system.
	Pressure	Pressure Control Failure	Incorrect cooling conditions, damaging the product.	3D	Regular manual checks and tests of the control system.

	Composition	Tempering and Depositing Unit Failure. Leaking Storage Vessel	Cooling conditions will not match new composition, so product will contain defects.	3E	Regular maintenance of tempering and depositing units.
Hazardous substances	Cooling Fluid (R-404A) contaminations	Leakage in the refrigeration unit	Health consequences, such as skin/eye irritation and symptoms of asphyxiation, loss of coordination and an increased pulse rate.	3C	Container for cooling fluid storage is secure and undergoes regular maintenance.
	Cooling Fluid (R-404A) Flammability	Leakage in the refrigeration unit	Flammable liquid can cause fires that can become out of control and cause damaged equipment and injury.	4B	Cooling fluid container is kept far away from any potential ignition sources.
Environment	Waste	Malfunctions and contaminants	Product that cannot be recycled is sent for waste disposal, causing environmental degradation.	3E	
		Pipe Failure	Air leakage and cooling fluid leakage can cause energy inefficiencies. Cooling fluid may be especially harmful to the environment.	3C	Addition of flow indicator to monitor any sudden changes in flow.

Table 5.6.2

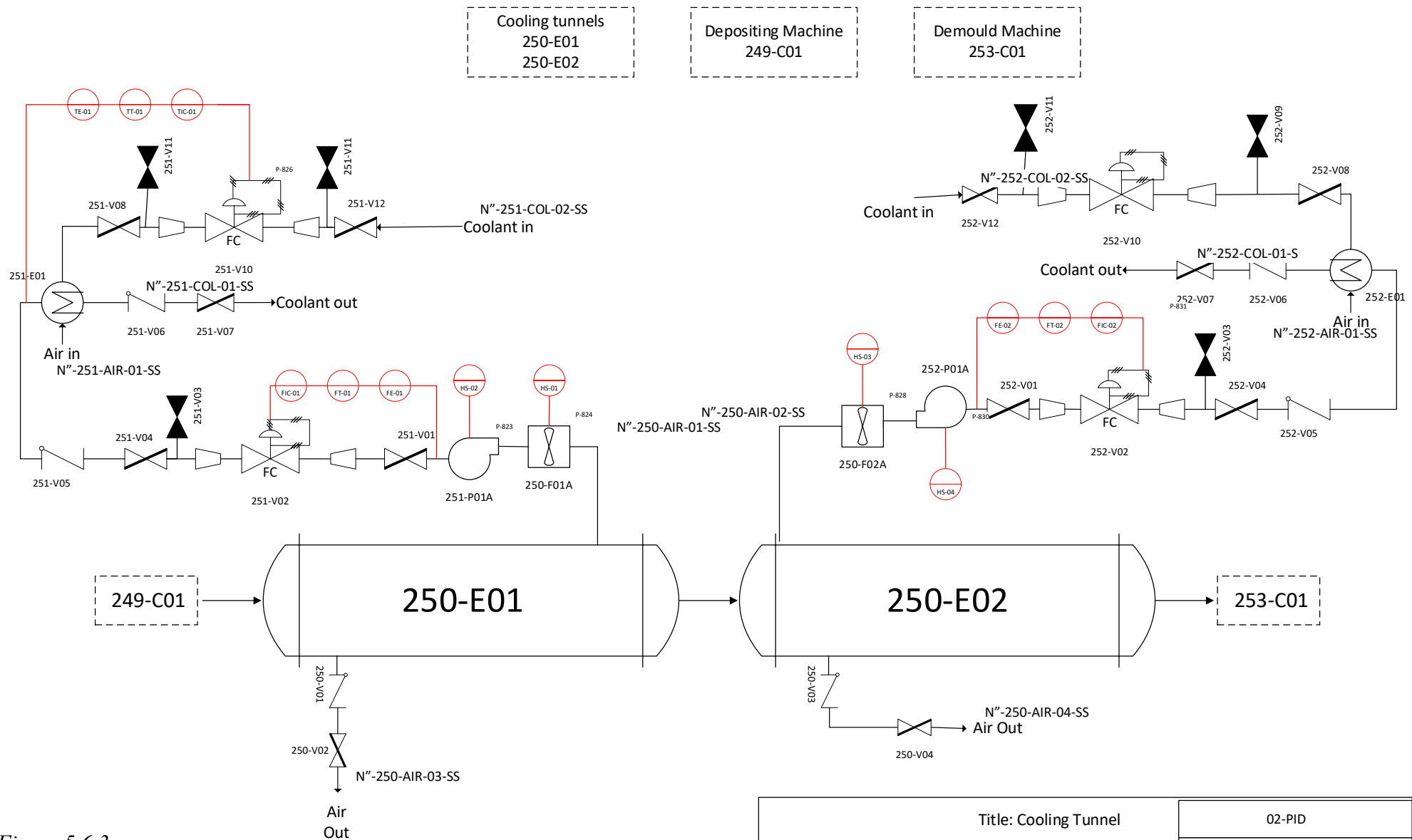


Figure 5.6.3

Title: Cooling Tunnel		02-PID	
Owner Group:		P&ID	
Drawn By:	Sohail Shaikh	18/04/2025	
Checked By:	Chak Lam Tam	18/04/2025	



University of Bath

Product and process design
Chocolate manufacturing with
water treatment facility

5.7 LOPA

A Layer of Protection Analysis (LOPA) is a risk assessment that evaluates the effectiveness of the safety systems that have been put in place. It looks at the likelihood of an event and the extent of severity of the event. A series of independent protection layers that could prevent the outcome are also considered. (Peters, n.d.) The objective is to demonstrate that sufficient Independent Protection Layers (IPL) are in place to reduce the likelihood of an event to an acceptable level. An IPL must be effective in preventing the unwanted event and independent on other IPLs taking place.

The Initiating event frequency (IEF) is the amount the event occurs per year, it shows the frequency of the event occurring. This is multiplied by the probability of an IPL failing (PFD) to get the Hazard Rate (H), which is the estimated frequency of the unwanted event.

A LOPA was carried out on the event of a cooling fluid leakage from the refrigeration unit.

Scenario	Cooling fluid leakage from the refrigeration unit, causing health damages or environmental impact.		
	Description	PFD	Frequency (yr ⁻¹)
Initiating event	Pipe leakage or burst in refrigeration unit		10 ⁻³
Condition Modifiers	Probability of fluid reaching accessible area	10 ⁻²	
	Probability of worker present	10 ⁻¹	
	Probability of fatal injury (severe irritation, asphyxiation)	10 ⁻¹	
	Flow control system failure	10 ⁻¹	
Unmitigated Frequency of Consequence			10 ⁻⁸
IPLs	Probability of flow control system failure	10 ⁻¹	
	Ventilation System failure	10 ⁻¹	
Total PFD for IPLs		10 ⁻²	
Frequency of Mitigated Consequence			10 ⁻¹⁰
Is the risk tolerance level met?: Yes			
Recommended Action :	Alarm for leak detection	10 ⁻¹	

Table 5.7.1

The maximum risk tolerance used in industry is 10⁻⁶ yr⁻¹, since the calculated frequency of mitigated consequence is 10⁻¹⁰ yr⁻¹ then the threshold is not met and the risk is acceptable. This shows that the current safeguards (IPLs) are sufficient in reducing the risk of hazards.

5.8 Critical Review

The design for the unit considers a range of chemical engineering fundamentals that would have a significant influence on the design. Heat transfer and fluid dynamics are both rigorously modelled. These principles comprehensively calculate process variables such as air temperature, air velocity, conveyor speed, air direction, residence time to a high degree of precision. The design was then optimised to make the process more economically and energy efficient, through analysing these variables with the methods used for design.

However, there are still areas where the process can be improved upon. The process is highly dependent on upstream process units, such as the temperer and the depositor. If there are variations in the product output from these units then the set process conditions in the cooling tunnel will not be suitable. Both the temperer and depositor must operate within the set parameters to ensure that the composition, structure, and temperature of chocolate enters the tunnel. Variation of these properties will compromise the tunnel's ability to produce uniform products.

This can be mitigated by the implementation of safeguards or buffers before the cooling tunnel. These can come in the form of control loops/ feedback systems in between the units that can detect variations and adjust the process suitably. The current cooling tunnel does not have a system to adapt to variations in temperatures or compositions of the inlet chocolate. A control system with a PLC could adjust airflow or air temperature to deal with the variations and ensure a consistent cooling profile.

A holistic overview of the unit highlights its dependency on the input data used for the parameters in the calculations. The rigorous design uses data based on the assumption that the data is complete, comprehensive and does not vary dramatically. If real world parameters such as the chocolate throughput, chocolate composition, chocolate viscosity, air flowrate, air velocity, air composition and air viscosity significantly vary from those in the theoretical calculations then the performance of the process will be compromised. Incomplete data might cause inadequate residence time, incorrect airflow and insufficient heat transfer.

An example of this would be if the heat transfer coefficient values of chocolate and air were incomplete or varied significantly then the rate of both conduction and convection heat transfer would be inaccurate. The rate of heat transfer is what the tunnel design was based off, so variations in the heat transfer coefficients would cause undercooling or overcooling, affecting product quality and uniform output.

A possible upgrade to mitigate this issue would be the addition of adjustable controls for process variables such as air temperature, air velocity and conveyor speed. Therefore, if the product quality was not up to standard the process can be refined. If the process variables are adjustable, then the system needs to be able to adjust to changes made. Therefore, the tunnel length, fan capacity and refrigeration capacity need to be upgraded to allow for variations.

For further upgrades, a PID control system (Proportional–Integral–Derivative) can be used to automate responses to the system. Instead of having on/off control, a PID can adjust cooling intensity smoothly and accurately. For example, if the temperature of the tunnel deviates from

the required temperature, then the PID controller can adjust the coolant flow accordingly. Also, if the chocolate enters the tunnel at an unexpected temperature, then the PID controller would again adjust either the coolant flow or the air velocity to cope with the corresponding inlet temperature. This will both increase energy efficiency and help ensure consistent high-quality product output.

6 Summary

6.1 Spec Sheet

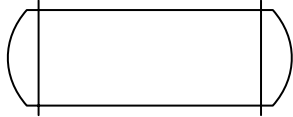
Project: Chocolate manufacturing with water treatment facility					
Cooling Tunnel	Segment 1		Date 13/03/2025		
Equipment Dimensions	Design		Sohail Shaikh		
Width	m	0.368			
Height	m	0.144			
Length	m	8.23			
Weight	Kg	6,611.10			
Outer Surface Area	m²	8.56			
Residence Time	S	633	Energy Requirements		
Conveyor Speed	m/s	0.052	Compressor	W	4.23x10 ⁻³
Heat Removed	W	63000	Conveyor	W	12.78
Function	To gradually cool and solidify the chocolate				
Number of Units	2				
Material of Construction	304 Stainless Steel (food grade)				
Air Flow System 1					
Pressure Drop	Pa	3.6 x 10 ⁻³	Pipe Diameter	m	0.394
Mass flowrate	kg/s	0.746	Reynolds		132,400
Volumetric Flowrate	m³/s	0.609	Change in Chocolate temperature	°C	-5
Superficial Velocity	m/s	1	Air Temperature	°C	21
Air Flow System 2					
Pressure Drop	Pa	3.6 x 10 ⁻³	Pipe Diameter	m	0.237
Mass flowrate	kg/s	0.284	Reynolds		39,780
Volumetric Flowrate	m³/s	0.220	Change in Chocolate temperature	°C	-6.5
Superficial Velocity	m/s	1	Air Temperature	°C	14.5

Table 8.1.1

6.2 Conclusion

The cooling tunnel is an essential part of chocolate manufacturing, ensuring that the deposited liquid chocolate solidifies in the correct manner. This way the chocolate product will have the desired structure, texture and gloss which makes it more likely to succeed commercially. To achieve these properties the chocolate needs to form the desired *Type V Crystals*, this will result in no fat bloom or visual defects in the final product. Forming these crystals requires gradual cooling within specific temperature ranges, therefore the cooling process needs to be precise and consistent.

To design a precise and consistent cooling unit, core principles such as heat transfer and fluid dynamics were rigorously considered. These were used to create models that simulated the thermal and aerodynamic behaviour that occurs in the process, these models were used as the baseline to design the equipment used in the process. Heat transfer via convection was investigated to find the temperature at the surface of the chocolate and thus the required residence time.

Heat transfer via conduction was modelled to find the internal thermal gradient in the vertical direction of the chocolate bar and its polycarbonate mould. This would be used to calculate the temperature of the system required to ensure full cooling of the bar. Fluid dynamics was investigated through CFD and the Navier-Stokes equations to predict the movement of fluid. This would visualise airflows in the tunnel and was used to find the required inlet velocity of air and the fan placement.

These were then further refined using the same models during the optimisation phase, where the tunnel length was reduced to increase energy efficiency and reduce footprint area, the final length was reduced to 8.23m. The air velocity was also refined to 1m/s through iterative analysis of the air distribution, again increasing energy efficiency.

The final design of the unit involves a conveyor-based system surrounded by stainless steel walls. The conveyor belt moves at 0.052 m/s and the total tunnel dimensions are 0.368m wide and 0.144m high. The tunnel is split into two different sections with a baffle, the first with a length of 4.61m and the second with a length of 3.62m. This aims to gradually cool the chocolate through having two different temperature zones, the first zone has a cooling air temperature of 21°C and the second has a temperature of 14.5°C. This will gradually and stably reduce the chocolate temperature from 30°C to 18°C, the optimal temperature for storing chocolate. The fans are both placed in the middle of the roof in each zone at the top of a 0.5m pipe, the pipe diameter varies in each zone and is dependent on flowrate.

Air is cooled through a refrigeration unit outside the tunnel, the air is then accelerated through a centrifugal fan into the tunnel. A duct guides the air to the top and bottom surfaces of the chocolate mould, ensuring that it is cooled from both sides. The conveyor belt is moved through a mechanical system involving motors, shafts, sensors, rollers and chains.

Material selection is an important stage in the process, the main bulk of the tunnel was made from 304 stainless steel. This includes the frame, base, body, baffle, fan housing, impeller blades. The conveyor belt was made from polyurethane and the system was insulated with

extruded polystyrene. The design of the tunnel was empirically validated against literature, particularly Grob (1991). The comparison showed a general consensus between the technical calculations and practical design of both projects.

Finally, a control strategy was put in place to both ensure an efficient process and increase safety. After the drawing and evaluation of a P&ID, temperature and flow sensors and regulators were placed strategically, to monitor process conditions and alter them correspondingly. Fan and conveyor motors are equipped with variable speed drives to alter the process dynamically based on the control system. This means that fluctuations in the process or environment will be dealt with accordingly in order to maintain a consistent and effective process.

Overall, the tunnel design demonstrates a successful integration between thermal modelling and aerodynamics to create a structurally optimal design that will ensure consistent, high-quality chocolate with the desired characteristics.

References

Executive summary

Richard Caines (2024). *UK Chocolate Confectionery Market Report 2021* | *Mintel.com*. [online] Mintel Store. Available at:.

IBISWorld (2024) Chocolate Production in the UK Industry Report (IBISWorld Report C10.820). Available at: <https://www.ibisworld.com/united-kingdom/market-research-reports/chocolate-production-industry/> (Accessed: 01/04/2025).

UK Health Security Agency (UKHSA) (2023) Sugar reduction and wider reformulation programme: Report on progress towards 20% sugar reduction guidelines. London: UKHSA. Available at: <https://www.gov.uk/government/publications/sugar-reduction-report-on-progress-between-2015-and-2020> (Accessed: [insert date]).

Introduction

Sato, K. (2018). *Polymorphism of Lipid Crystals*. [online] pp.17–60. Available at: <https://doi.org/10.1002/9781118593882.ch2> [Accessed 1 Apr. 2025].

New Food Magazine. (2017). *Chocolate cooling and demoulding*. [online] Available at: <https://www.newfoodmagazine.com/article/2048/chocolate-cooling-and-demoulding/> [Accessed 27 March 2025].

Beckett, S.T., 2000. *The science of chocolate*. Cambridge: Royal Society of Chemistry. Available at: https://muhammadsabchi.wordpress.com/wp-content/uploads/2010/04/beckett-the_science-of-chocolate.pdf [Accessed 9 Apr. 2025].

Staff (2022). *Chocolate Tempering: Beta Crystal Nucleation and the Purple Haze Phenomenon - Pastry Arts Magazine*. [online] Pastry Arts Magazine. Available at: https://pastryartsmag.com/general/chocolate-tempering-beta-crystal-nucleation-and-the-purple-haze-phenomenon/?utm_source=chatgpt.com [Accessed 10 Apr. 2025].

Demirel, Y. (2018). *Motor Efficiency - an overview* | *ScienceDirect Topics*. [online] Sciencedirect.com. Available at: <https://www.sciencedirect.com/topics/engineering/motor-efficiency>.

ISO (2024). *ISO 21182:2024 – Light conveyor belts — Determination of the coefficient of friction*. Available at: <https://www.iso.org/obp/ui/en/#iso:std:iso:21182:ed-2:v1:en> (Accessed: 18 April 2025).

Sntoom.net (n.d.). *How much power does an industrial fan consume?* [online] Available at: <https://sntoom.net/how-much-power-does-an-industrial-fan-consume/> [Accessed 18 Apr. 2025]

Unit brief

Beckett, S.T., 2000. *The science of chocolate*. Cambridge: Royal Society of Chemistry. Available at: https://muhammadsabchi.wordpress.com/wp-content/uploads/2010/04/beckett-the_science-of-chocolate.pdf [Accessed 9 Apr. 2025].

Kinta, Y. and Hatta, T. (2012). Morphology of Chocolate Fat Bloom. *Cocoa Butter and Related Compounds*, pp.195–212. doi:<https://doi.org/10.1016/b978-0-9830791-2-5.50011-6>.

Tewkesbury, H., Stapley, A.G.F. and Fryer, P.J. (2000). Modelling temperature distributions in cooling chocolate moulds. *Chemical Engineering Science*, 55(16), pp.3123–3132. doi:[https://doi.org/10.1016/s0009-2509\(99\)00578-3](https://doi.org/10.1016/s0009-2509(99)00578-3).

Sensitech. (2023). *Chocolate Transportation & Warehousing Best Practices* | *Sensitech Blog*. [online] Available at: <https://www.sensitech.com/en/blog/blog-articles/blog-transporting-warehousing-chocolates.html>.

ASHRAE Handbook. (2020). HVAC Systems and Equipment. American Society of Heating, Refrigerating and Air-Conditioning Engineers.

Rigorous design

Vantagehouse.com. (2024). *Chocolate Machines* | *Vantage House*. [online] Available at: <https://www.vantagehouse.com/chocolate-machines/> [Accessed 30 Apr. 2025].

Zografos, A.J., Martin, W.A. and Sunderland, J.E. (1987). Equations of properties as a function of temperature for seven fluids. *Computer methods in applied mechanics and engineering*, 61(2), pp.177–187. doi:[https://doi.org/10.1016/0045-7825\(87\)90003-x](https://doi.org/10.1016/0045-7825(87)90003-x).

Rodgers, T., 2013. *Heat Transfer*. [pdf] The University of Manchester. Available at: https://personalpages.manchester.ac.uk/staff/tom.rodgers/documents/HT_Notes.pdf [Accessed 14 Apr. 2025].

Dreger, M.M. (2014). The experimental determination of the thermal conductivity of melting chocolate: thermal resistance analogies and free convection boundary conditions. *Advanced Computational Methods and Experiments in Heat Transfer XIII*. [online] doi:<https://doi.org/10.2495/ht140431>.

FOW Mould, 2022. *A Complete Guide To Polycarbonate Molding Service - FOW Mould* [Online]. Available from: <https://www.immould.com/polycarbonate-molding/> [Accessed 19 March 2025]

Thermtest. (2024). *Thermal Conductivity of Polycarbonate Materials*. [online] Available at: <https://thermtest.com/application/thermal-conductivity-of-polycarbonate-materials>.

NASA (2015). *Navier-Stokes Equations*. [online] Nasa.gov. Available at: <https://www.grc.nasa.gov/www/k-12/airplane/nseqs.html>.

Grob, L. (1991). *Aero-and thermodynamical optimization of cooling tunnels for chocolate systems*. [online] Available at: https://www.research-collection.ethz.ch/bitstream/handle/20.500.11850/418909/1/LucasGrob_PhDThesis.pdf [Accessed 20 Apr. 2025].

Solitaire Overseas (2024). *Density of Stainless Steel 304 - Solitaire Overseas*. [online] Solitaire Overseas Blog. Available at: <https://www.solitaire-overseas.com/blog/density-of-stainless-steel-304/>.

Optimisation

Beckett, S.T., Fowler, M.S. and Ziegler, G.R. (2017) *Industrial chocolate manufacture and use*. 5th edn. Chichester: Wiley-Blackwell.

MakeItFrom.com (n.d.) *Polycarbonate (PC) vs. Polylactic Acid (PLA, Polylactide): Material Properties Comparison*. Available at: <https://www.makeitfrom.com/compare/Polycarbonate-PC/Polylactic-Acid-PLA-Polylactide> (Accessed: 22 April 2025).

Yu, F.W., Chan, K.T., Sit, R.K.Y. and Yang, J. (2014). Review of Standards for Energy Performance of Chiller Systems Serving Commercial Buildings. *Energy Procedia*, [online] 61, pp.2778–2782. doi:<https://doi.org/10.1016/j.egypro.2014.12.308>.

Mechanical design

National Refrigerants Ltd. (n.d.). *R410A*. [online] Available at: <https://nationalref.com/products/r410a/>.

Bsbeltfactory.com. (2025). Available at: <https://www.bsbeltfactory.com/the-5-best-material-for-food-conveyor-belts/> [Accessed 28 Apr. 2025].

www.alibaba.com. (2020). *Food Grade Transparent Pu Conveyor Belt for Elevator*. [online] Available at: https://www.alibaba.com/product-detail/food-grade-transparent-pu-conveyor-belt_1600087794748.html.

Rollers UK. (2023). *SS-PH4011HSL1 – Ø40 x 11mm Hex. Sprung One End – Rollers UK*. [online] Available at: <https://rollersuk.com/product/ss-ph4011hsl1-o40-x-11mm-hex-sprung-one-end/> [Accessed 28 Apr. 2025].

Durabelt.com. (2019). *DuraBelt - Elastic Urethane Flat Belting, Tracking Sleeves, Stretchy, Belts, Anti-Snag Flat Belts*. [online] Available at: <https://www.durabelt.com/flatbeltinfo.php> [Accessed 28 Apr. 2025].

AZoM (2019). *Stainless Steels - Stainless 304 Properties, Fabrication and Applications*. [online] AZoM.com. Available at: <https://www.azom.com/article.aspx?ArticleID=2867>.

Reclamet Limited. (2025). *Scrap Metal Prices*. [online] Available at: <https://www.reclamet.co.uk/scrap-metal-prices/> [Accessed 28 Apr. 2025].

indiamart.com. (2017). *Pu Ceramic Conveyor Belt*. [online] Available at: <https://www.indiamart.com/proddetail/pu-ceramic-conveyor-belt-7875016930.html> [Accessed 28 Apr. 2025].

www.easycomposites.co.uk. (n.d.). *XPS Extruded Polystyrene Foam (Styrofoam) 100mm - Easy Composites*. [online] Available at: <https://www.easycomposites.co.uk/xps-extruded-polystyrene-foam>.

Control

Marketing (2024). *The Role of Control Systems in Manufacturing - Corematic*. [online] Corematic. Available at: <https://corematic.com.au/blog/the-role-of-control-systems-in-manufacturing/>.

UNITRONICS (2023). *What is PLC ? Programmable Logic Controller*. [online] unitronics. Available at: <https://www.unitronicsplc.com/what-is-plc-programmable-logic-controller/>.

Siemens AG, 2017. Basics of PLC programming: Startup and operation. [online] Siemens Automation. Available at: <https://www.automation.siemens.com/sce-static/learning-training-documents/classic/basics-programming/a03-startup-en.pdf> [Accessed 29 Apr. 2025].

Refrigerants.com. (2025). Page Restricted. [online] Available at: <https://refrigerants.com/wp-content/uploads/2019/12/SDS-R404A> [Accessed 29 Apr. 2025].

Appendix 1- Short Cut Design

Time Required for cooling

$$\text{Heat transfer of the chocolate: } Q = mC_p\Delta T = mC_p(T_{\text{initial}} - T_{\text{final}})$$

$$\begin{aligned} \text{Heat removed from the system via convection: } Q &= -hA\Delta T \\ &= -hA(T_{\text{chocolate}} - T_{\text{air}}) \end{aligned}$$

$$mC_p(T_{\text{initial}} - T_{\text{final}}) = -hA(T_{\text{chocolate}} - T_{\text{air}})$$

$$mC_p \frac{dT}{dt} = -hA(T_{\text{chocolate}} - T_{\text{air}})$$

$$\frac{dT}{dt} = \frac{-hA}{mC_p}(T_{\text{chocolate}} - T_{\text{air}})$$

$$\frac{dT}{(T_{\text{chocolate}} - T_{\text{air}})} = \frac{-hA}{mC_p} dt$$

$$\int \frac{dT}{(T_{\text{chocolate}} - T_{\text{air}})} = \frac{-hA}{mC_p} \int dt$$

$$\ln(T_{\text{chocolate}} - T_{\text{air}}) = \frac{-hA}{mC_p} t + c$$

$$\text{Boundary conditions: when } T_{\text{chocolate}} = T_0 \therefore t = 0$$

$$\ln(T_0 - T_{\text{air}}) = 0 + c \therefore c = \ln(T_0 - T_{\text{air}})$$

$$\ln(T_{\text{chocolate}} - T_{\text{air}}) = \frac{-hA}{mC_p} t + \ln(T_0 - T_{\text{air}})$$

$$e^{\ln(T_{\text{chocolate}} - T_{\text{air}})} = e^{\frac{-hA}{mC_p} t} \times e^{\ln(T_0 - T_{\text{air}})}$$

$$T_{\text{chocolate}} - T_{\text{air}} = e^{\frac{-hA}{mC_p} t} \times (T_0 - T_{\text{air}})$$

$$\ln\left(\frac{T_{\text{chocolate}} - T_{\text{air}}}{T_0 - T_{\text{air}}}\right) = \ln e^{\frac{-hA}{mC_p} t}$$

$$\ln\left(\frac{T_{\text{chocolate}} - T_{\text{air}}}{T_0 - T_{\text{air}}}\right) = \frac{-hA}{mC_p} t$$

$$t = \ln\left(\frac{T_{\text{chocolate}} - T_{\text{air}}}{T_0 - T_{\text{air}}}\right) \times \frac{mC_p}{-hA}$$

Cooling Tunnel Conveyor Weight
(Assume belt is 0.05m thick)

Weight of conveyor belts: $10.18\text{kg} + 8.1\text{kg} + 13.79 = 32.07\text{kg}$ (Continental Belting Pvt. Ltd., 2024)

Weight of Chocolate bar on the conveyor at a certain time:

Length of mould = $(5 \times 0.185) + (6 \times 0.002) = 0.937\text{m}$

Number of moulds on the belt at any given time = $14.53\text{m} / 0.937\text{m} = 15.5$

Number of chocolate bars on the belt at any given time = $15.5 \times 20 = 310$ bars

Weight of mould on the belt at any given time = $15.5 \times 5.761 \text{ kg}$ (mass of the mould) = 89.3kg

Weight of chocolate bars at any given time = $310 \times 0.18\text{kg} = 55.8\text{kg}$

Total weight = $32.07\text{kg} + 89.3 \text{ kg} + 55.8\text{kg} = 177.17\text{kg}$

Appendix 2- Rigours Design

Surface Temperature of chocolate with time integration

$$\frac{dT}{dt} = \frac{UA(T_a - T)}{\dot{m}c_p}$$

$$\frac{dT}{T_a - T} = \frac{UA}{\dot{m}c_p} dt$$

$$\int_{T_{in}}^{T_{out}} \frac{dT}{T_a - T} = \int_0^{\Delta t} \frac{UA}{\dot{m}c_p} dt$$

$$-\ln|T_a - T_{out}| + \ln|T_a - T_{in}| = \frac{UA\Delta t}{\dot{m}c_p}$$

$$\ln\left(\frac{T_a - T_{in}}{T_a - T_{out}}\right) = \frac{UA\Delta t}{\dot{m}c_p}$$

$$\frac{T_a - T_{in}}{T_a - T_{out}} = e^{\frac{UA\Delta t}{\dot{m}c_p}}$$

$$T_a - T_{out} = (T_a - T_{in}) \cdot e^{-\frac{UA\Delta t}{\dot{m}c_p}}$$

$$T_{out} = T_a + (T_{in} - T_a) \cdot e^{-\frac{UA\Delta t}{\dot{m}c_p}}$$

Internal Temperature of chocolate with time integration

$$\frac{\partial T}{\partial t} = \alpha \frac{\partial^2 T}{\partial x^2}$$

$$\frac{\partial T}{\partial t} \approx \frac{T_i^{n+1} - T_i^n}{\Delta t}$$

$$\frac{\partial^2 T}{\partial x^2} \approx \frac{T_{i+1}^n - 2T_i^n + T_{i-1}^n}{\Delta x^2}$$

$$\frac{T_i^{n+1} - T_i^n}{\Delta t} = \alpha \frac{T_{i+1}^n - 2T_i^n + T_{i-1}^n}{\Delta x^2}$$

$$T_i^{n+1} - T_i^n = \frac{\alpha \Delta t}{\Delta x^2} (T_{i+1}^n - 2T_i^n + T_{i-1}^n)$$

$$T_i^{n+1} = T_i^n + \frac{\alpha \Delta t}{\Delta x^2} (T_{i+1}^n - 2T_i^n + T_{i-1}^n)$$